Improving the Durability of Thermally Insulated Historic Solid Masonry Walls

by

David Wach

A thesis submitted in conformity with the requirements
for the degree of Master of Applied Science
Graduate Department of Civil Engineering
University of Toronto

Abstract

Improving the Durability of Thermally Insulated Historic Solid Masonry Walls

David Wach

Master of Applied Science

Graduate Department of Civil Engineering

University of Toronto

2017

Providing means of drying from the inboard face of the masonry when walls are insulated on the interior assists the overall drying potential of the façade. Laboratory tests simulating inward vapour pressure drives induced by solar heating were carried out on Multiple samples of RSI3.9 (R22) and RSI4.2 (R24) mineral fibre. The testing revealed that the drying potential of mineral fibre insulation was roughly equivalent to a 3 mm (1/8 in.) vented clear airspace. Combining mineral fibre insulation with a 3 mm (1/8 in.) airspace was shown to be a very effective means of providing the ventilation necessary for drying solar heated walls. The laboratory test results were incorporated into a hygrothermal computer model to simulate the potential for drying walls exposed to moisture. The laboratory tests and computer modeling have revealed that using air permeable insulation can be an effective means of assisting the drying of internally insulated walls.

Acknowledgements

I would like to acknowledge and thank the following people and organizations who have made the completion of this thesis possible:

My supervisor, Professor K.D. Pressnail, for his encouragement, support and guidance. I knocked on Professor Pressnail's door four years ago with a faint vision of the completion of this work. Thank you for your encouragement to always move onward.

Paul Pasqualini and Engineering Link for providing me with the opportunity and means to complete this research.

I would like to thank Roxul Inc. for their support and input into the study. Also, I would like to acknowledge the National Science and Engineering Research Council for financial support.

To Aisling Curtin, your love and support made this happen. Thank you from the bottom of my heart.

To Gord and Steve Wach, I know there is no one prouder of me than the both of you.

To Beth Wach, I know you would have loved to read this. This is for you.

Table of Contents

List of Tables

List of Figures

List of Acronyms

SPF	Spray Polyurethane Foam

Chapter 1: Introduction

1.1 BACKGROUND

Buildings account for a substantial portion of primary energy usage worldwide, much of which is used for heating and cooling. Older buildings are prone to thermal inefficiencies because they were built at a time when energy conservation was not as large of a concern as it is today. In Canada, buildings account for roughly 30% of secondary energy usage [1]. In the residential sector, approximately 2/3 of this energy is used for heating [2]. Often it is not economical to replace these buildings because their structures are durable and are not close to the end of their service lives. A common energy usage reduction strategy has been to thermally retrofit existing buildings to improve their energy efficiency.

A large number of buildings in Canada, both residential and commercial, were constructed with load bearing solid masonry walls comprising their structure in the late 19th and early 20th centuries. These buildings were built without thermal insulation and relied upon their mass to resist heat transfer. The buildings are ideal candidates for thermal retrofits because they lack insulation and can have high rates of unintentional air leakage through the envelope which also contributes to undesirable heat movement.

1.1.1 CHALLENGES RELATED TO HISTORIC SOLID MASONRY BUILDINGS

The ideal thermal retrofit for a solid masonry wall occurs on the exterior for technical and economic considerations [3]. In this configuration, the thermal control layer, combined with moisture and vapour control layers, can keep the wall both warm and dry. A challenge is presented when considering historical solid masonry buildings in cold climates because often insulating at the exterior is not an option.

Solid masonry buildings in Canada that have been designated as “heritage” by local preservation boards must have the appearance of their facades maintained during retrofits. While it is often less expensive to insulate externally, internal insulation is often a necessity. For example, in the case of historic buildings, or buildings with set-back restrictions, internal insulation is often the only viable strategy. During heating seasons in cold climates, internal thermal insulation will reduce the amount of heat transfer through the solid masonry walls causing the walls to be colder on average. When the walls get wet they will stay wet for a longer period of time because less energy is available in the walls to help dry them. Common thermal retrofits of historical masonry buildings in cold climates have used spray polyurethane foam (SPF) as the thermal control layer, applied directly to the inside of the masonry wall. The SPF also acts as the moisture, vapour and air control layers in this configuration. If a vapour retarder is installed inboard of the brick masonry, the wall will only be able to dry to the outside by mechanisms including evaporation and vapour diffusion, whereas previously it could dry in two directions.

Cold and damp masonry walls may be less durable. Durability issues include an increase in frequency of spalling due to osmotic pressures and freeze-thaw action. As well, wood floor joists or steel members that are embedded in the wetter masonry may fail since wood floor joists may decay and steel members may corrode in high relative humidity environments.

1.1.2 MASONRY DURABILITY

Historic solid masonry walls generally consist of multiple wythes of clay brick masonry. Prior to advances in brick production in the mid-20th century, high levels of variability existed in the appearance, geometry and mechanical properties of historic clay bricks. These bricks were fired in stationary kilns, where temperature gradients existed, causing wide variations in the strength and absorption properties of the bricks, even in the same firing batch [4]. Weaker bricks with a less desirable appearance were referred to as ‘common’ brick. Common brick was generally used to construct the interior and supporting wythes of solid masonry walls because their substandard appearance would not be visible from the exterior [5]. Once the historic solid masonry wall is insulated from the interior, the interior wythes will now experience more cycles of freezing and thawing as the freezing front now penetrates deeper into the wall from the outside. Because the properties of the inner bricks are poor, they are susceptible to damage as they have a greater exposure to freeze-thaw action as a result of the freezing front moving deeper into the wall.

Whether a brick will be susceptible to freeze-thaw damage depends on its critical degree of saturation (S_{crit}) [6]. The critical degree of saturation is the moisture content at which damage from freeze-thaw action begins to occur divided by vacuum saturated moisture content of the material. Freeze-thaw action occurs when moisture contained in the pores of a brick begins to freeze, forcing water into capillary pores ahead of the freezing front which leads to hydrostatic pressures within the brick and eventually spall [7]. The question of whether freeze-thaw damage will occur within a historic solid masonry wall depends upon the moisture content of the masonry and whether it is equal to or greater than the masonry's S_{crit} during freeze-thaw cycles. The most susceptible walls are those in locations that are cold and wet. Interior thermal retrofits can lead to cooler, damper conditions and therefore, internal insulation can increase the risk of damage from freeze-thaw action in historic solid masonry walls.

The durability of framing members embedded within historic solid masonry walls can also be negatively affected by the introduction of interior thermal insulation. Common construction practice in buildings with solid masonry walls was to set wooden joists directly into the load bearing masonry wall. It was also common to embed steel framing members into the wall including columns, lintels and angles. The relative humidity threshold for decay to occur at building envelope surfaces is approximately 95% [8]. Corrosion risk is measured by the time in which a metal is exposed to temperatures greater than 0°C and a relative humidity in excess of 80% [8].

Recent research has focused on the risk of bio-deterioration (wood rot) due to solid masonry walls becoming colder and wetter, causing the relative humidity surrounding the wood to rise [9]. De Rose et. al have investigated methods utilizing a limit state approach to evaluating the durability risk of insulating solid masonry walls in a cold climate from freeze-thaw, wood rot and corrosion by comparing anticipated temperature and moisture loads to those that are necessary for the damage functions described [10]. Although there was low freeze-thaw risk after the interior insulation retrofit due to the relatively high S_{crit} of the bricks in two case studies investigated by De Rose et. al, wood rot and corrosion risk was increased. The properties of wall assemblies at different buildings should be specifically evaluated for susceptibility to damage functions before an internal retrofit is performed.

Bio-deterioration and high moisture levels of masonry in general may pose health risks through negatively affecting indoor air quality [11] [12]. Although an important potential implication of interior thermal retrofits, this research focuses on the durability implications of interior thermal retrofits.

1.1.3 VENTILATION THEORY

Air flow can be quantified by the simplified laws of fluid mechanics. Air is often assumed to be an incompressible ideal gas. Bulk air contains both water vapour and heat energy. When bulk air moves through building elements heat energy and water vapour can be gained or lost. When an airspace is provided behind a wall cladding, moisture can be removed by drainage, capillary transport and evaporation, and diffusion. When the airspace is ventilated, exterior air driven by natural convection can remove moisture or even add moisture to the wall assembly, depending upon the conditions within the cavity. Ventilation can be far more efficient for removing moisture than vapour diffusion.

When the analysis of airflow is constrained to the domain of movement through buildings, the airflow can be classified as laminar or turbulent. Laminar flow occurs when the air moves due to small pressure differences or when it flows through materials containing small cracks and pores. Airflow in mineral fibre insulation would likely be considered laminar as the air permeable insulation has relatively small pores. Flow due to high pressure differences, or that through larger openings, is more likely to be turbulent flow. Laminar flow can be described by Darcy’s equation where the air flow rate Q is linearly related to the driving air pressure difference by a constant:

$$Q = K \times A \times \Delta P \tag{1.1}$$

Q = airflow rate [m^3/s]

K = constant

A = area [m^2]

ΔP= pressure difference [Pa]

Turbulent flow through orifices is also a function of the driving air pressure difference. Turbulent flow is better described by adding a flow exponent that is considered to be 0.5 for purely turbulent flow:

$$Q = C_d \times A \times \left(\Delta P \times \frac{2}{\rho_{airspace}}\right)^{1/2} \tag{1.2}$$

Q = airflow rate [m^3/s]

C_d = discharge coefficient

A = area of the orifice [m^2]

ΔP = pressure difference [Pa]

ρ = density of the fluid [kg/m^3]

The discharge coefficient, calculated for circular sharp edged orifices, is 0.61 according to Kirchoff [8]. If experimental results are available, they should be used, because the discharge coefficient ignores losses due to turbulence and friction. In a ventilated cavity, there will always be friction with the sides of the cavity. It would be expected that the value of the C_d would be lower in field conditions in ventilated cavities. It would be a function of the roughness of the boundaries of the cavity, obstructions to the clear airspace, and the thickness of the clear airspace itself.

Baker et al. (1987) [8] found that a general power law as follows fits the data from building enclosure components that have been tested:

$$Q = C\Delta P^{n} \tag{1.3}$$

Q = airflow rate [m^3/s]

n = is a flow exponent

C = flow coefficient

The flow coefficient is a measure of the leakage of the enclosure assembly and includes the area, flow path, flow regime, friction, temperature, and density effects. As the air flows through an orifice, if the flow exponent is 0.5, the flow is turbulent. Laminar flow would have a flow exponent of 1.0, and the equation would resemble Equation 2.1 above that represents Darcy's equation for laminar flow. As the thickness of the clear airspace in the ventilated cavity becomes smaller, it can be expected that the airflow will change from turbulent to laminar within the flow path of the cavity. If we consider both vents and the cavity in the system, the flow may transition between laminar in turbulent in different regions of the flow path. The transition between one flow regime and another often displays variable flow rates and erratic behaviour [8].

Flow through ventilated airspaces results from pressure differences in the cavity. The primary mechanisms generating the pressure difference are wind and natural buoyancy. Friction with vent edges and the walls of the ventilated airspace resist the flow.

1.1.4 PREVIOUS VENTILATION RESEARCH

In general, existing modeling and field studies have consistently demonstrated that providing ventilation within wall assemblies can be an important means of drying the wall assembly when it becomes wet. Field studies have mostly shown that ventilation helps to dry wall assemblies, but in certain cases can add moisture to the wall assembly. The majority of modeling studies have shown good agreement with the results of the field studies.

ASHRAE Report 1091 [13] provides a review of literature and theory regarding ventilation use in wood framed walls and describes research into the development of rain screen and sheathing membranes in wood frame walls. The researchers concluded that in general, ventilation of the test wall encourages faster drying and significantly reduces the impact of solar-driven inward vapour drive condensation.

Popp, Meyer and Kuenzel [14] performed field studies on the impact of ventilation with wall assemblies including various cladding types and concrete back up walls. They concluded that ventilation provides a faster drying rate in wall assemblies containing concrete back-up walls with absorptive claddings if ventilated airspaces are present.

Stovall and Karagiozis [15] found that the most important factors for determining the ventilation flow rate through an airspace are wind pressure, thermal buoyancy, presence (or lack of) of obstructions, and the vent area. They developed a computational fluid dynamics model and compared it to field results. The model showed that ventilation was beneficial and that there was no significant difference in flow between a 19 mm airspace and a 50 mm airspace. They also concluded that vent slot size is the controlling factor for the ventilation rate as opposed to the clear airspace thickness.

Salonvarra et al. [16] compared the functions of airspaces behind various types of cladding, and compared hygrothermal modeling to published field data in various US climates. They concluded that an air cavity is beneficial in all wall constructions but is particularly beneficial when highly absorptive claddings such as bricks and stucco are used.

Kargiosis and Kuenzel [17] studied the effect of air cavity convection on the moisture performance of wood framed walls and generally found that results of hygrothermal modeling are in good agreement with established field data.

Straube and Burnett used both field experiments and modeling to evaluate the performance of ventilation within wall assemblies featuring masonry veneers [15]. Ventilation can be useful to control inward vapour drives behind brick veneers and the ventilated airspace adds significant drying potential to the wall. In general, brick veneers with ventilated airspaces behind them display better hygrothermal performance than do brick veneers with no ventilation or ventilation that is restricted. Field measurements confirmed sufficient pressures to drive convective air movement. Normal amounts of ventilation will not cool walls.

Langmans et al. [18] performed an experimental analysis to determine the impact of ventilation at eight full scale test walls at a test house. They used hot bead anemometry and air pressure registration to measure the ventilation rate. They found that the air flow resistance of the airspace is negligible as compared to the resistance of the vent holes. They found that the ventilation rate behind brick veneers was between 1-10 ACH and was about 100 ACH behind siding.

Ventilation can increase the moisture content of some wall assemblies depending on environmental conditions. Hansen [19] performed field studies with twelve wall assemblies and studied the impact of ventilation on the moisture content of wood framed walls. They noted that there was a greater moisture content in the wall assembly when a ventilated cavity was present.

This occurs when the moisture content of the outdoor air is greater than the moisture content of the ventilated cavity. Straube and Burnett also found that walls can be wet by ventilation in some instances [20]. This condition will occur if the dew point of outdoor air greater than temperature of cavity. This condition can be detrimental but the researchers concluded that this circumstance is rare in a cold climate.

In general, field studies and modeling results are in agreement that ventilated airspaces benefit the moisture performance of wall assemblies by increasing their drying potential.

1.1.5 VENTILATED AIRSPACES BEHIND SOLID MASONRY WALLS

One strategy to reduce the risk of issues relating to durability from insulating on the inside of a solid masonry wall that has been investigated by researchers at The University of Toronto, is to provide a ventilated airspace on the interior of the masonry wall. When insulating historic masonry walls from the interior, providing a means of drying from the inboard face of the masonry wall improves the drying potential of the masonry. The risk of durability issues such as freeze-thaw damage, steel member corrosion, and wood member rot is reduced.

Pearson [21] proposed a ventilated masonry retrofit in which a drying airspace was incorporated between SPF and the exterior masonry using a polypropylene mesh that is commonly used to protect airspaces during brick veneer construction. Using hygrothermal simulations, it was found that compared to the uninsulated walls, internally insulating walls resulted in the moisture content of non-vented solar exposed walls increasing by 3.6% at the south elevation and by 5.8% at the east elevation during the simulation year in the Toronto, Ontario climate. By contrast, when the same internally insulated walls were ventilated, there was an increase in moisture content of 0.7%

to 1.6% at the south and east elevations during the same time period. The non-vented wall will reach its critical moisture content after approximately 5-16 years. Once the non-vented wall reaches its S_{crit}, freeze-thaw action can be expected to cause damage to solid masonry walls. Walls that incorporate ventilation would not reach their S_{crit} for an additional 30 years.

To explore methods of improving the drying potential, two field studies were previously carried out on internally insulated historic masonry buildings in Toronto, Ontario. In these field studies, a drying airspace was incorporated into the wall assembly using the method proposed by Pearson as described above.

Field trials were conducted at the Gemini residential building and at the Barrymore commercial buildings. Both buildings are constructed with solid brick masonry walls and are located in Toronto, Ontario. At both buildings, test panels were installed in which a drying airspace was incorporated between polyurethane foam insulation and exterior masonry using a polypropylene mesh that is commonly used to protect airspaces during brick veneer construction. Tzekova analyzed the performance of both buildings [22].

The Barrymore building was originally constructed in the 1850s. Two vented masonry test wall sections were installed at the building and monitored from November, 2011 to September, 2013. One test section was installed at the south elevation and one was installed at the east elevation. The south elevation in Toronto experiences the maximum solar exposure in the winter and the east experiences the maximum wind driven rain. During the winter months, when the walls are most exposed to freeze-thaw damage, the ventilated airspace helped the masonry dry. Monitoring at the Barrymore [22] confirmed that a greater amount of moisture was removed from test walls that used the vented airspace retrofit as compared to the traditional retrofit but that Pearson's hygrothermal simulations had overestimated the amount of airflow through the vented airspace and the amount of moisture removed with the vented airspace retrofit. Although the degree of moisture reduction achieved at Barrymore was less than the hygrothermal models indicated, the risk of freeze-thaw was reduced.

The Gemini residential building was monitored between January 2014 and August 2014. The Gemini building represented a full-scale test of how vented airspaces can perform within solid masonry walls as the ventilated airspace was incorporated during a full building retrofit. The north and south walls were monitored because the east and west walls were not exposed as the building was approximately four feet from adjacent buildings. At the north wall, moisture was introduced during three of the eight monitored months in total, and was removed by ventilation during five of the months. At the south wall, moisture was removed during all months.

The field trials have shown the polypropylene mesh to be an effective means of assisting drying of the masonry because the ventilated airspace provided a secondary path for which the masonry could dry.

To reduce construction costs, alternative systems to assist the drying of solid masonry walls have been considered. One option investigated by Tzekova [22] utilizes air and vapour permeable mineral fibre insulation to assist ventilation drying. Preliminary laboratory tests simulating inward vapour pressure drives induced by solar heating were carried out on air-permeable mineral fibre insulation of various densities. By utilizing mineral fibre insulation in a wall configuration to promote ventilation drying, both material and labour costs could be reduced during an interior thermal retrofit, as compared to the approach using polypropylene mesh.

Preliminary laboratory tests simulating inward vapour pressure drives induced by solar heating were carried out on air-permeable mineral fibre insulation of various densities [22]. Test wall sections with various densities of mineral fibre insulation were installed in the climate simulator at the University of Toronto. A light array increased the temperature of moisture absorbent cladding of the test wall section inducing a vapour drive into the wall. A moisture mass balance was performed to determine the amount of ventilation achieved. 16% of the moisture that entered the walls was unaccounted for in the mass balance. An upper bound for ventilation assumed the unaccounted for moisture was removed by ventilation and a lower bound assumed that it was lost to air leakage from the test wall. Walls with vent holes but no clear airspace had approximately 52% - 90% of the total moisture entering the walls removed by natural ventilation. Results indicated that moisture can be removed from walls that do not incorporate a clear airspace. Further, air permeable insulation along with adequately sized vent holes can promote ventilation drying.

1.2 RESEARCH OBJECTIVES AND METHODS USED

The overall aim of this work is to examine the potential for air permeable thermal insulation to be used in lieu of, or in combination with, a clear vented airspace in order to promote moisture removal in wall assemblies. To measure how well mineral fibre insulation facilitates ventilation drying, a series of laboratory tests were carried out. In addition, hygrothermal model simulations were also carried out to investigate the potential impact of the ventilation drying on the moisture response of an internally insulated wall system.

1.3 THESIS ORGANIZATION

Chapter 2 presents the results of a laboratory study which examined the impacts on moisture removal while utilizing mineral fibre insulation in varying vented air space configurations. Chapter

3 presents the results of hygrothermal simulations. Simulation parameters and assumptions are described. Conclusions and recommendations follow in Chapter 4.

Chapter 2: Laboratory Study: Venting via Air Permeable Insulation

The traditional thermal retrofit involving SPF applied directly to the interior of the solid masonry wall cuts off a direction of drying. By providing a ventilated clear airspace between the solid masonry and the SPF, a potential path for drying of moisture is created. The moisture can either move to the clear airspace through capillary action or diffusion, evaporate, and be removed by convective air flow due to stack action within the clear airspace. Field studies in Toronto, Ontario have demonstrated that the ventilated airspace is an effective means of assisting drying of the solid masonry walls. The clear airspace had been created by installing polypropylene mesh that is commonly used to protect clear airspaces during brick veneer construction inboard of the masonry wall. To reduce construction costs, alternative systems to provide a ventilated airspace were examined. One option investigated by Tzekova was to use mineral fibre insulation to assist ventilation drying (Tzekova, 2015). Preliminary laboratory tests were conducted to test whether the air permeable insulation itself could act as a ventilated airspace in that convective airflow promoting drying would occur within the mineral fibre insulation itself. Reported results were favourable.

Following Tzevova's preliminary tests, experimental procedures were refined to improve the quantification of the amount of drying that was occurring through mineral fibre insulation. The focus of this chapter is to describe the refined test methods and the results of the testing.

2.1 APPROACH

The overall objective of this laboratory testing was to determine how much solar driven moisture can be removed through ventilation using air permeable insulation in various venting configurations. In addition, this work attempts to determine an equivalent airspace thickness of air permeable mineral fibre insulation given its density. The work presented here builds upon previous work described by Tzekova [22] with a modified apparatus and experimental method. The intention of modifying the apparatus and experimental method was to reduce the amount of unaccounted for moisture experienced during previous laboratory testing. To quantify the effectiveness of mineral fiber insulation to function as a vented airspace, a series of laboratory tests were carried out. Multiple samples of RSI3.9 (R22) and RSI4.2 (R24) mineral fibre batts were tested with various airspace thicknesses. Controlled variables include the vent area ratio, the clear airspace thickness and the insulation density. The main variable of interest is the amount of moisture that can be removed from the test assembly by ventilation.

2.2 EXPERIMENTAL PROCEDURE

This section describes the experimental procedure used for the laboratory testing that attempts to quantify the amount of ventilation that can be achieved using mineral insulation as a venting medium. The apparatus is described, followed by discussion regarding the procedure.

2.2.1 APPARATUS

Testing was performed in the climate simulator in the Building Science Laboratory at the University of Toronto. Figure 1 shows the layout of the climate simulator. The climate simulator was divided into two rooms, the Warm Room and the Cold Room. The Cold Room contained a chiller, and the set point of the room was set to -15°C. The temperature of the Warm Room was influenced by the temperature of the main laboratory which was approximately 21-23°C throughout the testing. Two guard rooms, one within each of the warm room and the cold room were constructed. The temperatures of the guard rooms were controlled by a combination of heaters and fans. The temperature of Guard Room 1 was maintained between 19-21°C during and the temperature of Guard Room 2 was maintained between 18-21°C. The heaters and fans were controlled through relays by a program called HTBasic using data collected from thermocouples throughout the climate simulator.

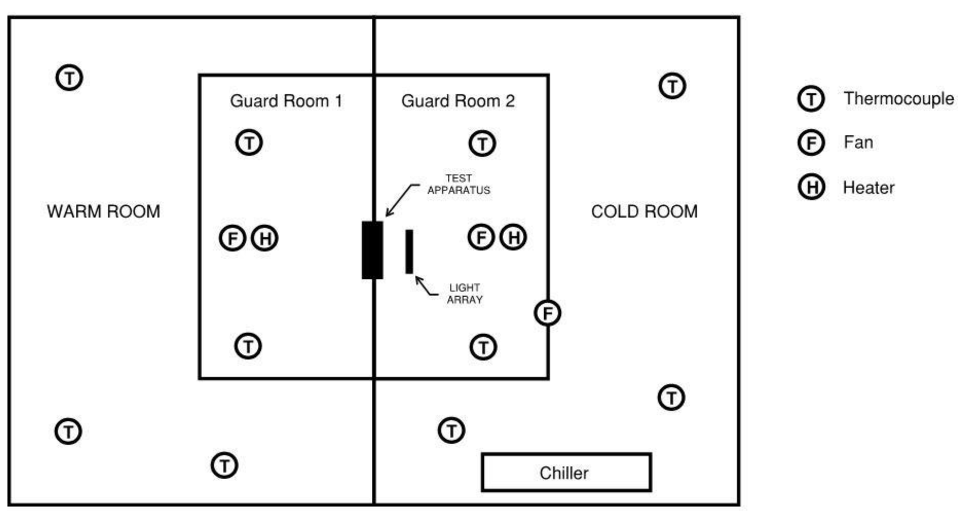

Figure 2.2.1: Plan View of Climate Simulator Set-up

To minimize evaporation losses during assembly and disassembly, the experimental apparatus and procedures used by Tzekova were refined. Figure 2 shows a photograph and Figure 3 shows a cross section of the test apparatus used to simulated moisture removal by ventilation (Refer to Appendix A for additional photographs). The test box cavity was loaded with mineral fibre insulation. Saturated ship lapped pine siding acted as the moisture source. The pine siding board pieces were placed over the test cavity onto the rails of the test box and held in place with wood stringers. The face and sides of the pine siding boards were sealed with 0.15 mm polyethylene and construction tape. Uniform airspace thicknesses were created between the mineral fibre insulation and the pine siding boards by installing wood shims of varying thicknesses upon the rails and styles of the test box. Any exposed wood was covered with construction tape to avoid moisture absorption. Twenty-five mm diameter circular ventilation holes were drilled into the pine boards at top and the bottom of the test apparatus. Corresponding holes were cut within the polyethylene sheet. A plastic grommet and tape were used to seal the circular vent hole ensuring that all airflow through the ventilation hole entered the test box cavity and did not leak between the boards and the polyethylene.

Figure 2.2.2: Photo of Test Apparatus

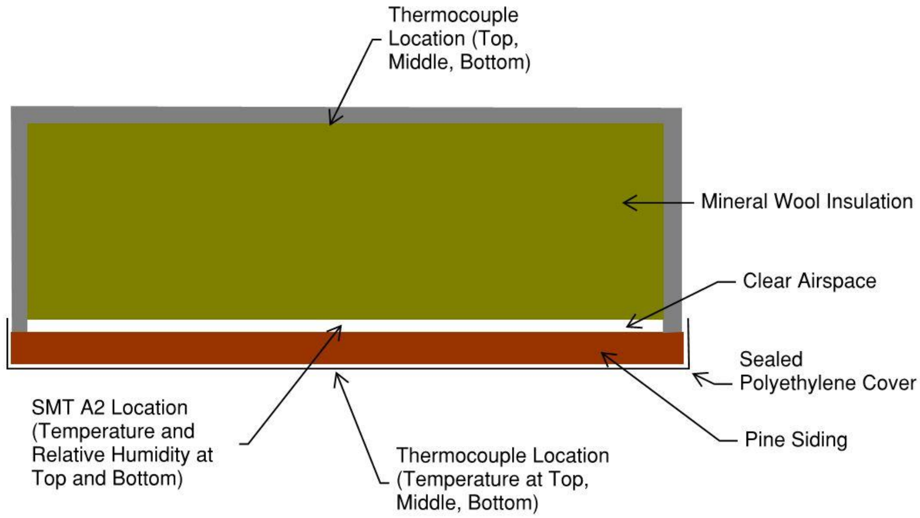

Figure 2.2.3: Cross Section of Plywood Box/Test Apparatus Showing Measurement Locations

A light array increased the pine board temperatures creating a vapour pressure gradient to drive moisture from the pine boards into the test box cavity to simulate sun driven moisture from cladding into the wall assembly. Six bulbs in a single column delivered approximately 1110 Watts to the polyethylene-covered pine siding. Considering the total area of the pine boards, the normalized supplied power was 1288 W/m^2. The light array was positioned 30 cm away from the pine siding surface during testing. Thermocouples were installed at top, middle and bottom of the testing apparatus at the back of test box and mineral fibre interface, to monitor temperatures. Thermocouples were also installed at the top, middle and bottom of the polyethylene in order to measure the surface temperature of the pine siding. SMT A2 wireless data loggers were used to record the temperature and relative humidity at the mineral fibre and pine siding interface (SMT, 2017). These sensors were positioned at the top and bottom of each wall, and were nested within cut-outs of the mineral fibre insulation.

2.2.2 METHOD

Pine siding boards were immersed in cold water for approximately 24 hours. The pine boards were then removed from the water 30 minutes prior to installation to allow most of the surface moisture to evaporate. The pine boards and mineral fibre insulation were weighed immediately prior to assembly. After the insulation was loaded into the test box cavity and the pine siding boards were installed, the apparatus was sealed. The assembled test apparatus was mounted into the wall separating the two guard rooms and was exposed to the light array for 6 hours. The test apparatus was then disassembled and all the components were reweighed. A moisture mass balance was carried out to determine the quantity of moisture removed during the test.

In order to determine how much ventilation drying had occurred, it was necessary to do a mass accounting of the moisture. Difficulties arose in estimating the amount of moisture removed by ventilation because some of the moisture evaporated from the apparatus into the laboratory air during set up and disassembly. Further, surfaces including the polyethylene cover, the test box, and taped rails could not be readily weighed. So evaporation losses and losses on surfaces that could not be weighed became “unaccounted for moisture”. Finally, there was one more possible source of unaccounted for moisture. Although care was taken to ensure the testing apparatus was airtight, it is likely that some moisture may have been lost through unintentional air leakage. The quantity of moisture lost due to unintentional air leakage from the testing apparatus was also a source of unaccounted for moisture.

To estimate the quantity of the unaccounted for moisture, a base case test was set up. In the base case test, the apparatus was completely air sealed using polyethylene sheeting, and no ventilation holes were provided. This test revealed that the total quantity of moisture that was unaccounted for was found to be 10% of the total moisture supplied by the pine boards. Since the experimental procedures were the same for all of the testing, it was assumed that 10% of the moisture supplied was unaccounted for in all of the subsequent tests.

Once testing was completed, and the moisture accounting was carried out, two cases were considered. In the first case, it was assumed that none of the unaccounted for moisture was removed by ventilation. In the second case, it was assumed that all of the unaccounted for moisture was removed by ventilation. The former assumption likely leads to an underestimate of the amount of ventilation drying and is, therefore, a lower bound value. The latter assumption likely leads to an overestimate of the amount of ventilation drying and is an upper bound value. The actual amount of moisture removed by ventilation likely lies somewhere between the lower bound and the upper bound. In the analyses that follow, the average of the lower bound and the upper bound values is used to estimate the quantity of moisture removed by ventilation.

2.3 LABORATORY RESULTS AND ANALYSIS

Section 2.3.1 begins by describing the procedure used for analysis for determining the amount of moisture that was removed by ventilation during testing. Next, Section 2.3.2 begins by examining how much moisture was removed through different venting configurations of the apparatus in the R22 Series. R22 mineral fibre insulation used in this testing has a resistance value of 3.87 m^2K/W and a density of 37 kg/m^3. Modifications to the experimental procedure were incorporated into the R24 series which is described in Section 2.3.3. R24 insulation has a resistance value of 4.23 m^2K/W and a density of 55 kg/m^3. Temperature and relative humidity conditions in the testing apparatus during testing are analyzed in Section 2.3.4. Section 2.3.5 theoretically examines the impact of air permeable insulation as the venting medium upon the flow within the ventilated airspace. Section 2.3.6 compares results obtained by Tzekova to results obtained in the R24 Series. Lastly, data from both the R22 Series and R24 Series are evaluated and discussed in Section 2.3.7.

2.3.1 PROCEDURE FOR DETERMINING MOISTURE REMOVAL VIA VENTILATION

The quantity of moisture removed from the test apparatus during a test represents the quantity of moisture that was removed via ventilation, neglecting unaccounted for losses. The difference between the amount of moisture dried from the pine siding (supplied moisture), and the amount of moisture recovered from the test apparatus (recovered moisture), represents the amount of moisture that was removed via ventilation from the apparatus during the test. The following equation represents a non-conservative estimation of moisture removed by ventilation:

$$\begin{aligned} &Moisture\ Removed\ via\ Ventilation\ (g) \\ &\quad = Moisture\ Lost\ from\ Pine\ Siding\ (g) \\ &\quad - Moisture\ Recovered\ in\ Test\ Apparatus\ (g) \end{aligned} \tag{2.1}$$

Although care was taken to ensure that environmental conditions (including temperature and relative humidity) were consistent between tests, small variations existed. Two measures were used to compare the quantities of moisture that were removed in different tests.

The first measure, ‘Normalized Moisture Removal Rate’, normalizes the moisture removal rate by the estimated stack pressure difference in the ventilated airspace of the test apparatus, according to the following equation:

$$Moisture\ Removed\ \left(\frac{g}{hr * Pa}\right) = \frac{Moisture\ Removed\ (g)}{Time\ of\ Test\ (hr) * Stack\ Pressure\ Difference\ (Pa)} \qquad (2.2)$$

The second measure, 'Moisture Removal Percentage', compares the moisture removed as a percentage of the total moisture supplied. Moisture removal is calculated according to the following equation:

$$Moisture\ Removed\ (\%) = \frac{Moisture\ Removed\ (g)}{Moisture\ Supplied\ (g)} \qquad (2.3)$$

Further, to aid in comparisons between different test series and previous testing by others, a normalized vent area ratio is determined. For the R22 Test Series, a vent area ratio of 1175 mm^2/m^2 was explored. For this testing, the wall area is taken to be the area of the cavity within the test apparatus. The vent area ratio is calculated as follows:

$$Vent\ Area\ Ratio\ (\%) = \frac{Vent\ Hole\ Area\ (mm^2)}{Wall\ Area\ (m^2)} \qquad (2.4)$$

During previous testing performed by Tzekova (Tzekova, 2015), the amount of moisture that was unaccounted for was approximately 16% of the total moisture supplied. It was assumed that this moisture was lost because the test walls were not airtight during the experiments, resulting in moisture loss through air leakage. The testing in this laboratory study attempted to improve the testing apparatus and procedure to maximize the airtightness of the apparatus. In addition, this laboratory work attempted to minimize the set-up time and disassembly time during testing where moisture loss can occur through evaporation into the ambient air of the laboratory. A full description of the experimental procedure is explained in Section 2.2.

Revisiting Equation 2.1, the total moisture removed from the apparatus is the difference between the amount of moisture supplied and the amount of moisture recovered from the test apparatus. Included in the amount of moisture recovered is an estimate of the evaporative drying of moisture from the pine boards into the laboratory air during set-up time before the apparatus was considered sealed. The time of set-up typically ranged from 9 to 11 minutes. Tests were conducted in the laboratory to determine the rate of evaporation from the boards, allowing the total amount of loss through evaporation during set-up to be estimated. Also included in the amount of moisture recovered is the evaporation of moisture of the pine siding boards during disassembly. The first board removed was weighed, then re-weighed after the remaining boards were weighed. The quantity of moisture lost from the first board during the time it took to weigh all the boards represents the maximum amount of evaporative loss of a single board. This maximum loss was attributed to the last board weighed. The first board removed and weighed was assumed to have zero evaporative moisture loss because it was weighed directly after the opening of the apparatus seal. A linear relationship was assumed between the maximum quantity of moisture lost for a board and zero moisture lost to determine the moisture loss for those boards between the first and last weighed. A similar procedure was used to estimate the amount of evaporative drying loss from the mineral fibre batt pieces during disassembly. The quantity was added to the amount of moisture recovered from the test apparatus.

Difficulty exists in estimating the amount of moisture that would evaporate from the apparatus into the laboratory ambient air during disassembly from surfaces including the polyethylene cover, the test box, and taped rails. These elements were too large and heavy to be individually weighed. The amount of moisture loss associated with these elements is assumed to be included in ‘unaccounted for moisture’. Although care was taken to ensure the testing apparatus was airtight during testing, if it was not airtight, moisture may have been lost through unintentional air leakage. Any amount of moisture lost due to unintentional air leakage from the testing apparatus would also be considered as unaccounted for moisture.

A base test was completed to determine the amount of unaccounted for moisture that could be expected during testing. The apparatus in this test was air sealed using polyethylene sheeting, and no intentional venting was incorporated. The total quantity of unaccounted for moisture was 10% of the total moisture supplied. Two cases were created for estimating the quantity of moisture removed via ventilation based upon the amount of moisture that was recovered from the testing apparatus:

- Case 1: Moisture Removed by Ventilation = A-B

  A = Moisture Removed (from Equation 2.1)

  B = Unaccounted for moisture based on the base test

Case 1 is conservative in that it assumes that none of the unaccounted for moisture is removed via ventilation airflow in the ventilated airspace. Case 1 can be considered a lower bound for moisture removed by ventilation. 10% of the moisture lost from the pine boards is considered to be unaccounted for moisture as set by the base test.

- Case 2: Moisture Removed by Ventilation = A

Case 2, the upper bound for moisture removed via ventilation, considers all the unaccounted for moisture to have been removed by ventilation. Case 2 is optimistic. The amount of moisture actually removed by ventilation is likely between these two estimates. Throughout the following analysis, the average between the lower bound and the upper bound (Case 1 and Case 2) is taken to be the estimated moisture removed by ventilation. Moisture removed by ventilation as a percentage is presented as a range. The normalized moisture removal rate takes the midpoint of the range between Case 1 and Case 2 ventilation then normalizes by the average stack pressure difference during the test.

2.3.2 R22 TEST SERIES

All tests in the R22 Series used either R22 (3.87 m^2K/W) mineral fibre insulation as the venting medium, or a combination of R22 insulation and a clear airspace of a given thickness as the venting media. The term venting configuration refers to the combination of these venting media as throughout the rest of the analysis. The density of R22 is 37 kg/m^3. The R22 batts were either in a 'fresh' condition, in that it they had not been used for a previous test, or a 're-used' condition, meaning that they had been used in one previous test. Batts in a re-used condition are assumed to have been through one cycle of placement into the test apparatus, wetting during the test, and drying in the laboratory in preparation for the next test.

Table 2.3.1 summarizes the R22 test results. A full summary of the testing conditions are provided in Appendix B. The difference in vapour pressure between the inboard surface of the pine siding and the back of the apparatus cavity is presented. In addition, the stack pressure difference between the top and the bottom of the ventilated airspace, caused by air density differences between the guard room and the ventilated airspace, is presented.

Temperatures were recorded in the guard room, at the polyethylene apparatus cover surface facing the guard room, and at the back of the testing apparatus using thermocouples. Temperatures were recorded at the inboard pine surface using SMT A2 sensors [23]. Relative humidity data were recorded in the guard room and at the inboard pine surface using SMT A2 sensors. Numerous sensor failures occurred during testing the relative humidity of the guard room and the ventilated airspace during testing. The average relative humidity for tests in which malfunctions did not occur was approximately 20% in the guard room, and approximately 90% in at the inboard pine surface. The guard room had a very low relative humidity because it contained conditioned air that had first been cooled to -15^{o}C. Thus, the average relative humidity over a test was assumed to be 20% in the guard room and 90% at the inboard surface of the pine for all tests.

Test Set	Test	Insulation Type	Clear Airspace Thickness	Vent Area Ratio (mm2 / m2)	Moisture Lost from Wood Siding (g)	Vapour Pressure Difference (Pa)	Stack Pressure Difference (Pa)
1	Base	R22	None	None	215	5070	1.64
2	2A	R22 (re-used)	None (6 mm batt compression)	1175	250	2870	2.01
	2B	R22	None (6 mm batt compression)	1175	222	2730	1.92
	2C	R22	None (6mm batt compression)	1175	222	4750	2.43
	2D	R22 (re-used)	None (6 mm batt compression)	1175	238	3410	2.16
3	3A	R22	6mm	1175	221	2770	1.76
	3B	R22	6mm	1175	275	3300	1.98
4	4A	R22	None	1175	225	2770	1.94
	4B	R22	None	1175	255	2800	2.23
5	5A	R22 (re-used)	13 mm	1175	273	2310	1.84
6	6A	R22 (re-used)	19 mm	1175	290	1880	1.76

Table 2.3.1: R22 Test Series Data

Varying the airspace thickness throughout the testing provided two main functions. The first was to determine if moisture could be removed from the apparatus by ventilation when no clear airspace was provided in the venting configuration. If moisture is removed when no clear airspace is provided, it is assumed to have occurred through ventilation air moving through the mineral fibre insulation batt. When no clear airspace was provided, the pine siding boards were installed such that the pine surface was in direct contact with mineral fibre insulation. To guarantee intimate contact between the mineral insulation and the pine surface, the apparatus was adjusted during some tests so that the pine siding compressed the insulation by 6 mm once installed. In this manner, no local areas of separation between the pine surface and the mineral fibre batt could develop during a test.

The second function of varying the clear airspace thickness was to help determine an equivalent airspace thickness of the mineral fibre insulation batt in terms of venting potential. By comparing how much moisture was removed in venting configurations with no clear airspace, to that of when a clear airspace was incorporated, an estimate of the equivalent airspace thickness of R22 insulation could be determined. During the R22 Series, various airspace thicknesses were tested. These airspaces thicknesses included: 0 mm with batt compression, 0 mm, 6 mm, 12 mm and 19 mm.

The average temperature in the guard room throughout R22 Series testing ranged from 18.0 to 19.1 °C. The average temperature at the polyethylene surface ranged between 41.8 and 50.1 °C. The larger variability in these surface temperatures was likely due to differences in positioning of the thermocouples during testing. Higher average temperatures were observed when the light array bulbs were shining directly on a sensor. The average temperature at the inboard surface of the pine siding ranged between 30.2 and 41.9°C. The minimum average temperature at this location occurred during the test with a 19 mm clear airspace and the maximum temperature occurred during the base test when no venting was provided. The average temperatures at the back of the test apparatus ranged from 20.5 to 25.1°C throughout the R22 Series. The variations in the average temperatures between tests led to variations in the air vapour pressures and the stack pressure difference that drives ventilation airflow.

Air vapour pressures were calculated at the interior surface of the pine (at the insulation interface or within the clear airspace depending on the venting configuration) using the temperature and relative humidity data. Air vapour pressures were also calculated at the back of the testing apparatus. The relative humidity was assumed to be 100% since the pine was always moist and condensation was always present at the back of the apparatus cavity at the end of each test. Figure 2.3.1 plots the average vapour pressure difference for each test in the R22 Series. Average vapour pressure differences between the inboard face of the pine and the back of the apparatus cavity ranged from between 1880 to 5070 Pa throughout the test series, indicating that there was always a vapour pressure drive into the wall.

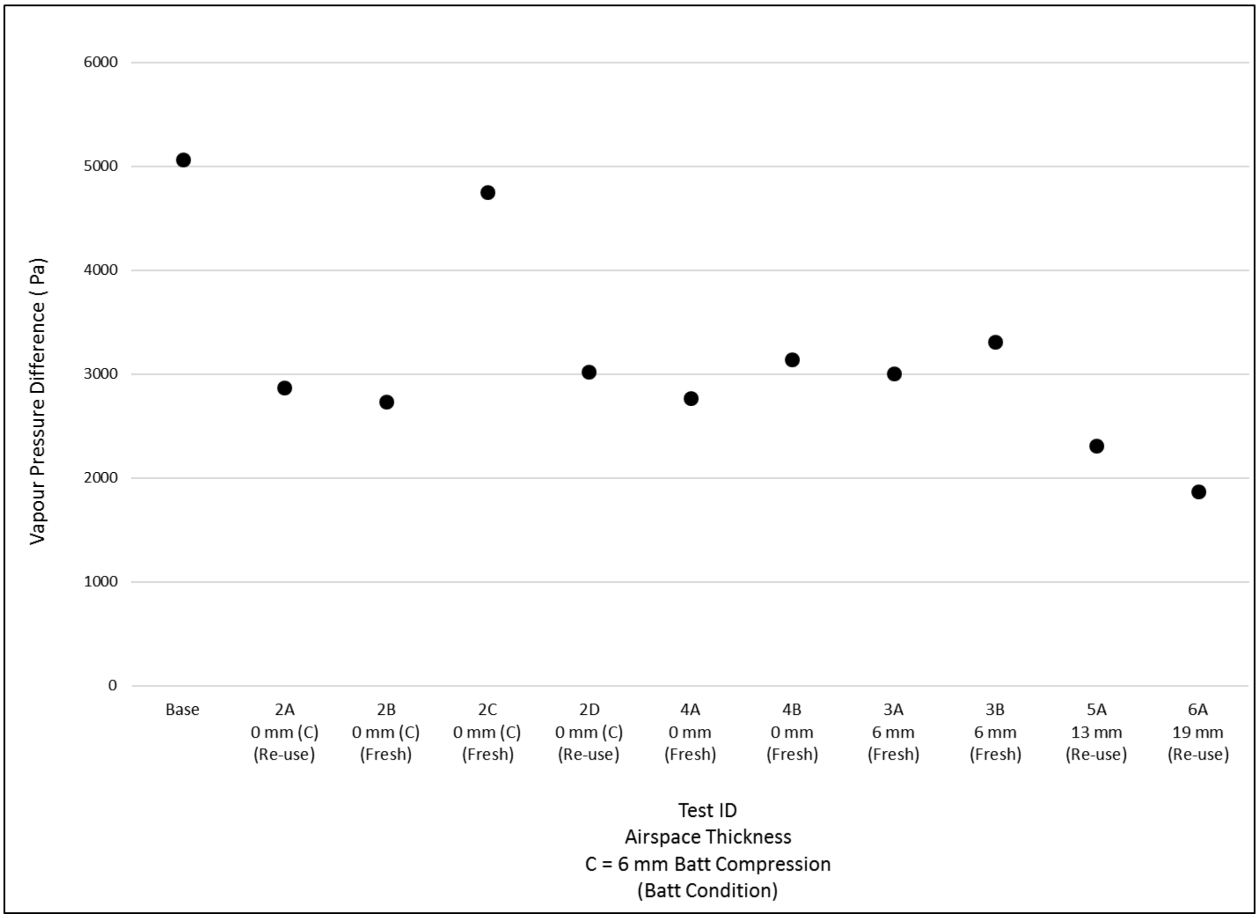

Figure 2.3.1: R22 Testing – Average Vapour Pressure Difference

The vapour pressure drive causes moisture evaporating from the interior pine surface to diffuse into the apparatus cavity toward the back of the test apparatus. Condensation at the back of the apparatus cavity indicated that moisture was driven into / through the mineral fibre insulation in all tests. The quantity of moisture lost from the pine siding during the R22 Series ranged from 215 g to 290 g.

Due to calculated differences in the density between the air in the guard room and in the apparatus cavity, a stack pressure difference between the top and bottom vent holes of the ventilated airspace developed. Density differences in the air at the top and bottom of the test apparatus are caused by temperature differences between tests, given the assumed relative humidity. Air moves due to the difference in pressure that results. Wind pressure is neglected in laboratory conditions. Therefore, air movement is a function of thermal buoyancy and moisture buoyancy. The stack pressures ranged from between 1.76 Pa and 2.43 Pa throughout the testing of the R22 Series.

The range of moisture removed by ventilation as a percentage of moisture supplied for the tests in the R22 Series are plotted in Figure 2.3.2. The assemblies included a variety of venting configurations that included no clear airspace with mineral fibre insulation and a clear airspace of varying thicknesses in combination with the mineral fibre insulation. The normalized moisture removal rate is plotted in Figure 2.3.3.

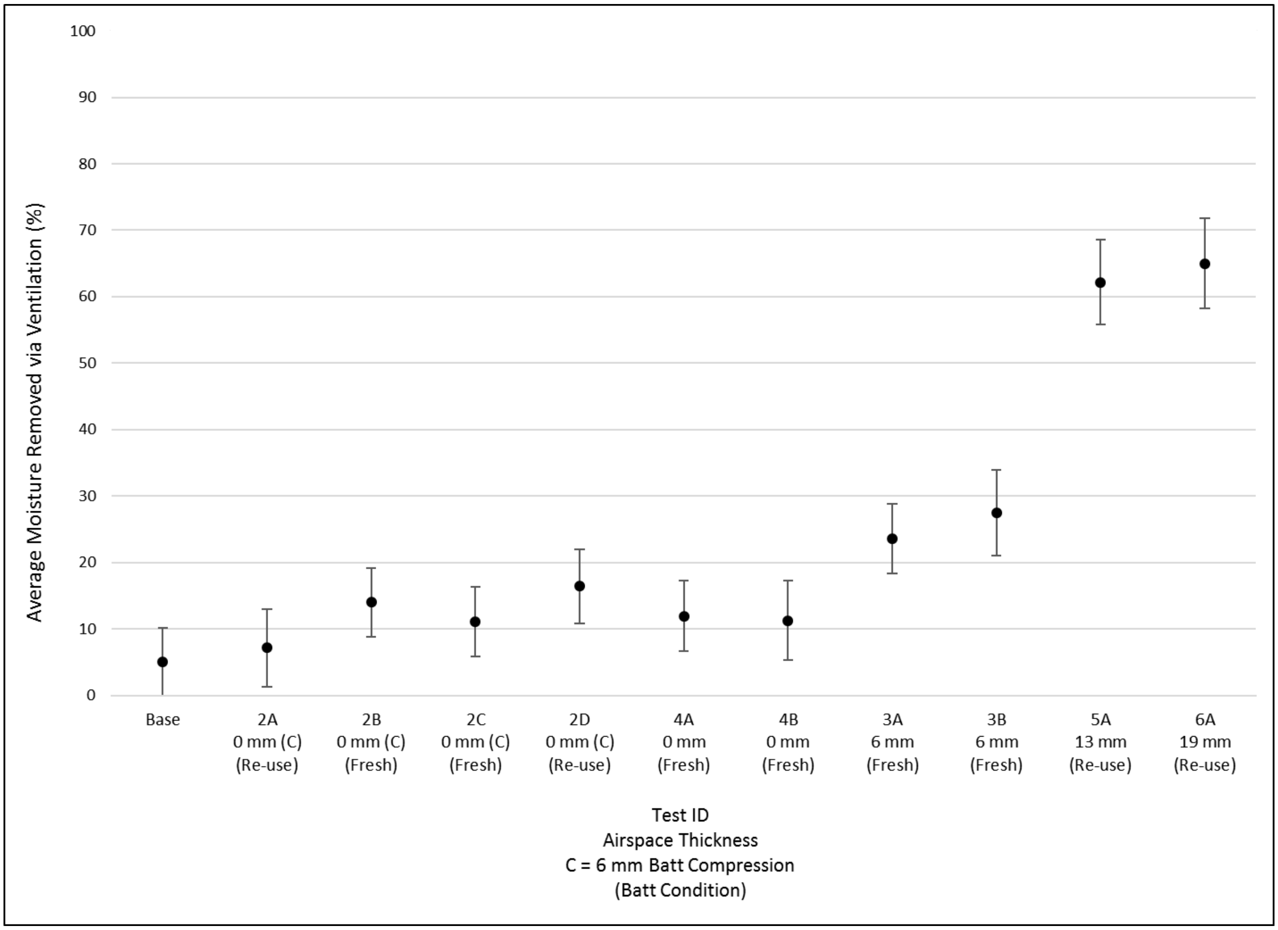

Figure 2.3.2: R22 Testing – Average Percentage of Moisture Removed for Various Air Space Thicknesses

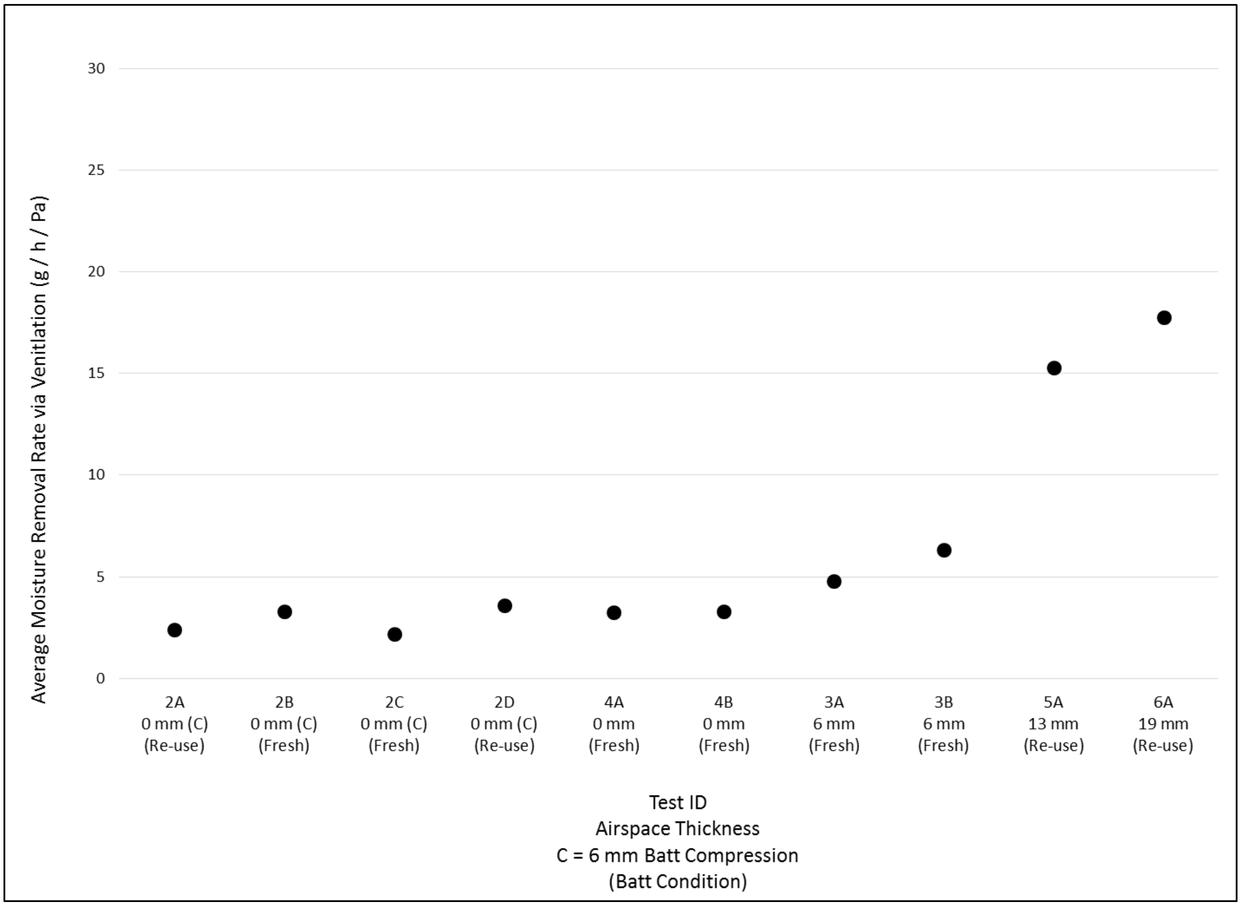

Figure 2.3.3: R22 Testing – Average Normalized Rate of Moisture Removal

Test Set 2 featured four tests with the venting configuration of 0 mm airspace combined with R22 mineral fibre insulation that was compressed by 6 mm. Ventilation removed between 1-22% of the total moisture lost from the pine boards. The rate of moisture removed ranged from 2.2-3.6 g/h/Pa.

Test Set 4 also featured no clear airspace in the venting configuration, but in these tests the batts were not compressed by 6 mm. Care was taken to ensure that there was contact between the pine boards and the insulation in lieu of the insulation being compressed. In the two tests of Test Set 4, the moisture removed by ventilation was between 11-12% of the total moisture supplied. The rate of moisture removed 3.3 g/h/Pa in both tests.

Compressing the batt in Test Set 2 served the purpose of ensuring intimate contact between the pine siding boards and the mineral fibre insulation. This would slightly increase the density of the batt locally at the interface with the pine boards. It was expected that the amount of moisture removed would be slightly lower than the tests in Test Set 4 when the mineral fibre batts were not compressed. The results between the tests of Test Set 2 were more variable than those of Test Set 4, and more moisture was removed in two of the tests in Test Set 2 then in both of the tests in Test Set 4. The effect of compressing the batt locally is uncertain. Test Set 2 also featured two tests in which the batts were in the re-used condition. The effect of re-using a batt is uncertain because one test was at the low end of the range of moisture removed from Test Set 2 while the other test incorporating a re-used batt was at the upper end of the range. If only tests using fresh batts are considered, the results of Test Set 2 are more similar to Test Set 4. This suggests that compressing the batts by 6 mm does not have an appreciable impact on the quantity of moisture removed by ventilation if only fresh batts are considered. The properties of the re-used batts were likely affected by settling during the first test in which they were used, by handling between the tests, and by drying and re-wetting of the batts.

In both Test Set 2 and Test Set 4, moisture was removed by ventilation. Although no clear airspace was provided in the venting configuration. Convective air flow due to the stack pressure difference must have occurred, removing the moisture from the test apparatus by ventilation. The results of these test sets suggest that moisture can be removed by providing ventilation airflow through the air permeable mineral fibre insulation.

Test Sets 3, 5 and 6 introduced a clear airspace to act in conjunction with the mineral fibre insulation in the venting configuration. A consistent thickness of the airspace throughout the cavity profile was achieved by adding shims around the outside of the test apparatus as described in

Section 2.2.1. The airspace is located between the pine siding boards and the mineral fibre batts. Airspaces of 6 mm, 13 mm and 19 mm were tested.

Test Set 3 contained two tests, and featured a 6 mm airspace using fresh batts. The moisture removed by ventilation was between 18-34% of the total moisture supplied. The normalized rate of moisture removed ranged from 4.8-6.3 g/h/Pa. Adding a clear airspace of 6 mm increased the amount of moisture removed by venting as compared to when no clear airspace is provided in the venting configuration. This trend continues when air spaces of 13 mm and 19 mm were tested in Tests 5 and 6. The difference in the moisture removed by ventilation is much larger between the 6 mm airspace and the 13 mm airspace as compared to the difference between the 13 mm airspace and the 19 mm airspace, although the increase in airspace thickness is equivalent. This suggests that the airflow in the 6 mm airspace is more restricted by friction with the boundaries of the clear airspace (the pine surface and the batt) than when a 13 mm airspace is provided. When a 6 mm airspace or lower is provided, the thickness of the airspace itself may become the limiting factor to airflow as compared to the relative size of the vent holes.

The mean percentage range of moisture removed by ventilation of total moisture supplied for each test set is plotted in Figure 2.3.4. The mean normalized moisture removal rate, averaged for each airspace thickness, is plotted in Figure 2.3.5.

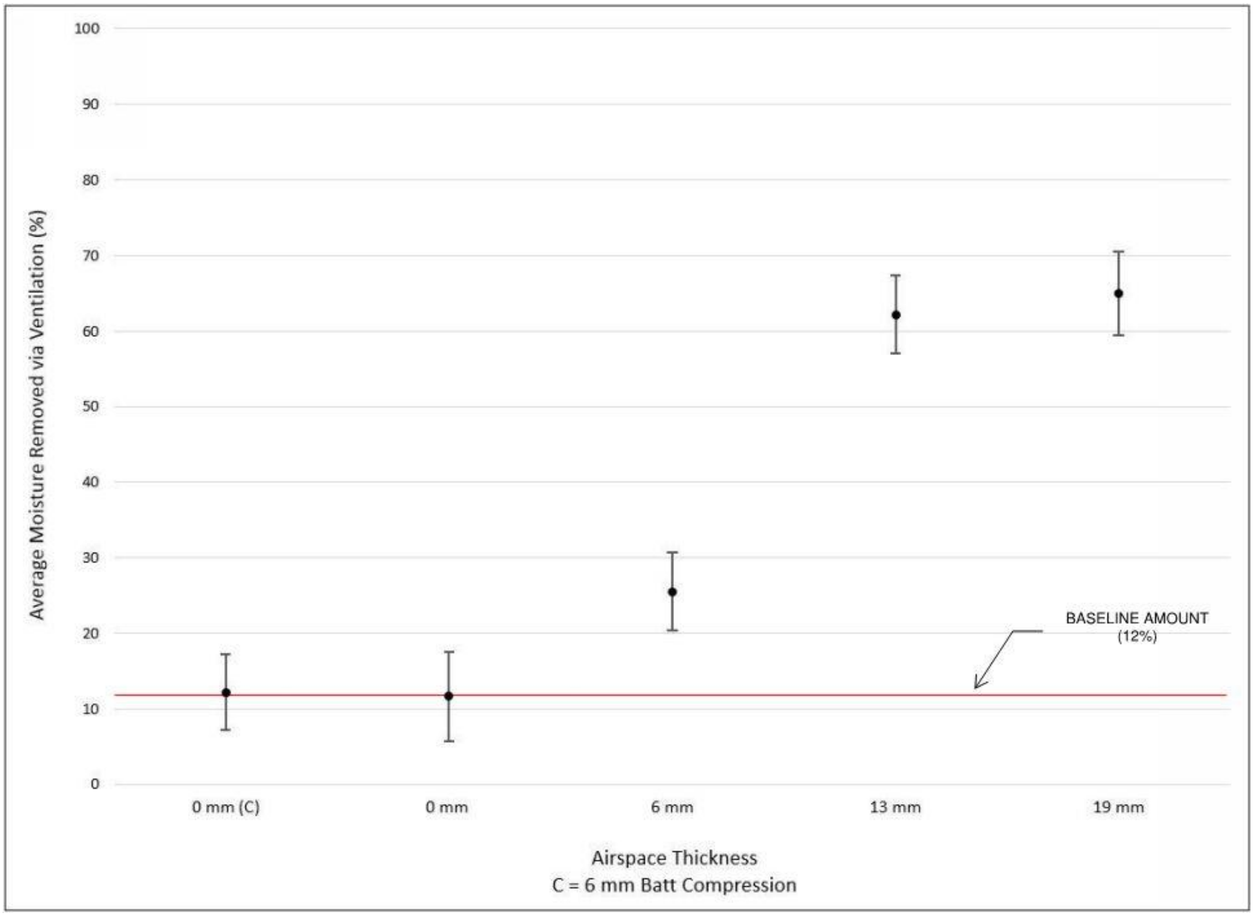

Figure 2.3.4: R22 Testing – Mean Percentage of Moisture Removal by Ventilation for Various Airspace Thicknesses

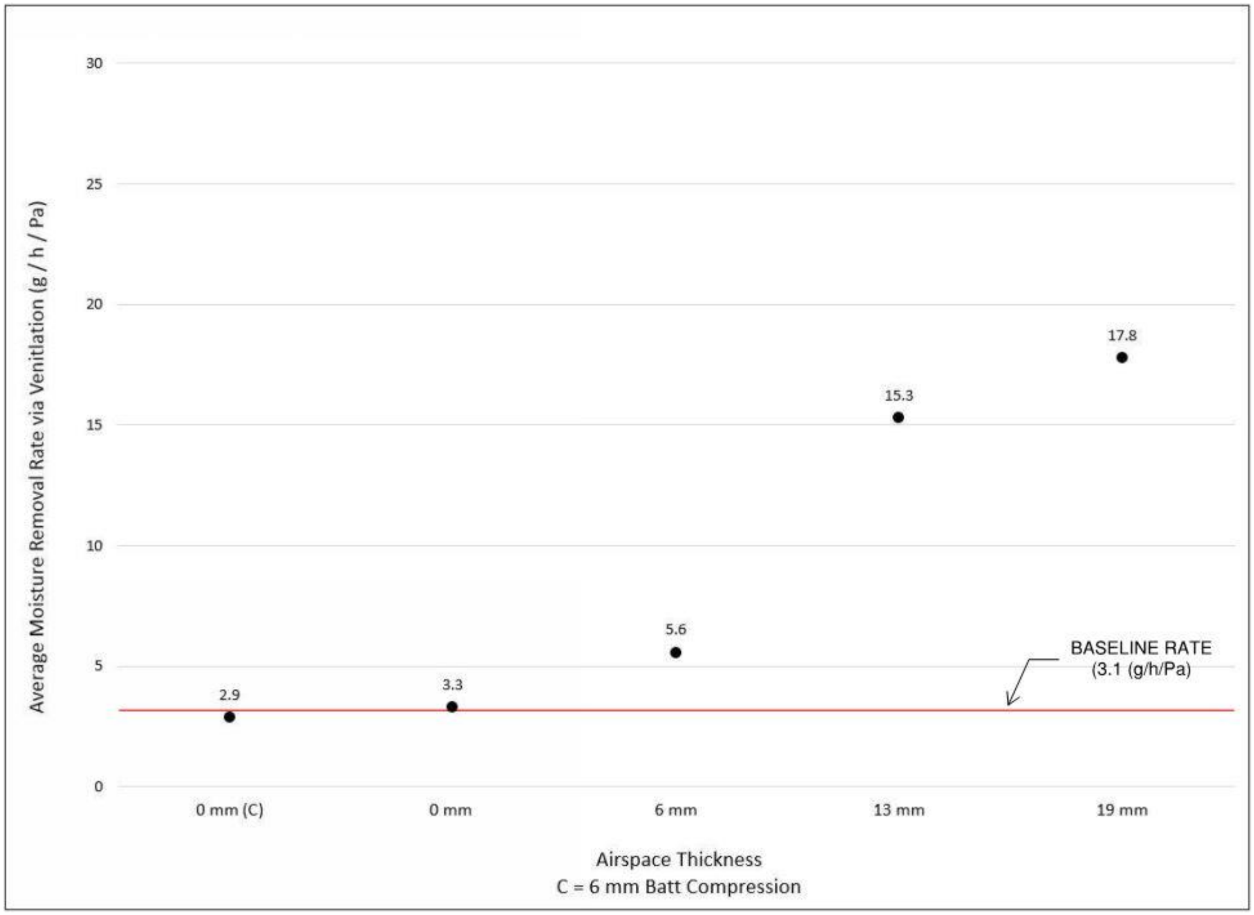

Figure 2.3.5: Average Normalized Moisture Removal Rate – Mean of Set at Airspace Thickness

The mean moisture removed by ventilation of the 0 mm with compression tests and the 0 mm tests were both 12% of the total moisture removed from the assembly. The amount of moisture removed in the combination of the 0 mm compression and 0 mm tests can be taken as the baseline for the moisture that is vented through the mineral fibre insulation during testing. Thus, the baseline moisture removal by ventilation as a percentage of moisture supplied is 12 percent. The 6 mm tests averaged 26 percent moisture removal. If the baseline ventilation of 12 percent is assumed to occur in the mineral fibre insulation of the venting configuration during the 6 mm tests, then the difference, 14 percent, is assumed to be vented through the clear airspace. The venting in the clear airspace is comparable to the baseline mineral fibre venting (14 percent vs. 12 percent). This finding suggests that the amount of ventilation drying that is occurring through mineral fibre insulation is roughly equivalent to the amount of ventilation drying that occurs through a 6 mm clear airspace.

The same analysis can be applied for the normalized moisture removal rate. When normalized stack pressure, the average rate of moisture removed was 2.9 g/h/Pa for the 0 mm with compression tests and 3.3 g/h/Pa for the 0mm with no compression tests. The mean normalized rate of moisture removed was 5.6 g/h/Pa for the 6 mm tests, double that of the tests when no clear airspace was provided. This suggests that the mineral fibre insulation is approximately equivalent to a 6 mm clear airspace in terms of venting potential.

Comparing the baseline set with the tests with no clear airspace in both measures to the tests with a 13 mm airspace and a 19 mm airspace, further suggests that the 6 mm airspace is more restricted by the boundaries. The increase in moisture percentage removed and normalized moisture removal rate is much more pronounced when moving between 6 mm and 13 mm than it is when moving from 13 mm to 19 mm. If it is assumed that the batt is more restrictive to airflow than the clear airspace, it raises the possibility that when an airspace of sufficient width is provided, the proportion of the air that flows through the batt is reduced. The clear airspace becomes less restrictive to airflow as its thickness increases.

Physical evidence of this reduced flow through the batt when a larger airspace is incorporated, can be found in observing condensed moisture within the batt. The proportions of moisture that were found in the test apparatus as condensation on different apparatus elements for each test was analyzed (See Appendix B). In Test Sets 1 to 4, approximately half of the moisture that was recovered from the test assembly was in the mineral fibre insulation batts (44-56%). Figure 2.3.6 shows the proportions of moisture of the total moisture recovered, that were found at different apparatus elements for Test 2A. This proportion dropped to 26% and 25% for Tests 5 and 6 respectively, when large clear airspaces were incorporated, further suggesting that when a large enough clear airspace is provided, a larger proportion of the moisture is removed from the system by ventilation before it is driven into the batts through vapour diffusion.

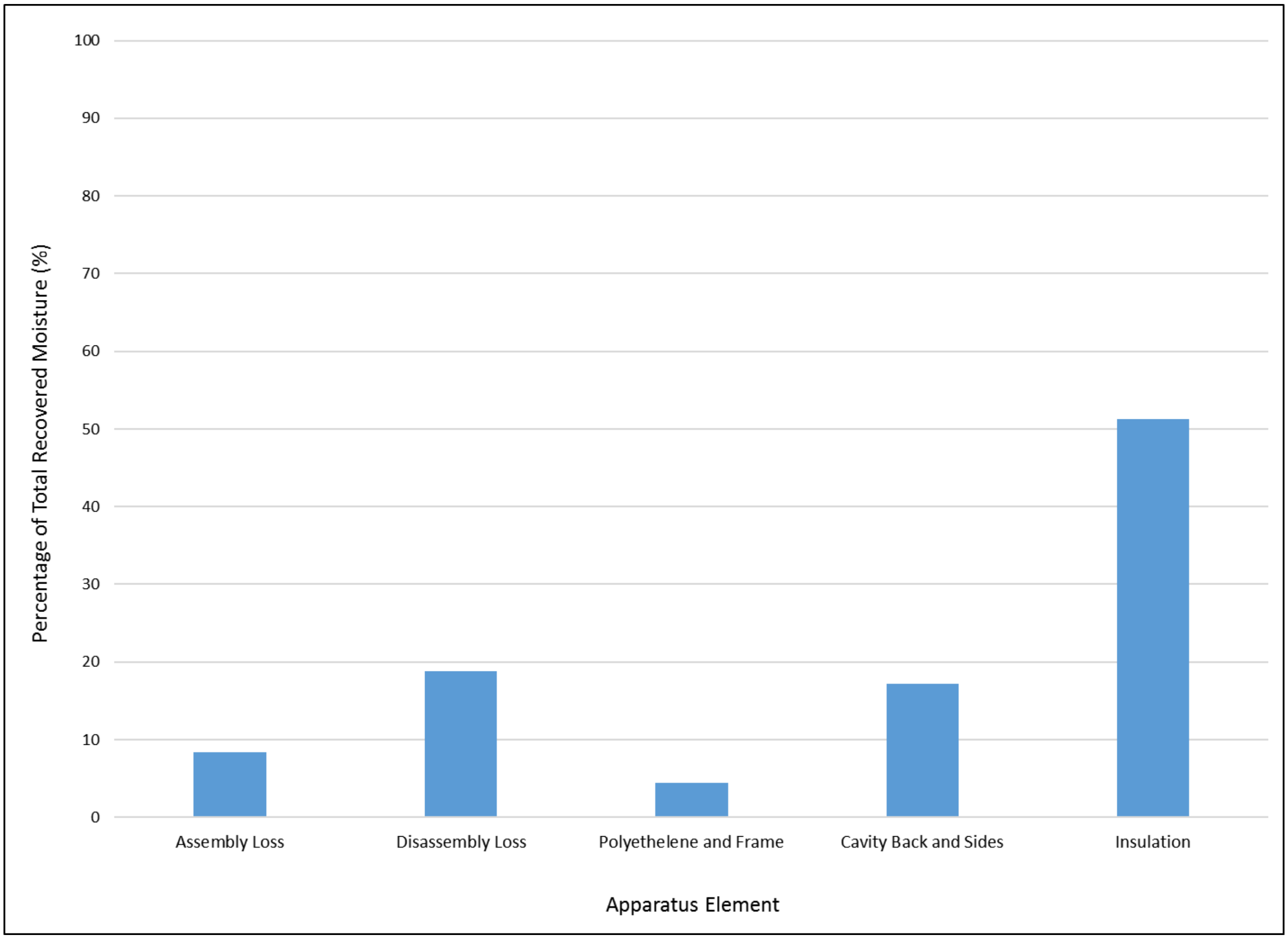

Figure 2.3.6: Recovered Moisture Distribution for Test 2A

Consistently throughout testing, a larger proportion of moisture was gained by batts near the top of the test apparatus than near the bottom. The effect was more pronounced when a clear airspace was provided in the venting configuration. Figure 2.3.7 shows the percentage of moisture found within the topmost and bottommost batts for each test.

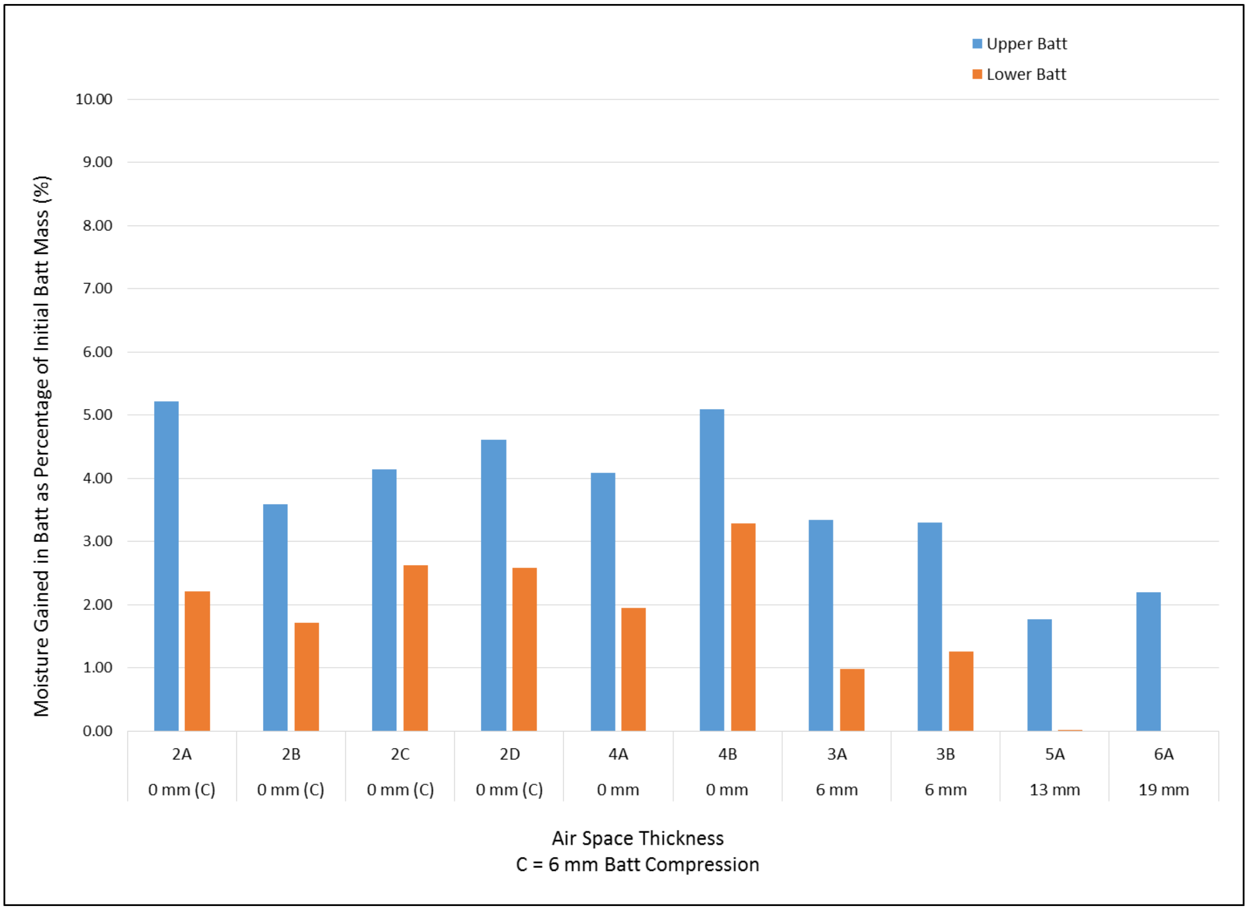

Figure 2.3.7: Moisture Gained in Batt as a Percentage of Initial Mass of Batt

Air carrying moisture flowed up through the batt due to the stack effect. At a certain point, the vapour pressure of the air within the batt being carried up through the batts would reach the saturation vapour pressure and the moisture would condense within the batt at that point. The top of the test apparatus was consistently warmer than the bottom due to warm air rising because of stack action. This suggests that the vapour pressure gradients would be from top to bottom vertically, and from the pine boards toward the back of the cavity, laterally. As moisture-laden air flowed vertically in the apparatus, in the opposite direction to the vapour pressure gradient, water vapour was transported upward within the moving air because of convective flow due to the stack pressure difference.

2.3.3 R24 TEST SERIES

R24 (4.23 m^2K/W) insulation was used for the R24 series of tests. The main difference between the R22 Test Series and the R24 Test Series was the density of mineral fibre insulation used. The density of the R22 mineral was 37 kg/m^3 while the R24 insulation had a density of 55 kg/m^3. Additional changes to airspace configurations and larger vent area ratios are displayed in C – Compressed batt

Table 2.3.2.

In the R24 Test Series, clear airspaces of 0 mm with compression, 0 mm, 3 mm and 6 mm were tested. To explore the impact of increasing the vent area ratio on ventilation airflow, the vent area ratio was doubled for Test Sets 14 through 17. Two vent holes were spaced along the width of the apparatus, at the top and bottom, such that each hole accounted for half the tributary area of the apparatus cavity. Tests Sets 10 and 12 incorporated a sheet of spun bonded polyolefin (SBPO) between the clear airspace and the mineral fibre insulation. The intention of these tests was to isolate airflow to the clear airspace because the SBPO acts as an air barrier. Any moisture driven into the mineral batts could not be removed due to ventilation airflow. C – Compressed batt

Table 2.3.2 provides a summary of the testing performed in the R24 Series.

Test Set	Test	Insulation Type	Clear Airspace Thickness	Vent Area Ratio (mm^2 / m^2)	Moisture Lost from Wood Siding (g)	Vapour Pressure Difference (Pa)	Stack Pressure Difference (Pa)
8	8A	R-24	6mm	1175	241	1040	1.84
	8B	R-24	6mm	1175	282	1490	1.82
	8C	R-24	6mm	1175	292	1870	2.09
9	9A	R-24	None	1175	219	3180	1.94
	9B	R-24	None	1175	215	3270	1.81
	9C	R-24	None	1175	243	4090	2.44
10	10A	R-24	10mm SBPO	1175	296	1760	1.64
11	11A	R-24	0mm (C)	1175	232	2640	1.82
	11B	R-24	0mm (C)	1175	252	3340	2.07
	11C	R-24	0mm (C)	1175	238	3300	2.00
12	12A	R-24	6mm SBPO	1175	288	1790	1.56
13	13A	R-24	3mm	1175	288	2809	2.05
	13B	R-24	3mm	1175	281	1940	1.63
	13C	R-24	3mm	1175	261	3370	2.30
	13D	R-24	3mm	1175	276	1870	1.78
14	14A	R-24	0mm (C)	2350	237	3780	2.07
15	15A	R-24	0mm	2350	216	5040	2.60
16	16A	R-24	3mm	2350	290	3530	2.09
	16B	R-24	3mm	2350	262	3540	2.09
17	17A	R-24	6mm	2350	288	2050	1.90

C – Compressed batt

Table 2.3.2: R24 Series Testing Summary

The procedure for analysis described in 2.4.1 is used for the R24 series. 10% of the total moisture supplied is considered to be removed by ventilation as the upper bound. The same 10% is considered to be lost from the test apparatus through unintentional air leakage in the lower bound for moisture removal by ventilation airflow.

Average temperatures were recorded in the guard room, at the guard room side polyethylene surface covering the pine siding, at the inboard pine surface and at the back of the testing apparatus. The average temperature in the guard room throughout the R24 Series ranged from 17.8 to 18.8 °C. The average temperature at the polyethylene surface ranged from 43.7 to 50.1°C. The average temperature at the inboard siding, representing the siding and insulation interface or clear airspace temperature ranged between 29.9 and 40.4°C. The average temperatures at the back of the test apparatus ranged from 20.7 to 24.7°C. The variations in the average temperatures between tests cause variations in both the air vapour pressures and the stack pressure between tests.

Vapour pressures were calculated at the interior surface of the pine (at the insulation interface or within the clear airspace depending on the venting configuration), and at the back of the testing apparatus. In all cases, the relative humidity was assumed to be 100% since the pine was always moist and condensation was always present at the back of the testing apparatus at the end of each test. The resulting average vapour pressure differences between the two locations for each test is shown in Figure 2.3.8.

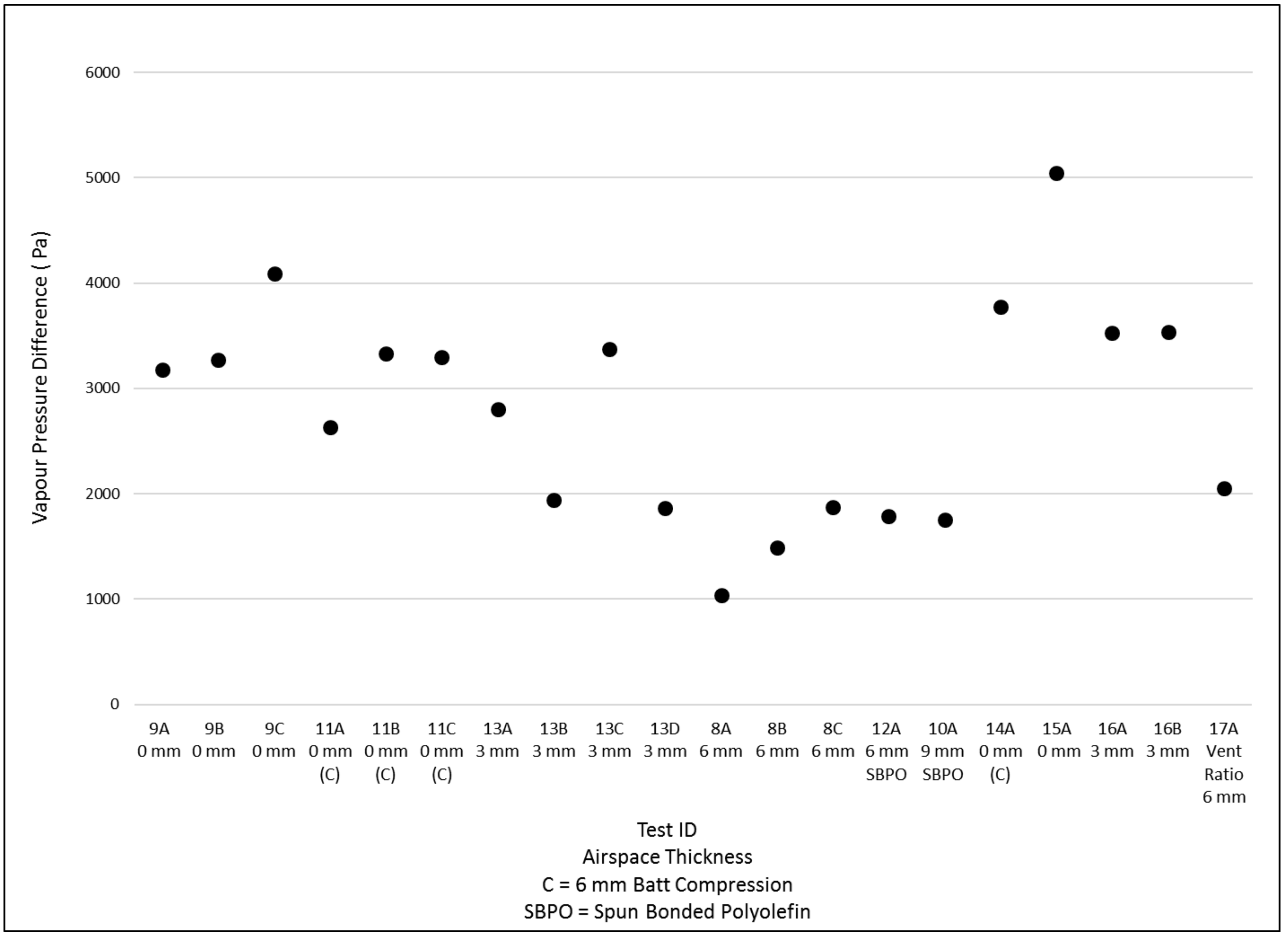

Figure 2.3.8: R24 Testing - Average Vapour Pressure Difference

Average vapour pressure differences ranged from between 1500 to 5200 Pa throughout the test series, indicating that there was always a vapour pressure drive from the pine surface into the apparatus cavity. The vapour pressure differences in Test Sets 9 and 11, when no clear air space was provided in the venting configuration, were generally higher than in the test sets when a clear airspace was provided. When a clear airspace was provided, ventilation air is able to flow directly adjacent to the pine siding. This likely led to cooling of the inboard pine surface and therefore, a smaller vapour pressure difference resulted.

The vapour pressure gradient caused evaporating moisture from the pine surface to diffuse inward toward the back of the test apparatus. Condensation at the back of the apparatus cavity indicated that moisture was driven into / through the air permeable insulation in all tests. The quantity of moisture supplied during the R24 Series ranged from 215 g to 296 g.

A stack pressure difference between the bottom vent and the top vent within the venting airspace existed. The temperature was measured with thermocouples in the guard room and relative humidity was assumed to be 20%. The temperature in vented airspace or insulation was measured with the SMT A2 sensor and the relative humidity were assumed to be 90%. The calculated stack pressure difference ranged from between 1.56 Pa and 2.44 Pa.

The percentage range of moisture removed by ventilation of the moisture supplied, for the R24 Series Test Sets 8 through 13, is plotted in Figure 2.3.9. The normalized rate of moisture removal has been plotted in Figure 2.3.10.

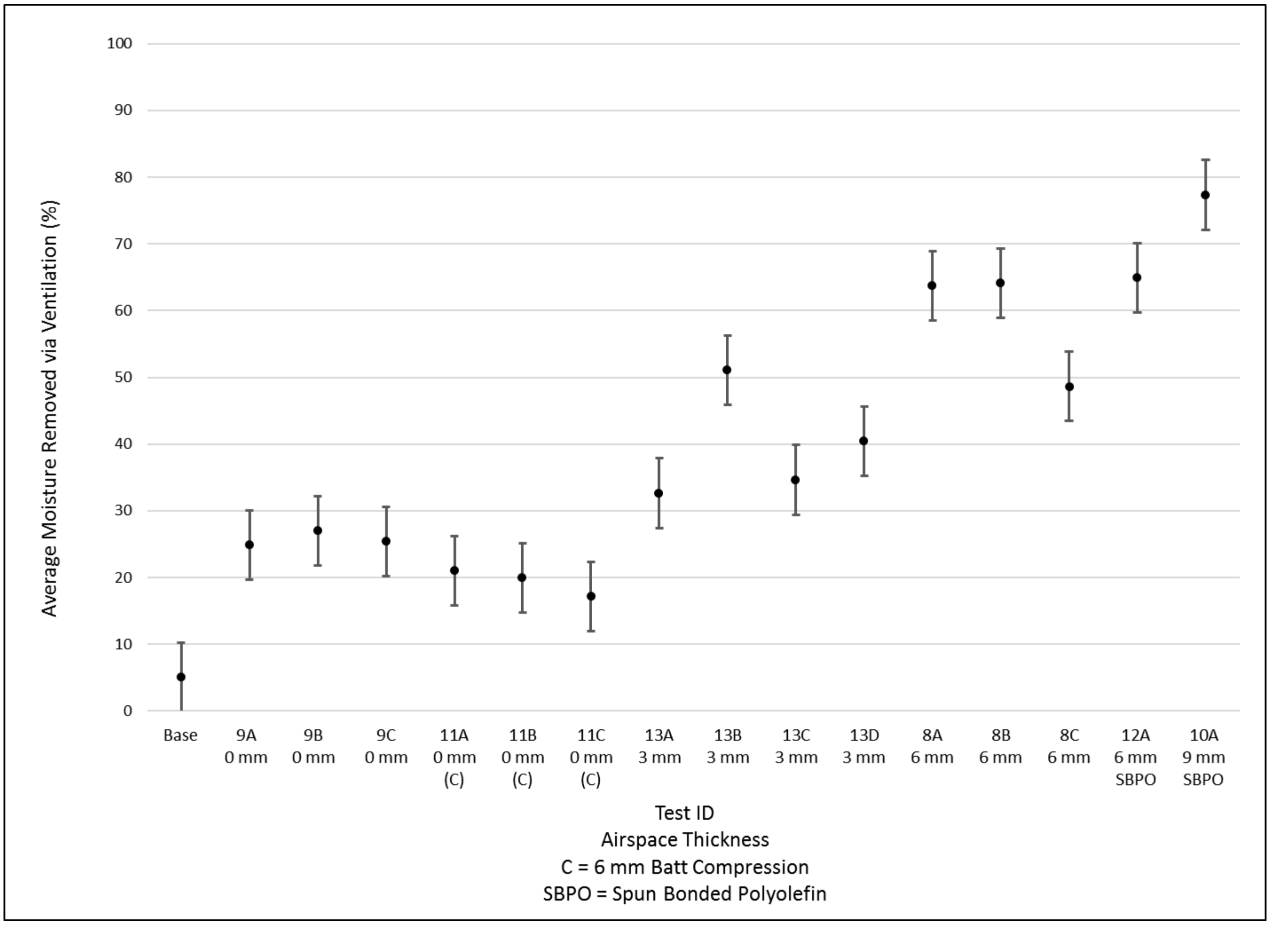

Figure 2.3.9: R24 Testing – Average Percentage of Moisture Removed for Various Air Space Thicknesses

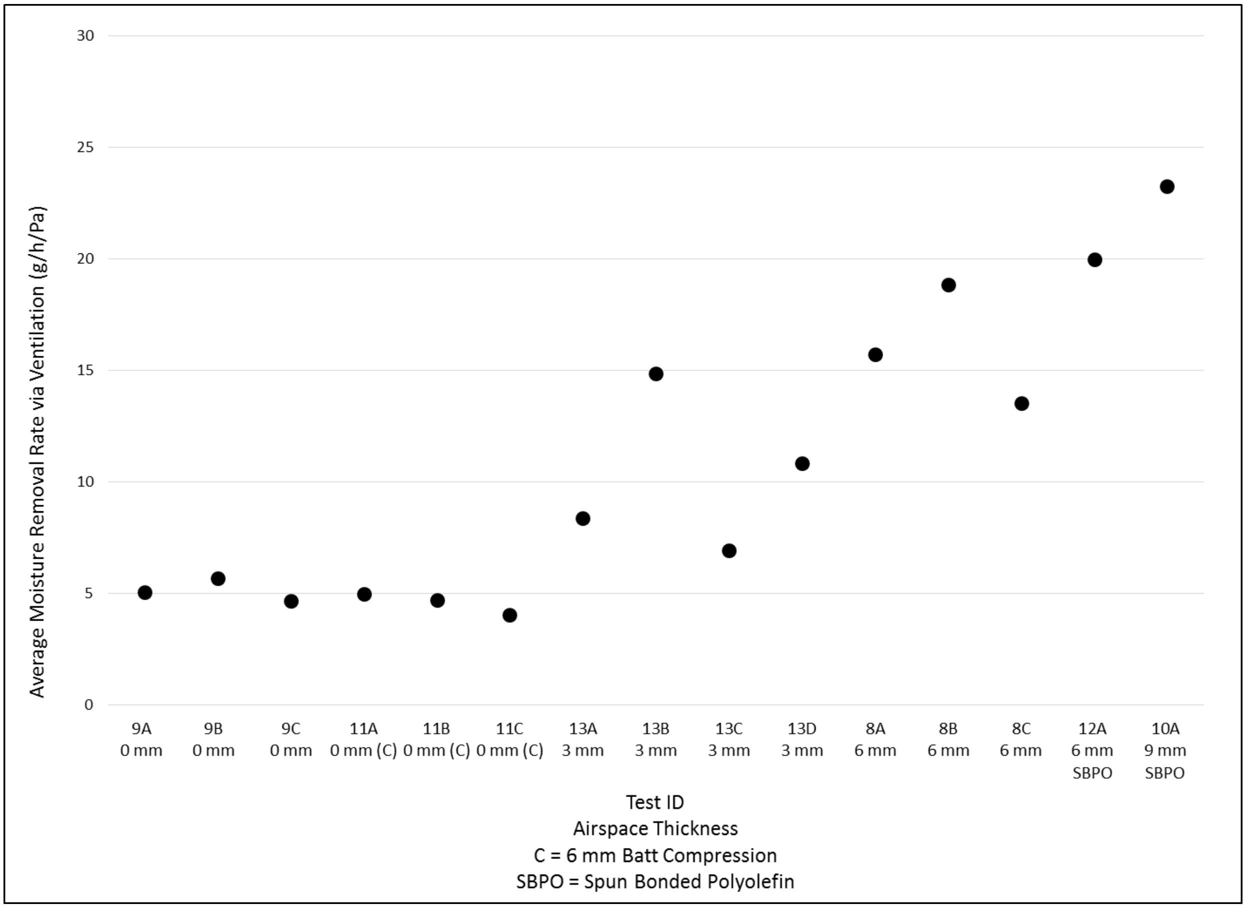

Figure 2.3.10: R24 Testing – Average Normalized Rate of Moisture Removed by Ventilation for Various Airspace Thicknesses

Test Sets 9 and 11 both featured a venting configuration that included no clear airspace between the pine siding boards and the mineral fibre insulation. The insulation batts used in Test Set 11 were installed with 6 mm of compression. The moisture removed by ventilation was between 20-32% for Test Set 9 (no compression). In Test Set 11, the percentage removed was between 12-26%. When normalized by the stack pressure, the rate of moisture removed ranged from 4.7 to 5.0 g/h/Pa in Test Set 9 and ranged from 4.0-5.0 g/h/Pa in Test Set 11. Moisture removal by ventilation as a percentage of the amount of moisture supplied is slightly lower when the mineral fibre insulation batts are compressed. Similarly, the normalized rate of moisture removal from the test apparatus was lower when the batts were compressed. The observed difference in the natural ventilation rate when the batts were compressed versus no compression may be within experimental error. However, when the batts are compressed, two effects occur. First, compression causes the local density of the batts to increase slightly, particularly at the interface with pine siding. This increase in density may lead to a slight increase in the resistance to air flow through the batts. Secondly, since the surface of the batt is not a plane surface, small interconnected void spaces likely exist between the surface of the batt insulation and the pine siding. When the batt is compressed, interconnected void spaces are less likely to occur and therefore fewer channels for airflow would exist. In both Test Set 9 and Test Set 11, moisture was removed by ventilation. In both of these test sets, no clear airspace was provided in the venting configuration. Convective air flow due to the density differences must have occurred within the mineral fibre insulation, removing the moisture from the test apparatus by ventilation. The results of these test sets suggest that moisture can be removed by providing ventilation airflow through the mineral fibre insulation.

Test Sets 8 and 13 introduced a clear airspace to act in conjunction with the mineral fibre insulation in the venting configuration. A consistent thickness of the airspace throughout the apparatus cavity profile was achieved by adding shims onto the rails and styles of the test box as described in Section 2.3. The clear airspace was located between the pine siding boards and the mineral fibre batts. Clear airspaces of 3 mm and 6 mm were tested.

Test Set 8 contains three tests, featuring a 6 mm airspace and mineral fibre batts in the venting configuration. The moisture removed by ventilation removed between 42-71% of the total moisture supplied. The normalized rate of moisture removal ranged from 13.5-18.9 g/h/Pa. Adding a clear airspace of 6 mm to the venting configuration increased the amount of moisture removed by venting as compared to when no clear airspace was provided.

Test Set 13 contains four tests, featuring a 3 mm airspace in the venting configuration. The moisture removed by ventilation was between 26-58% of the total moisture. The normalized rate of moisture removal ranged from 7.4-14.9 g/h/Pa. Adding a clear airspace of 3 mm increased the amount of moisture removed by venting as compared to when no clear airspace is provided in the venting configuration. The amount of moisture removed was less than when a 6 mm airspace was included in the venting configuration.

The mean range of moisture removed by ventilation percentage for each test set is plotted in Figure 2.3.11. The mean normalized moisture removal rate is plotted in Figure 2.3.12.

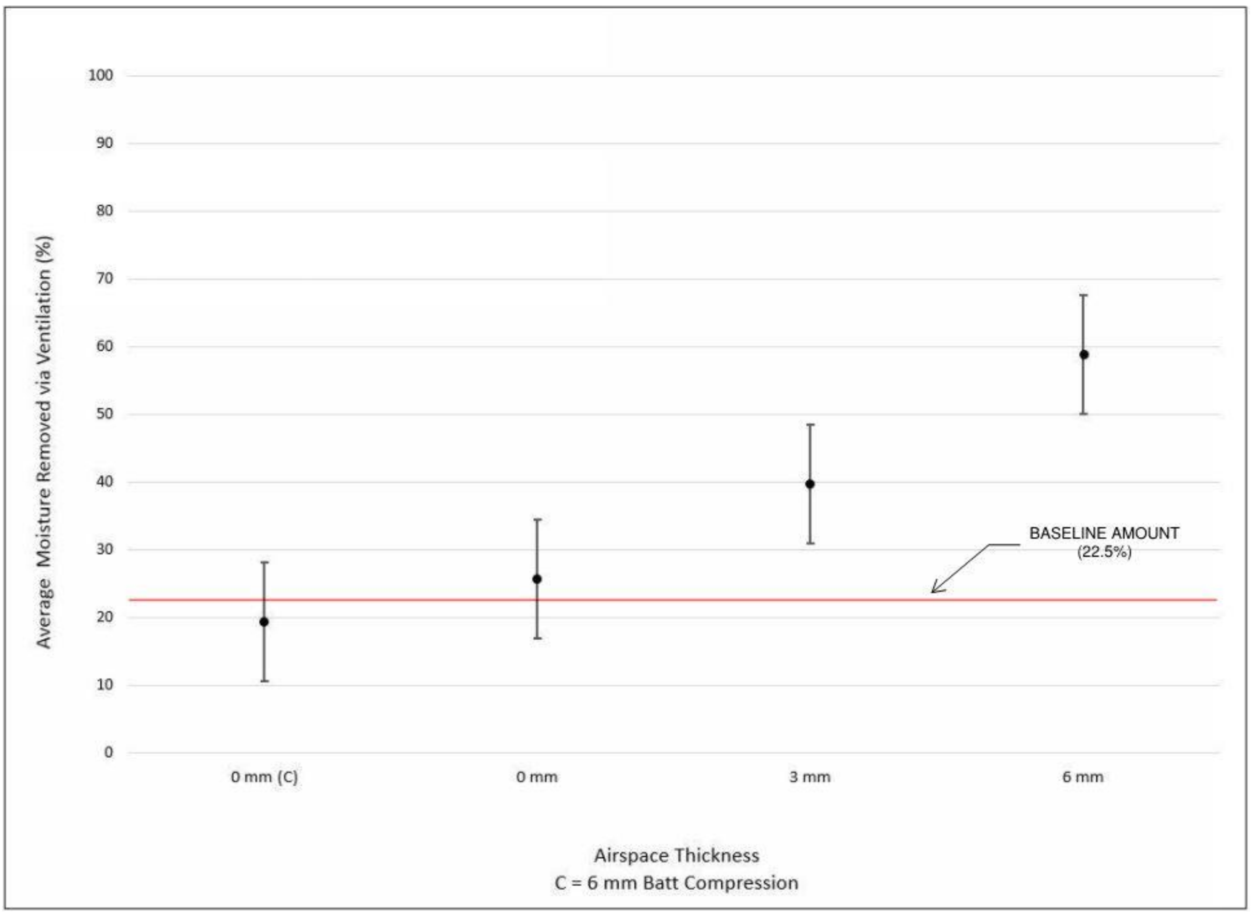

Figure 2.3.11: R24 Testing – Average Percentage of Moisture Removed by Ventilation for Various Airspace Thicknesses

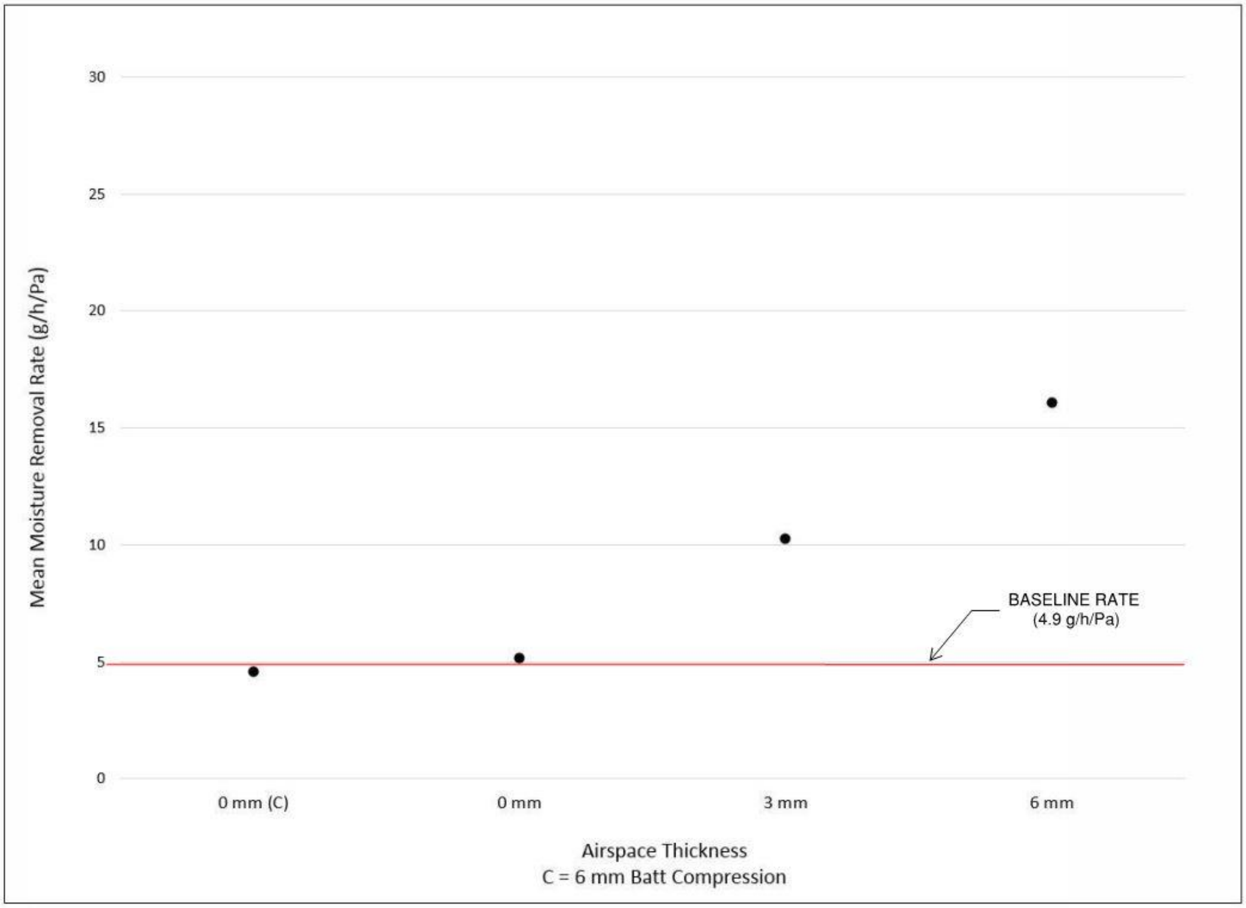

Figure 2.3.12: R24 Testing – Average Normalized Moisture Removal Rate – Mean of Set at Airspace Thickness

The mean moisture removed by ventilation of the 0 mm with compression tests, and the 0 mm tests, were 19 percent and 26 percent of the total moisture removed from the assembly, respectively. The 3 mm tests averaged 40 percent moisture removed by ventilation and the 6 mm tests averaged 59 percent moisture removed by ventilation. If we consider the amount of moisture removed in the 0 mm compression and 0 mm tests combined as the baseline for the moisture that is vented through the mineral insulation during testing, then approximately 22.5 percent of moisture can be removed through mineral fibre insulation as the baseline (average between the two sets). When the 3 mm tests are considered, 40 percent of moisture was removed by ventilation. 22.5 percent of the venting in the 3 mm tests can be assumed to occur in the mineral fibre insulation and the remainder. The remainder, 17.5 percent, is assumed to occur in the clear airspace. Comparing this difference of 17.5 percent to the 22.5 percent baseline mineral fibre venting indicates that the mineral fibre insulation is approximately equivalent to slightly more than a 3 mm clear airspace in terms of venting potential. The same analysis can be applied for the normalized moisture removal rate. When normalized by the stack pressure difference, the average rate of moisture removed was 4.6 g/h/Pa for the 0 mm with compression tests and 5.1 g/h/Pa for the 0 mm with no compression tests. The mean normalized rate of moisture removed was 10.3 g/h/Pa for the 3 mm tests. This suggests that the mineral fibre insulation is approximately equivalent to slightly less than a 3 mm clear airspace in terms of venting potential. When considering the equivalent airspace thickness of an R24 batt in a venting configuration, these results suggest that the R24 is equivalent to approximately a 3 mm clear airspace in terms of venting potential.

The amount of moisture removed by ventilation continues to increase when the 6 mm clear airspace is compared to the 3 mm clear airspace venting configuration. The relative increase in both the percentage of total moisture removed and normalized moisture removal rate between the 3 mm and 6 mm averages is comparable to the increase between 0 mm with compression / 0 mm and the 3 mm clear airspace test averages. Thus, the increase in moisture removed from the baseline set at 0 mm when no clear airspace is provided, looks linear between the no airspace venting configuration and the 6 mm airspace venting configuration.

The proportions of moisture that were found in the test apparatus at different elements for each test was analyzed and is presented in Appendix C. In test Sets 9 and 11, when no clear airspace was provided in the venting configuration, more than half of the moisture that was recovered from the test assembly was located in the batts (52-58%). Figure 2.3.13 shows the proportions of moisture of the total moisture recovered, that were found at different apparatus elements for Test 11A. This proportion decreased to 46% and 37% for Test Sets 13 (3 mm) and 8 (6 mm) respectively. This suggests that, as the thickness of the clear airspace within the venting configuration increases, a larger proportion of the moisture is removed from the system by ventilation before it is driven into the batts through vapour diffusion. As a result, less moisture ends up in contained within the mineral fibre insulation at the end of the test.

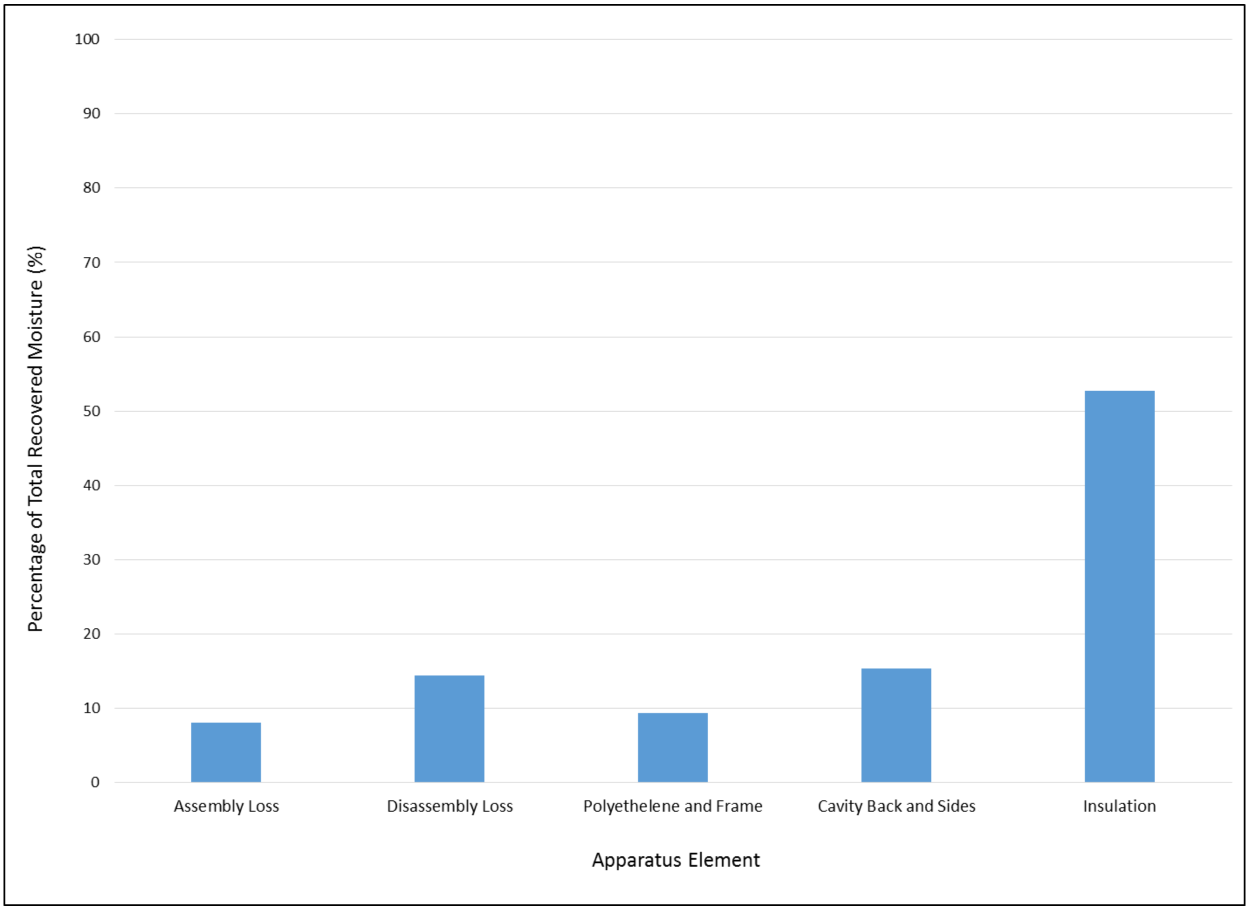

Figure 2.3.13: Recovered Moisture Distribution for Test 11A

A larger quantity of moisture was gained in mineral fibre batt pieces near the top of the test apparatus as compared to the bottom, in the R24 Series. Moisture was carried up through the mineral fibre insulation by convective airflow. At a certain point, the vapour pressure of the air within the insulation being carried up through the batts would reach the saturation vapour pressure and the moisture would condense within the insulation at that point. The top of the test apparatus was consistently warmer than the bottom due to stack action. This suggests that the vapour pressure gradient would be from top to bottom vertically. As moisture flowed in the apparatus in the opposite direction, it was likely transported as water vapour within the air as a result of air density differences. Figure 2.3.14 shows the percentage of moisture found within the uppermost and lowermost batt for each test.

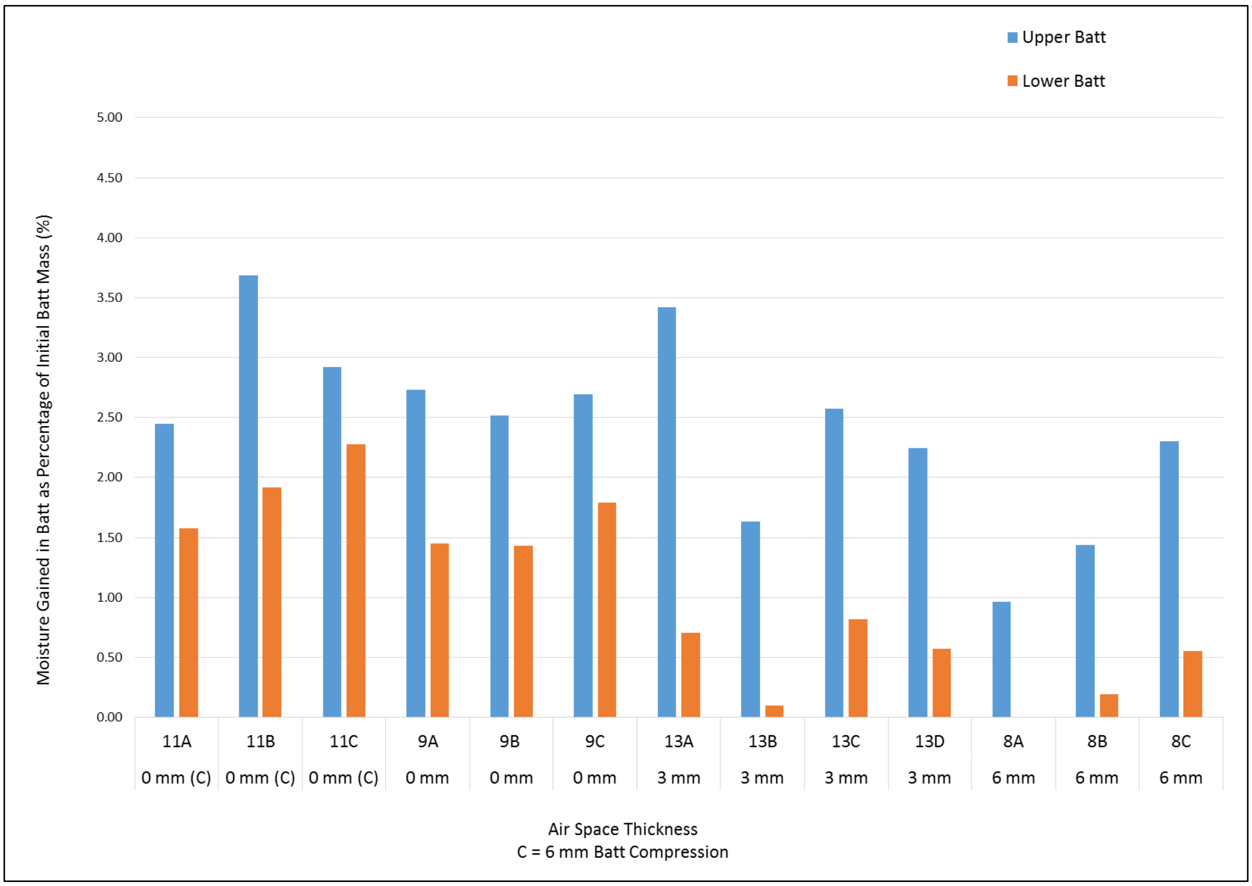

Figure 2.3.14: Moisture Gained in Batt as a Percentage of Initial Mass of Batt

Tests 10 and 12 incorporated a sheet of SBPO between the clear airspace and the mineral fibre insulation to isolate the insulation from convective airflow. A convective loop could still develop within the insulation itself, but it would be isolated from the airflow occurring through the ventilation holes in the clear airspace. SBPO has a high vapour permeance [3200 ng / Pa s m^2] [24] so moisture was expected to enter the mineral fibre insulation due to the vapour pressure gradient. In Test 10, 7 percent of the moisture recovered was located in the batts and in Test Set 12, 21% of the moisture recovered was in the batts. Test Set 12, which had a 6 mm clear airspace, can be compared to the Test Set 8, which also had a clear airspace without SBPO. A greater normalized rate of moisture removal by ventilation was displayed in Test Set 12 than the average of Test Set 8 (20.1 g/h/Pa vs. 16.0 g/h/Pa). Because the insulation batts were isolated from convective ventilation airflow, the moisture in the bulk air did not enter the air permeable insulation and condense within the batt itself. Less moisture became ‘trapped’ in the insulation resulting in more removal by the ventilation air in the clear airspace. When considering the moisture that did not end up in the batt, a greater proportion was found condensed upon the SPBO air barrier itself and also on the inside of polyethylene apparatus cover.

Previous work by Tzekova had shown that the quantity of moisture removed by ventilation increased as the vent area ratio increased [22]. The impact of the vent area ratio was examined in Test Sets 14 through 17. During these tests, the vent area ratio was doubled to 2350 mm^2/m^2 from the 1175 mm^2/m^2 used in the remainder of the R24 Series. Holes were drilled in the pine boards such that an equal tributary width of the test apparatus was allocated to each vent hole. The range of moisture removed by ventilation in Test Sets 14 through 17, as well as the mean moisture removal percentage for R24 tests at various airspace thicknesses, is plotted in Figure 2.3.15 for comparison. The normalized moisture removal rate is plotted in Figure 2.3.16.

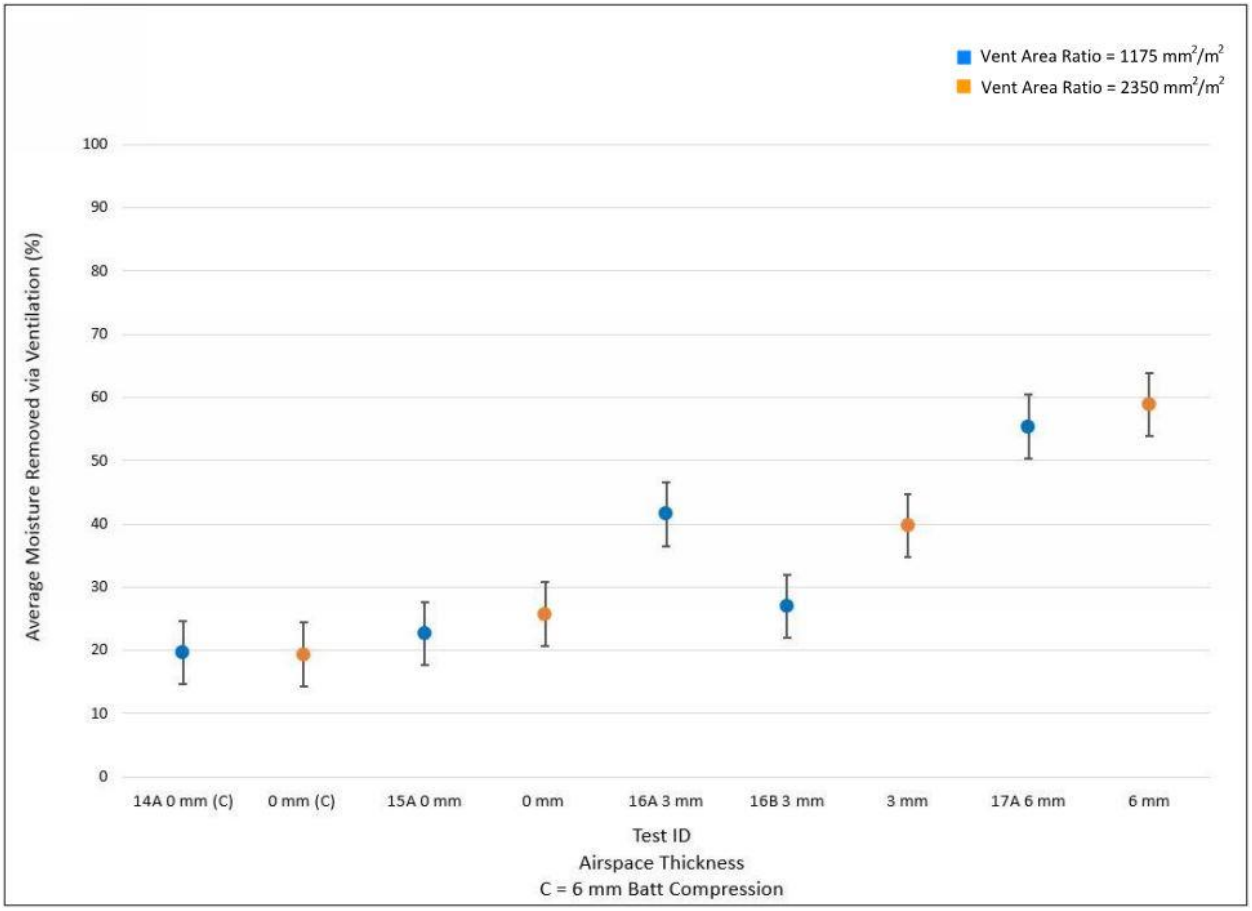

Figure 2.3.15: R24 Testing – Moisture Removal Percentage at Standard Vent Area Ratio (1175 mm^2/m^2) and Increased Vent Area Ratio (2350 mm^2/m^2)

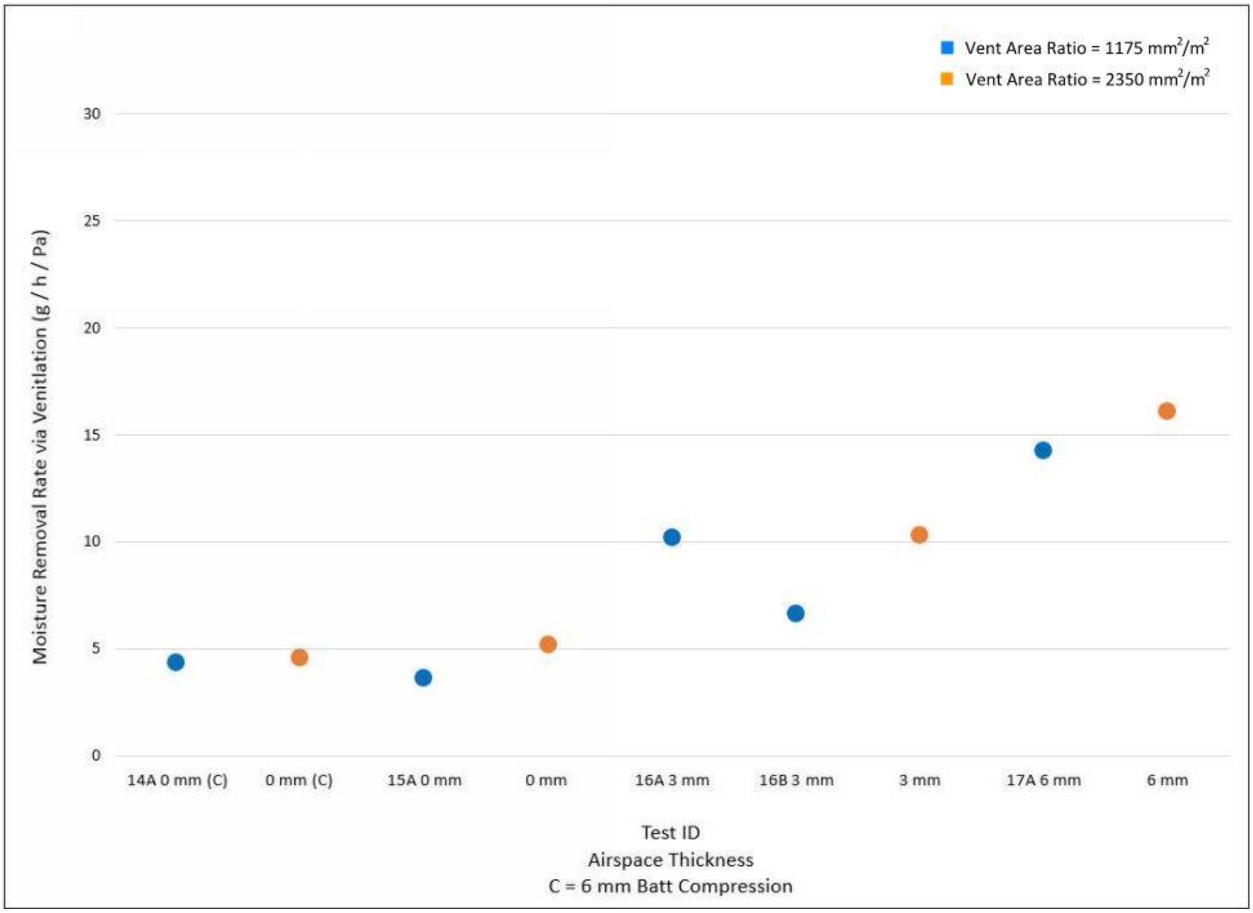

Figure 2.3.16: R24 Testing – Normalized Moisture Removal Rate at Standard Vent Area Ratio (1175 mm^2/m^2) and Increased Vent Area Ratio (2350 mm^2/m^2)

To evaluate the results of Test Sets 14 through 17 where the vent area ratio was doubled, comparisons are made with the mean results from Test Sets 8, 9, 11 and 13, where equivalent clear airspace thicknesses were used. By comparison, the results of doubling the vent area ratio had no significant effect on the amount of moisture removed by ventilation. The percentage of total moisture supplied that was removed by ventilation and the normalized moisture removal rate were both slightly below the mean of the same measures when considering equivalent airspace thicknesses. This indicates that increasing the vent area ratio is not significant given the testing conditions. This suggests that the flow in the vented cavity is limited by the airspace thickness when the airspace thickness is small (ie. 6 mm or less).

Overall, the results of the R24 Series testing suggest that airflow is occurring in the mineral fibre insulation. Moisture is removed by ventilation when no clear airspace is provided in the venting configuration. Further, the distribution of moisture within the insulation of the test apparatus upon test completion provides evidence that convective airflow is transporting moisture within the insulation. The amounts of moisture removed when no clear airspace is provided is assumed to set a baseline for venting that is able to occur through convective airflow within the insulation, both as a percentage of the total supplied and as a normalized rate based the stack pressure. When the venting baseline is compared against the tests that used clear airspaces within the vented cavity, results indicated that the equivalent airspace thickness of the R24 insulation was approximately equal to a 3 mm clear airspace in terms of venting potential.

2.3.4 VENTING INFLUENCE ON TEMPERATURE AND RELATIVE HUMIDITY

Temperature and relative humidity values were analyzed for each of the venting configurations tested. As previously discussed, temperature at the outboard face of the polyethylene apparatus cover was measured at the top, middle and bottom, and was taken to be the temperature of the outboard face of the pine siding boards. Temperature and relative humidity readings were recorded at the pine/insulation interface near the top and bottom of the apparatus. For venting configurations incorporating a clear airspace, the sensors measured the airspace conditions. Lastly, temperature at the back of the apparatus cavity was measured at the top and the bottom of the apparatus.

As discussed in Section 2.3.2, two problems were encountered with the SMT A2 sensors that recorded data at the top and bottom of the pine/insulation interface or at the clear airspace. First, the sensors delivered null values for some of the 15 minute averaging intervals, during some of the tests. Second, the relative humidity sensors were prone to failure during tests when exposed to liquid moisture and would return readings of -25% (the default error value). If a relative humidity sensor failed during a test, the SMT A2 unit would be replaced for the next test. Failures occurred approximately 20% of the time. Appendix B contains temperature and relative humidity graphs of all the R22 tests while Appendix C summarizes the R24 tests.

Figure 2.3.17 shows sample temperature measurements for Test 11A from the R24 Series at the pine surface and back of the apparatus cavity. These temperatures represent the boundary conditions for the testing apparatus. The pine surface temperatures were higher than the temperatures recorded at the back of the cavity of the test apparatus. This produced the vapour pressure gradient necessary to drive moisture from the pine siding boards into the cavity of the testing apparatus. The higher temperatures at the pine surface were achieved by the light array radiation that was located 30 cm from the polyethylene cover sheet. The pine surface temperatures were generally higher at the top of the test apparatus. This condition was consistent through the testing of both the R22 and the R24 series. The temperatures rose during the duration of the test at both the pine surface and at the back of the vented cavity. The temperature rise was generally smaller at the back of the test apparatus cavity than at the pine surface. The back of the cavity was protected from radiation of the light array by the thermal resistance of the mineral fibre insulation. The top of the back of the apparatus cavity was warmer than the bottom throughout the testing of both series, due to less dense, warmer air rising in the test apparatus cavity.

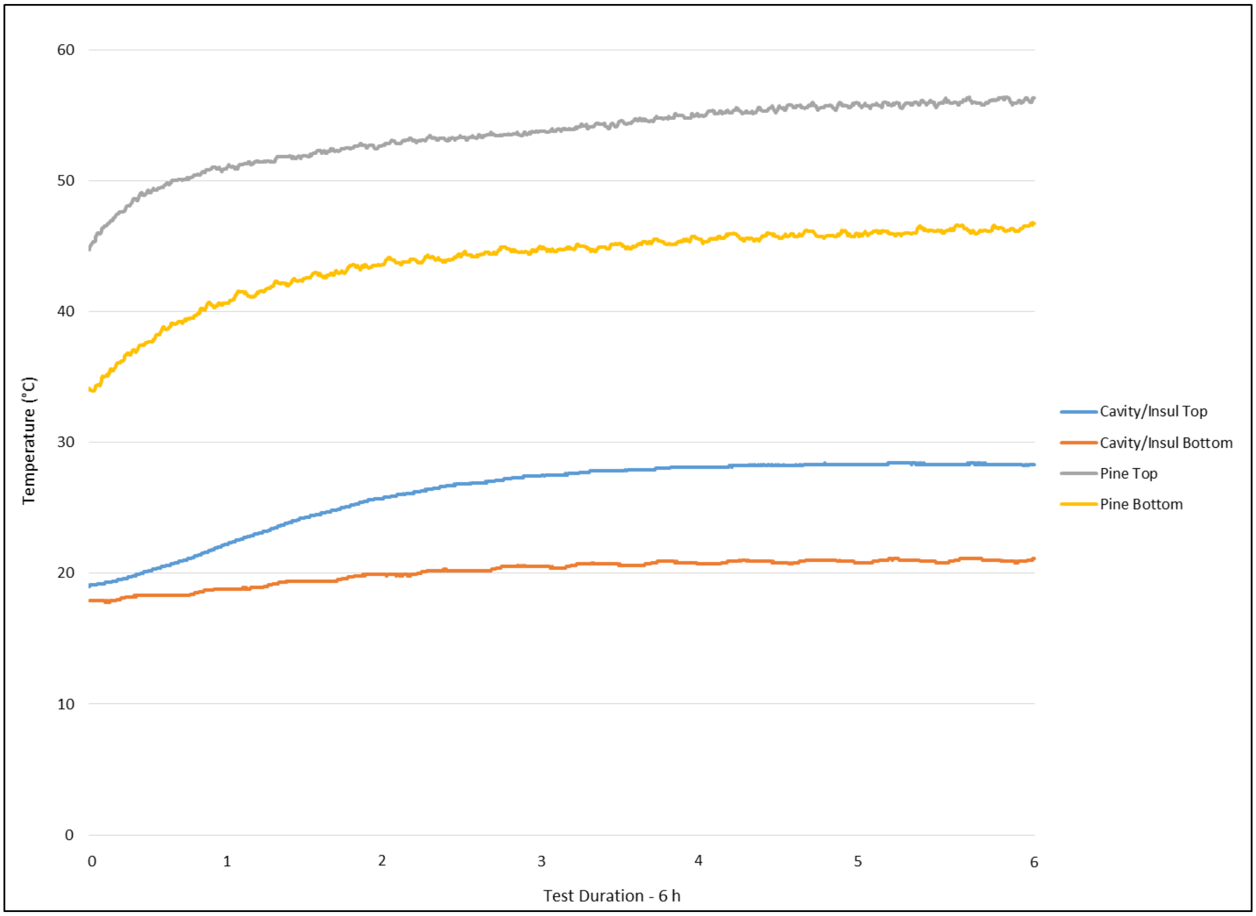

Figure 2.3.17: Sample Temperature Data for Test 11A

Figure 2.3.18 shows the temperature at the pine/insulation interface for Test 11A and at the clear airspace for Test 8C. Figure 2.3.19 shows the relative humidity at the same locations for Test 11A and Test 8C. Test 11A represents a venting configuration where no clear airspace was incorporated (0 mm with compression). Test 8C incorporated a 6 mm clear airspace.

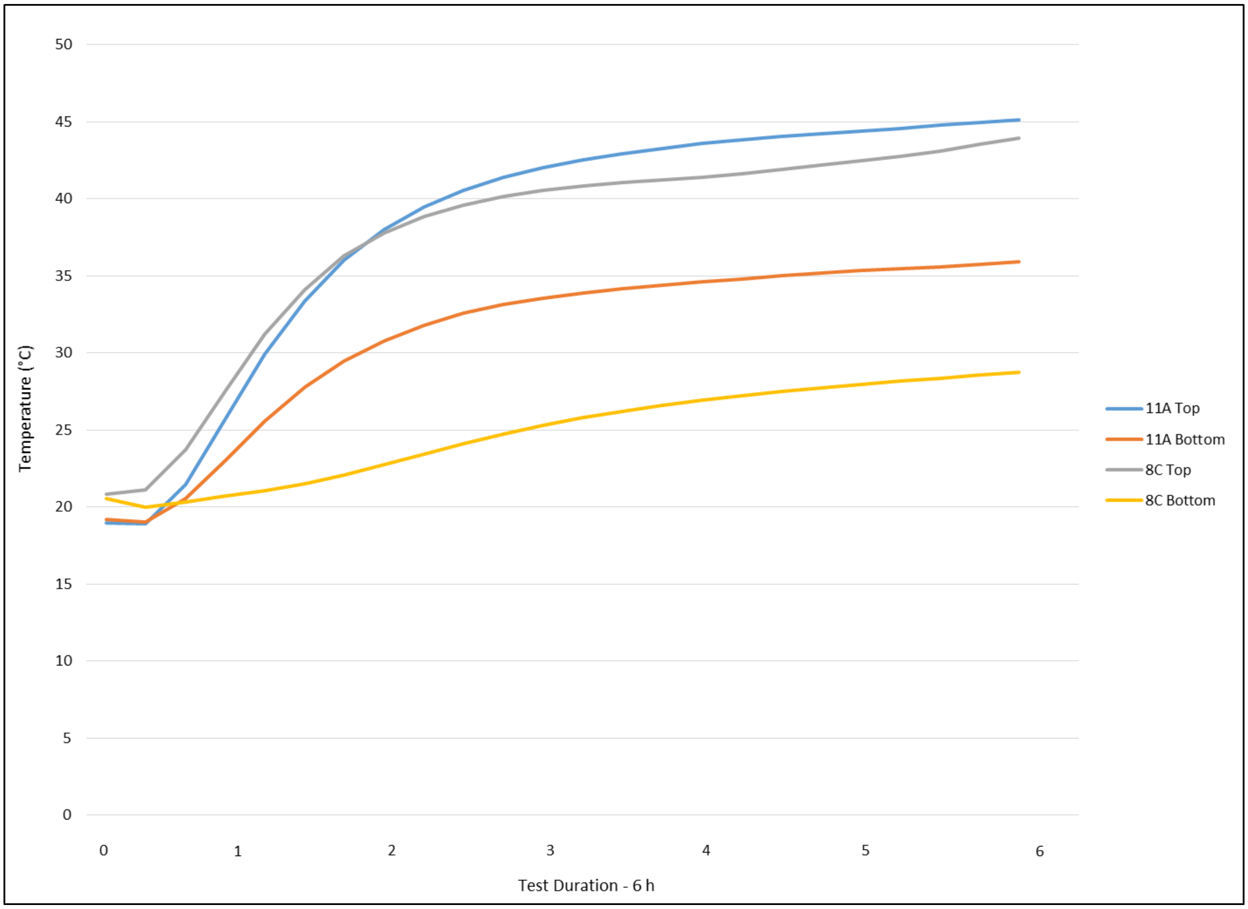

Figure 2.3.18: Temperature Data at Inboard Pine Surface for Test 11A and 8C

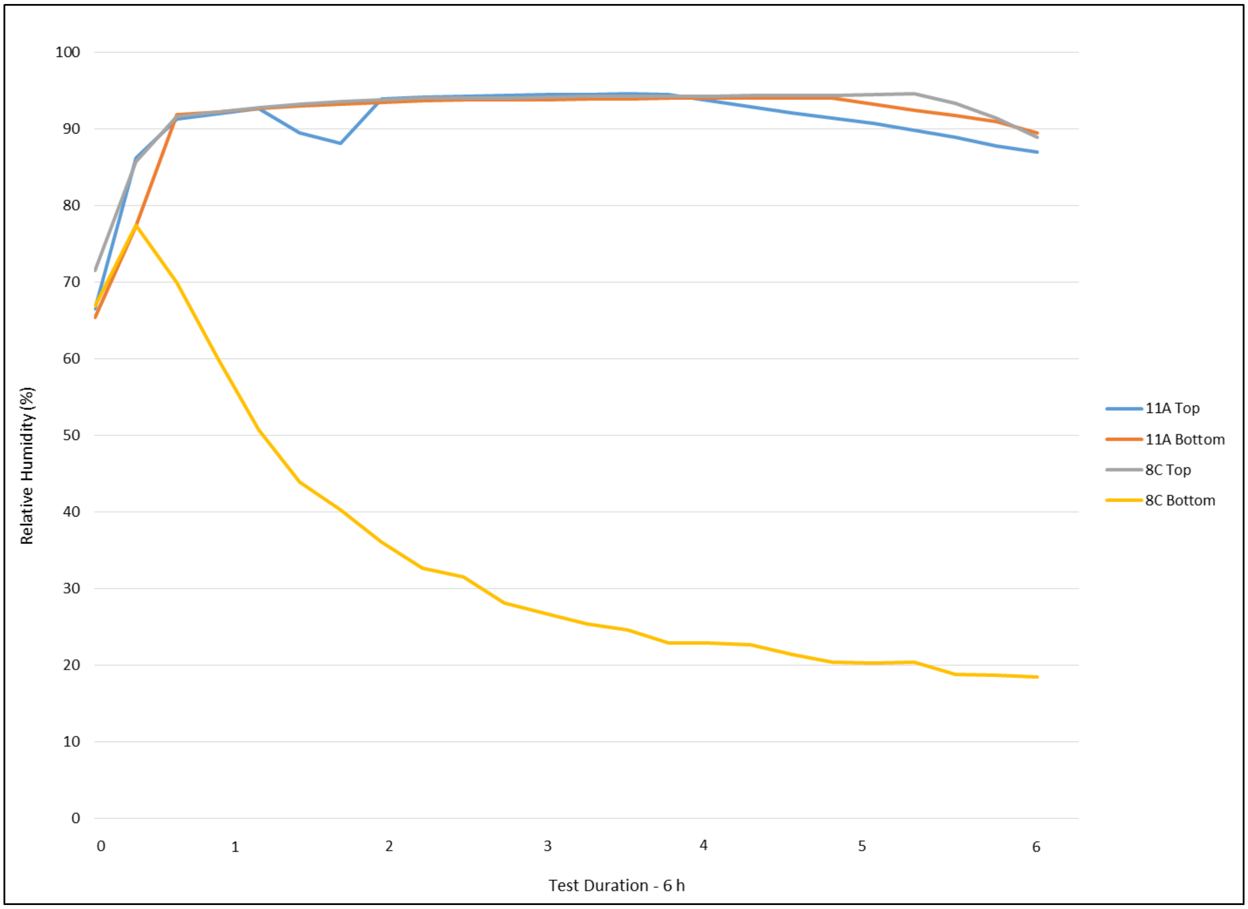

Figure 2.3.19: Relative Humidity Data at Inboard Pine Surface for Test 11A and Test 8C

Temperatures were always warmer near the top as less dense, warm air would rise in the direction of the stack pressure difference. This observation was consistent across all tests. For venting configurations with no clear airspace, this suggests that warm air was rising within the mineral fibre insulation. Thus, convective airflow was occurring within the air permeable insulation. The difference between the temperatures at the top and bottom of the apparatus cavity were more pronounced when a clear airspace was incorporated, as shown by the results of Test 8C. Convective air flow due to the stack pressure difference occurred in the apparatus cavity regardless of the clear airspace, but cooler air from the guard room was introduced to the apparatus cavity at the bottom ventilation hole at a greater flow rate when the clear airspace was present.

Relative humidity levels stayed more consistent between the top and bottom of the apparatus cavity in tests where no clear airspace was incorporated in the venting configuration. Moisture was removed during these tests, but at a much lower normalized rate than in tests with a clear airspace in the venting configuration. Absolute moisture levels within the batts stayed at a high enough level to keep the relative humidity stable.

In tests where a clear airspace was incorporated into the venting configuration, the relative humidity at the bottom of the apparatus cavity fell significantly over the duration of the test. This suggests that airflow within the cavity was removing moisture as it entered the ventilation hole near the bottom of the test apparatus. As moisture was removed by air circulating through the clear airspace, relative humidity levels decreased.

Overall, laboratory testing has shown that moisture can be removed by ventilation from the test apparatus when no clear airspace is provided in the venting configuration. When a clear airspace is incorporated into the venting configuration, moisture is removed at a greater rate.

2.3.5 THEORETICAL ANALYSIS

The theoretical moisture removal rate for a clear airspace in the R24 series using the orifice equation is examined in Section 2.3.5.1. Next, the flow coefficient for the R24 series is estimated in Section 2.3.5.2. The air permeability of R24 mineral fibre insulation is estimated in Section 2.3.5.3. A combined flow equation is developed in Section 2.3.5.4 and is used to estimate the theoretical moisture removal from the R24 Series. A discussion of the theoretical results is contained in Section 2.3.5.5.

2.3.5.1 THEORETICAL MOISTURE REMOVAL RATE FOR CLEAR AIRSPACE

Using observed air temperature and assumed relative humidity conditions, the stack flow and orifice flow equations were used to estimate the amount of moisture that could be removed from the test apparatus in Test Sets 8, 10, 12 and 13 of the R24 Series. These Test Sets were chosen because they incorporated an unobstructed clear airspace in the venting configuration where air movement due to stack flow can be theoretically approximated. The theoretical amount of moisture that could be removed by drying stack action through the clear airspace was compared to the laboratory results. Airflow through mineral fibre insulation is neglected for simplicity. The methodology used for this theoretical analysis follows work by Tzekova and is presented below. The airflow in the ventilated airspace is assumed to be based on the amount of air that passes through the vent holes. Tzekova had found that estimates yielded by the procedure presented below matched theoretical moisture removal by ventilation to actual moisture removal reasonably in three tests. The tests incorporated a 19 mm clear airspace between pine siding boards and mineral fibre insulation in the venting configuration.

The capacity of air to hold moisture was calculated using the following:

$$w_{capacity} = w_{airspace} - w_{GR} \tag{2.5}$$

$$w_{airspace} = \frac{P_{wairspace}}{R_w \, T_{airspace}} \tag{2.6}$$

$$w_{GR} = \frac{P_{wGR}}{R_w \, T_{airspace}} \tag{2.7}$$

$w_{capacity}$ = *amount of moisture that can be picked up by the air [kg/m^3]*

$w_{airspace}$ = *amount of moisture in the airspace [kg/m^3]*

w_{GR} = *amount of moisture in the guard room [kg/m^3]*

$T_{airspace}$ = temperature in the guard room [K]

T_{GR} = temperature in guard room [K]

$P_{wairspace}$ = partial pressure of water vapour in the airspace [Pa]

P_{wGR} = partial pressure of water vapour in the guardroom [Pa]

R_w = gas constant for water vapour [461.5 J/kgK]

The stack pressure difference was calculated using the following:

$$\Delta \mathrm{P_s} = \left(\rho_{airspace} \times g \times h\right) - (\rho_{GR} \times g \times h) \tag{2.8}$$

$$\rho_{GR} = \frac{1}{T_{GR}}\left(\frac{P_{wGR}}{R_w} + \frac{101325 - P_{wGR}}{R_a}\right) \tag{2.9}$$

$$\rho_{airspace} = \frac{1}{T_{GR}}\left(\frac{P_{wairspace}}{R_w} + \frac{101325 - P_{wairspace}}{R_a}\right) \tag{2.10}$$

ΔP_s = stack pressure difference [Pa]

g = gravitational constant [m/s^2]

ρ_{GR} = density of air in guard room [kg/m^3]

$\rho_{airspace}$ = density of air in airspace [kg/m^3]

h = height between vent holes [m]

P_{wGR} = partial pressure of water vapour in the guardroom [Pa]

$P_{wairspace}$ = partial pressure of water vapour in the airspace [Pa]

R_a = gas constant for dry air [287.1 J/kgK]

The flow rate was calculated using the following:

$$Q = C_d \left(\Delta P_s \times \frac{2}{\rho_{airspace}} \right)^{1/2} \tag{2.11}$$

Q = *airflow rate [m^3/s]*

C_d = *discharge coefficient*

ΔP_s = *stack pressure [Pa]*

$\rho_{airspace}$ = *density of air in airspace [kg/m^3]*

The moisture removal rate is the product of the capacity of moisture and the flowrate:

$$Moisture\ Removal\ Rate\ = Q \times w_{capcity} \tag{2.12}$$

Table 2.3.3 contains the actual moisture removed and compares it to the theoretical moisture removal by the orifice equation. Figure 2.3.20 plots actual moisture removal against theoretical moisture removal.

Test	Moisture Removed (g)	Theoretical Moisture Removed (g)	Difference (g)	Ratio of Theoretical to Actual
13A 3 mm	108	566	458	5.24
13B 3 mm	154	378	224	2.45
13C 3 mm	101	674	573	6.67
13D 3 mm	123	430	307	3.50
8A 6 mm	157	369	212	2.35
8B 6 mm	189	363	174	1.92
8C 6 mm	155	443	288	2.85
12A 6 mm SBPO	197	353	156	1.79
10A 9.5mm SBPO	240	386	146	1.61

Table 2.3.3: Actual and Theoretical Moisture Removal based on Orifice Equation

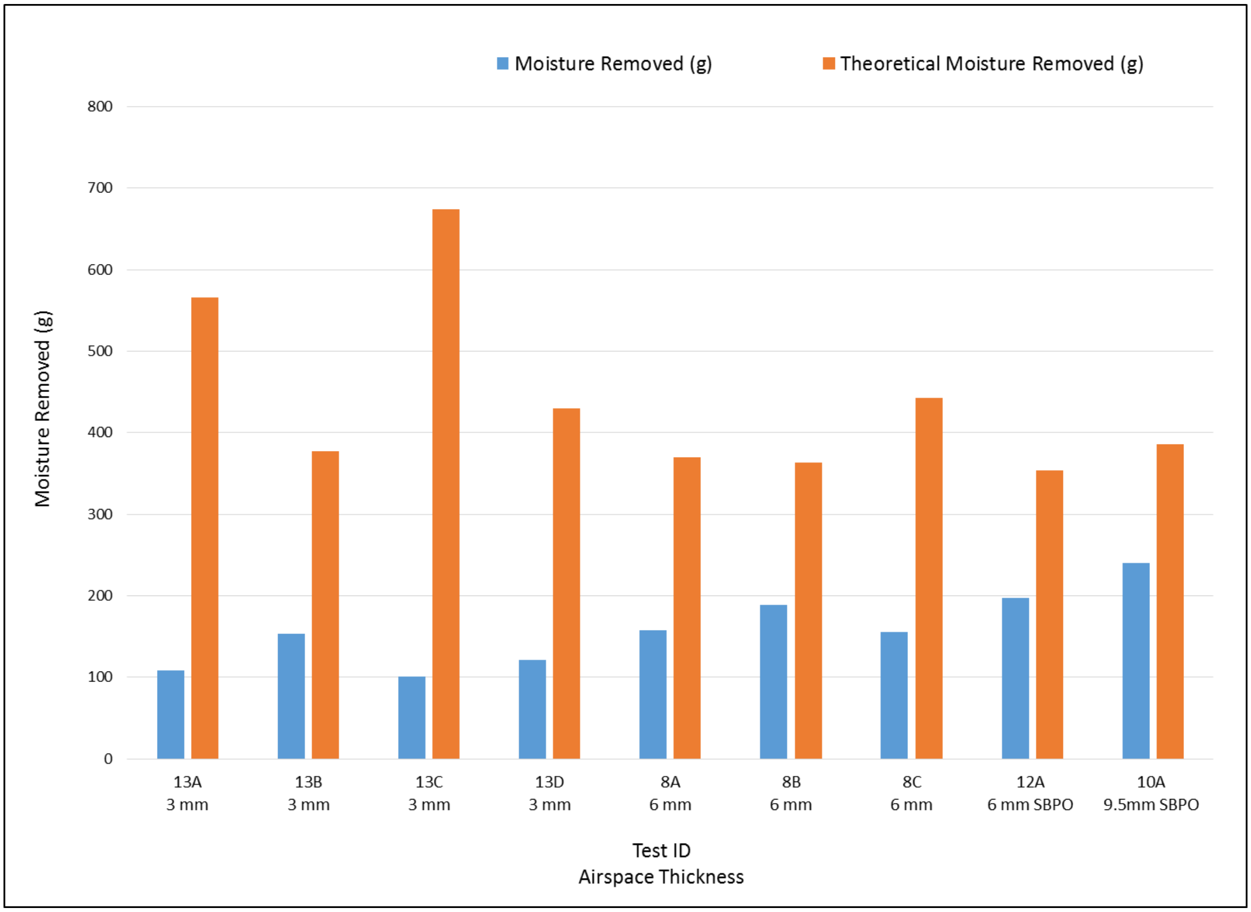

Figure 2.3.20: Actual vs. Theoretical Moisture Removal for Orifice Flow Equation

The theoretical amount of moisture removed is closer to the actual moisture removed by ventilation in Test Set 8 than in Test Set 13, but does not match the moisture removed as closely as the results reported by Tzekova. Test Set 8 has a larger clear airspace than does Test Set 13 (6 mm vs. 3 mm). This suggests that as the thickness of the clear airspace is reduced, the orifice flow equation becomes less useful in predicting the flow through the ventilated airspace. The area of the ventilated airspace itself may be the limiting factor controlling the flow. The airspace is rectangular as opposed to circular and the rectangular airspace has a large surface area for friction compared to the cross sectional area. In the tests above, the most influential boundaries of the clear airspace are the pine surface and the mineral fibre insulation.

The possibility that the discharge coefficient C_d was incorrect in the above analysis was explored. C_d is a product of the contraction coefficient, C_c, and velocity coefficient, C_v. The value of 0.6 is assumed for turbulent flow through a circular sharp edge orifice. The vent hole used in the laboratory experiments is a circular sharp edge orifice, but there is doubt as to whether the flow is in the tests is turbulent. The relatively small clear airspaces tested of 3 mm and 6 mm are likely more heavily influenced by the boundary walls, the pine siding and by the mineral fibre batt than larger airspaces such as 19 mm tested by Tzekova. Note, the mineral fibre batt is assumed to take no airflow, but this assumption will be adjusted later in the analysis.

The tests with SBPO reinforce the idea that the mineral fibre insulation has an effect on the airflow. The theoretical quantity of moisture removed by ventilation in Tests 10 and 12 that incorporated SBPO in the venting configuration more closely match the actual amount of moisture removed. The SBPO essentially shields the airflow from the effects of the mineral fibre insulation as a boundary, suggesting that the mineral fibre insulation affects the moisture removal. The SBPO blocks air from entering into the mineral fibre batt. This suggests the assumption used in the above analysis that no flow enters the batt is incorrect, and is more incorrect when a smaller clear airspace is used in the venting configuration.

2.3.5.2 DETERMINING THE FLOW COEFFICIENT

Often, building components are tested for their flow characteristics. It has been found that for components such as windows and walls, a general power law can fit the data from most leakage situations as proposed by Baker et al. in 1987 (Straube, 2005).

$$Q = C(\Delta P_s)^n$$

Q = airflow rate [m^3/s]

ΔP_s = stack pressure [Pa]

C = flow coefficient

n = flow exponent

The flow coefficient includes the area, flow path, flow regime, friction and temperature/density effects. The required flow through the system was calculated based upon the actual moisture removed due to ventilation in Test Sets 8 and 13. Regarding the flow exponent, 0.5 holds for perfectly turbulent flow and 1.0 holds for perfectly laminar flow. Often a value of n = 0.65 is assumed in practice. Knowing the moisture capacity of the clear airspace, and the actual moisture removed, the required flow rate can be calculated. The three flow exponents mentioned above are tested to determine the resulting flow coefficients. A value, C_{norm}, which normalizes the flow coefficient by the area of the clear airspace is presented. Calculated averages for C and C_{norm} are shown in Table 2.3.4 for the clear airspace thicknesses of the Test Sets examined.

	Clear Airspace Thickness (mm)	Flow Coefficient C (x 10^{-6})	C_{norm}
n = 0.5	3mm	105	0.11
	6mm	176	0.09
n = 0.65	3mm	96	0.10
	6mm	163	0.08
n = 1.0	3mm	78	0.08
	6mm	137	0.07

Table 2.3.4: Calculated Flow Coefficients given Airspace Thicknesses and Flow Exponents

The values of C_{norm} for the clear airspace thicknesses of 3 mm and 6 mm, with the given flow exponents of 0.5, 0.65 and 1.0 are approximately 6 times smaller than the sharp orifice discharge coefficient C_d. This further suggests that the boundaries of the clear airspace in the venting configuration of these tests have a significant impact on the ventilation airflow that can be achieved.

2.3.5.3 THEORETICAL MOISTURE REMOVAL RATE FOR MINERAL FIBRE INSULATION

Air flow within permeable materials can be calculated using Darcy's Law:

$$Q = K(\Delta P_s)^n \tag{2.13}$$

K = air permeance value

n = flow exponent

ΔP_s = *stack pressure [Pa]*

A similar analysis above in Section 2.3.5.2 can be applied here to determine the estimated effective air permeance value for R24 mineral fibre insulation. The required flow rate is calculated from the actual moisture removal rate for Test Sets 9 and 11. These Test Sets used only mineral fibre in the venting configuration and thus had a 0 mm clear airspace thickness. The flow in the mineral fibre insulation was assumed to be laminar and thus the flow exponent was assumed to be 1.0. The estimated air permeance value, K, was calculated and is presented in Table 2.3.5.

Test	Moisture Removed (g)	Q required (m^3/s)	Air Permeance K
9A 0 mm	61.8	0.0694	0.0358
9B 0 mm	65.1	0.0802	0.0444
9C 0 mm	72.0	0.0608	0.0249
11A 0 mm (C)	57.5	0.0689	0.0378
11B 0 mm (C)	61.7	0.0658	0.0318
11C 0 mm (C)	51.1	0.0566	0.0283

Table 2.3.5: Estimated Air Permeance Values of R24 Mineral Fibre based upon Observed Moisture Removal

It should be noted that airflow is assumed to be in the longitudinal direction within the batt as opposed to the transverse direction. This should increase the air permeance value because the mineral fibre strands of the batt are generally oriented in the longitudinal direction.

2.3.5.4 TOTAL FLOW THROUGH VENTING CONFIGURATION

The total flow through the venting configuration is a combination of flow in the clear airspace and flow in the mineral fibre insulation when both are combined in the venting configuration. Flow through venting configuration can be described by the following equations:

$$Q_{venting\ configuration} = Q_{airspace} + Q_{mineral\ wool} \tag{2.14}$$

$$Q = C(\Delta P_s)^n + K(\Delta P_s)^n \tag{2.15}$$

Theoretical moisture removal was calculated for Test Sets 13 and 8 using the above equations combined with the analysis method described in Section 2.3.5.1. The flow coefficient was chosen assuming the flow exponent for turbulent flow, as calculated in Section 2.3.5.2. The air permeance value for mineral fibre insulation in the longitudinal direction is chosen as the average of the values calculated in Section 2.3.5.3. The assumptions are summarized in Table 2.3.6 below:

Parameter	**Material**	**Assumed Value**
Flow Exponent (n)	Clear Airspace	0.5
Flow Exponent (n)	Mineral Fibre	1.0
Flow Coefficient (C)	Clear Airspace	105×10^{-6}
Air Permeability (K)	Mineral Fibre	33.8×10^{-6}

Table 2.3.6: Assumed Values for Theoretical Moisture Removal Calculations

Table 2.3.7 contains the actual moisture removed and compares it to the theoretical moisture removal by the orifice equation. Figure 2.3.21 plots actual moisture removal against theoretical moisture removal.

Test	Moisture Removed (g)	Theoretical Moisture Removed (g)	Difference (g)	Theoretical / Actual
13A 3 mm	108	196	88	1.81
13B 3 mm	154	161	7	1.05
13C 3 mm	101	233	132	2.30
13D 3 mm	122	174	52	1.43
8A 6 mm	157	203	46	1.29
8B 6 mm	189	245	56	1.30
8C 6 mm	155	238	83	1.53

Table 2.3.7: Actual and Theoretical Moisture Removal based on Equation 2.14

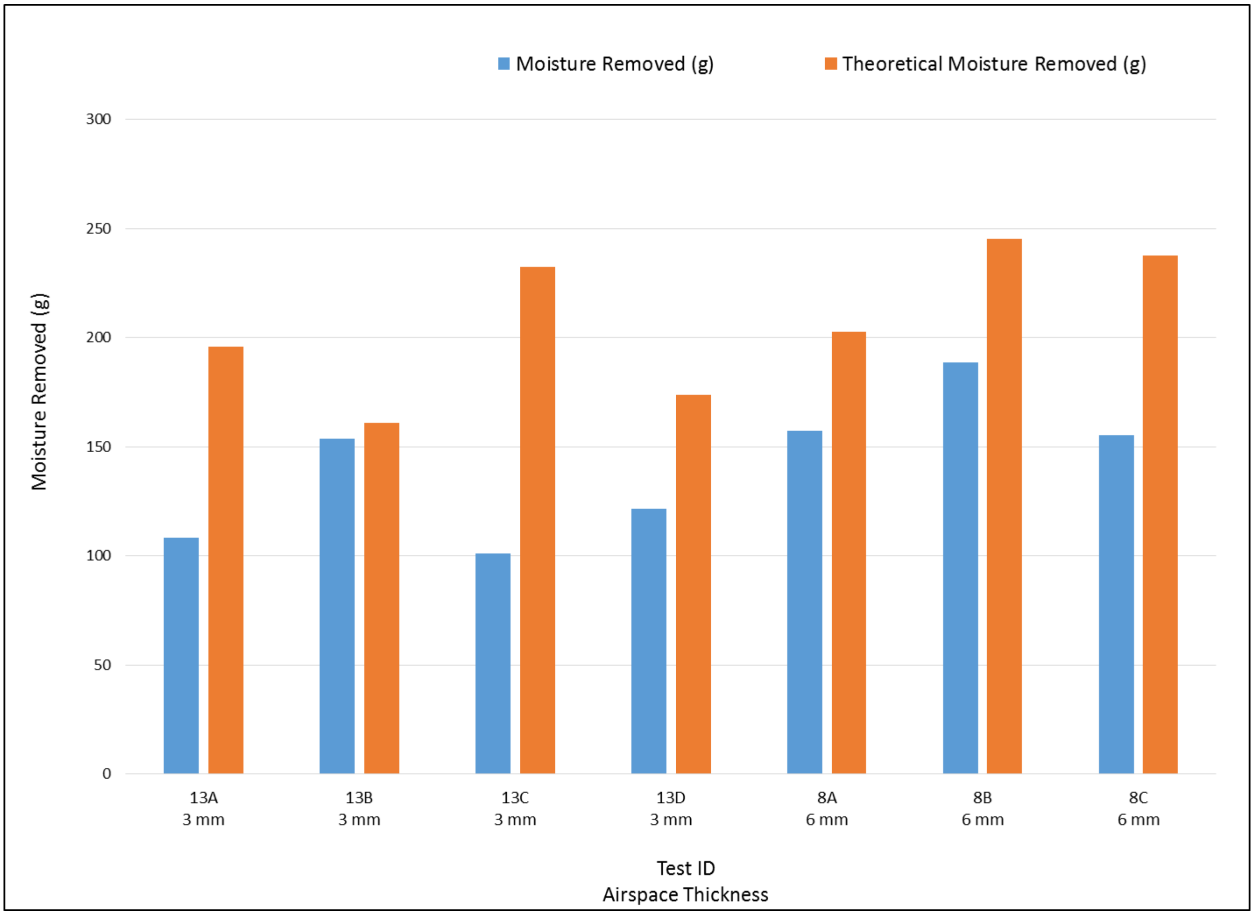

Figure 2.3.21: Actual vs. Theoretical Moisture Removal for Combined Flow Equation

Equation 2.14, for the values assumed, more closely approximates the actual moisture removed than does the orifice flow equation presented in Section 2.3.5.1. In all cases, the theoretical moisture removal was greater than the actual moisture removal. The equation provided a better estimate for Test Set 8 which incorporated a 6 mm clear airspace in the venting configuration, than it did for Test Set 13 which incorporated a 3 mm clear airspace.

Limitations of the above analysis include the estimate of the flow coefficient (C). C was calculated based upon limited number of tests and neglected flow through batts. The actual C is therefore likely smaller than the estimated value because the estimated neglects the influence of the mineral fibre batts. As the difference between the theoretical moisture removed and the actual was always positive, this would bring the theoretical closer to the actual.

2.3.5.5 DISCUSSION OF THEORETICAL DRYING

As the thickness of the clear airspace in the venting configuration is reduced, the flow coefficient is also reduced due to the increased influence of boundaries of the clear airspace. The combination of flow in clear airspace and flow through batts more closely approximates moisture removed for the 3 mm and 6 mm plus mineral fibre venting configurations than does the orifice flow equation. Both of the above observations suggest that the ventilated airspace characteristics is the limiting factor as opposed to the vents when the clear airspace is less than or equal to 6 mm.

Interfaces between laminar and turbulent (air from orifice or clear airspace entering batt) can result in variable flow rates and erratic, hysteretic behaviour [8]. This erratic behaviour will have an impact on the overall flow rate and is not accounted for in the combined equation. If it reduces the airflow efficiency in the venting configuration, the predicted moisture removal of the combined equation may become closer to the actual.

2.3.6 TZEKOVA TEST RESULTS REVISITED

The ‘Refined Test Series’ results obtained by Tzekova were analyzed using the normalized moisture removal rate by ventilation described in Section 2.1.1. Tzevoka tested two ventilation cavity configurations, 0 mm and 19 mm with two types of mineral fibre insulation, R15 Dual

Density and R24 [22]. Various vent area ratios ranging from 1000 mm^2/m^2 were also examined. The normalized results are plotted in Figure 2.3.22:

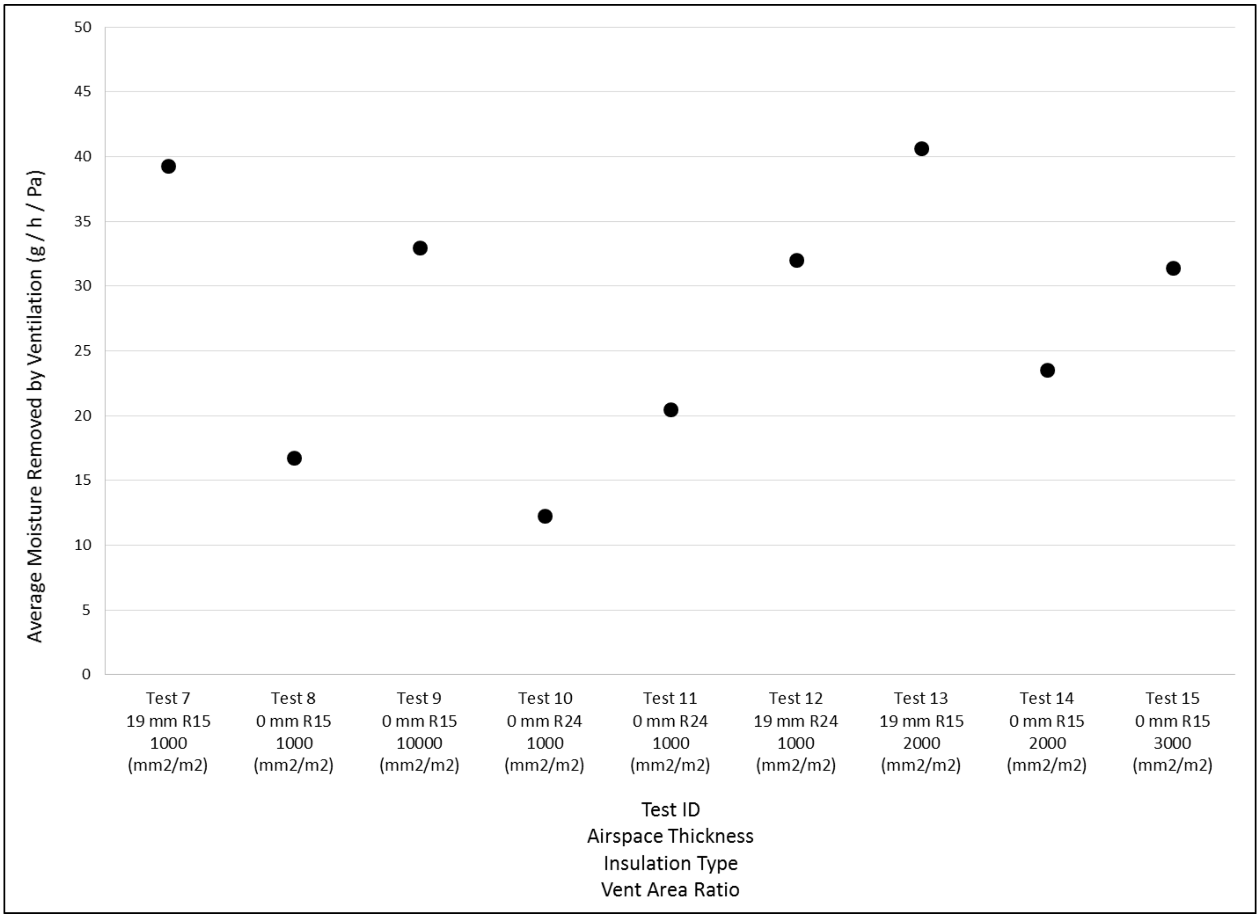

Figure 2.3.22: Average Normalized Rate of Moisture Removal by Tzekova (2015)

Tests 10 and 11 from Tzekova's data can be compared against the data from Test Sets 9 and 11 from the R24 series. In both cases no clear airspace was provided in the venting configuration, R24 mineral fibre insulation was used, and similar vent area ratios were used (1000 mm^2/m^2 for the above and 1175 mm^2/m^2 for the R24 series).

Test 10 removed 12 g/h/Pa while Test 11 removed 20.5 g/h/Pa of moisture by ventilation in Tzekova's refined tests. In Test Set 11 of the R24 series that included compression to the batt in the apparatus cavity, the mean normalized moisture removal rate was 4.8 g/h/Pa while in Test Set 9 where no compression was present, the mean normalized moisture removal rate was 5.4 g/h/Pa.

The moisture removed from the R24 series with a 3 mm clear airspace (Test Set 13) was 10.8 g/h/Pa and it was 16.9 g/h/Pa when a 6 mm airspace was included in the venting configuration. The results obtained from Tzekova in Test 10 and Test 11 more closely match the data from the R24 Series that used a 6 mm airspace. The average of these two tests, 16.4 g/h/Pa, is in the vicinity of the R24 Series 6 mm tests.

As explained in Section 2.3, Tzekova's procedure was refined for this laboratory study to ensure that contact was made between the pine surface and the mineral fibre insulation when no clear airspace was included in the venting configuration. Due to the experimental procedure used by Tzekova, an unintended clear airspace of 3 mm to 6 mm may have developed during assembly when no clear airspace intended.

2.3.7 DISCUSSION

Overall, the results of the R22 Series testing suggest that airflow is occurring in the mineral fibre insulation. Moisture is removed by ventilation when no clear airspace is provided in the venting configuration. As well, the vertical distribution of moisture within the insulation that was found upon test completion provides further evidence that convective airflow is transporting moisture within the insulation. A venting baseline for mineral fibre insulation is created by the results of moisture removal in tests where no clear airspace is provided in the venting configuration. When the venting baseline is compared against the tests that used clear airspaces within the venting configuration, results suggested that the equivalent airspace thickness of the R22 insulation was approximately equal to a 6 mm clear airspace in terms of venting potential.

Several limitations to the results were discovered throughout the preliminary series testing. The physical properties of the R22 batts were not uniform between bundles of insulation. Achieved loft of the mineral fibre insulation was not consistent between bundles affecting the effective density of the batt. Inconsistent loft also led to concerns regarding the uniformity of the clear airspace during testing. Some insulation batts were able to keep their shape better than others when cut into pieces during testing preparation. This leads to concerns that ‘softer’ batts would be more prone to settling during the test. If a batt were to settle, airflow characteristics would change and could lead to inconsistent results. If the batt were to settle enough it could reduce the thickness of the clear airspace and possibly block it altogether. Through experimentation, it was determined that higher density R24 insulation has better properties for testing than does the R22 mineral fibre insulation, including more consistent loft, higher density, and higher rigidity. The combination of these properties allowed the batt to hold its shape when cut, and more consistently achieved the desired loft. This led confidence in the consistency of the clear airspace in the venting configuration. R24 batts were used throughout the R24 Series testing and test results were found to be more consistent.

The average temperatures displayed throughout the R24 Series are similar to those of the R22 Series. As the experimental procedure did not change from the R22 Series, this was to be expected, and suggests consistency between the environmental boundary conditions between the two series.

The range of the vapour pressure drive was approximately 400 Pa larger in the R24 Series than it was in the R22. The range of moisture supplied from the pine siding in the R24 Series was similar to the range of moisture supplied by the pine siding in the R22 Series.

The results of Test Set 8 in the R24 Series can be compared to the Results of Test Set 3 of the R22 Series. The R24 batts have a higher density than the R22 batts. One would expect that the moisture removed through ventilation in the R24 Series would be lower when the same venting configurations are examined. On the contrary, the venting in the R24 series was much greater than equivalent tests of the R22 Series. This is evidenced by the larger quantities of moisture removed in Test Set 8 compared to Test Set 3. The inconsistency of the physical properties of the mineral fibre insulation in the R22 series may have affected the airflow within the ventilated airspace. The results between tests of Test Set 8 are more consistent than those of Test Set 3 in that the ranges of moisture removal between tests in each test set was smaller.

When comparing the R24 Series (Test Sets 9 and 11) to the R22 Series (Test Sets 2 and 4) when no clear airspace is provided based on the amount of moisture removed by ventilation, similar differences exist. More moisture removal by venting was achieved when R24 batts were used in the venting configuration. This is counter to the author's intuition based upon the densities of the batts. Test Set 2 included two tests where re-used batts were included, leading to more inconsistent results. The relative difference between the R22 Series and the R24 Series was smaller when considering moisture removed when no airspace was incorporated than it was when a 6 mm airspace was incorporated. The results of the R24 Series are more consistent between tests. Again, it is suggested that the variation in the physical properties of the batts in the R22 Series led to variation in the results between tests. In general, the results of the R24 series was more consistent than the results of the R22 Series upon the basis that test results within Test Sets had less variation.

The results of the R22 Series and the R24 Series both indicated that airflow is occurring through mineral fibre insulation. Drying occurred when no clear airspace was present in the venting configuration. In addition, insulation near the top of the test apparatus gained more moisture throughout tests than did insulation near the bottom of the assembly. The moisture was carried higher into the batt by convective ventilation airflow, where it condensed due to the saturation vapour pressure being reached. This effect was more pronounced when a clear airspace was present in the venting configuration and also increased when the thickness of the clear airspace was larger. Airflow through batts may introduce moisture during high moisture load conditions during the test. The vapour pressure drives during the test mimic solar reversal. When solar reversal is “shut off”, ventilation airflow will continue to dry the wall assembly as long as moisture content in the air of the ventilated airspace and mineral fibre insulation is less than the moisture content of the air outside.

In the field, higher density rigid mineral fibre insulation may be desired for design and constructability purposes. The venting potential of the mineral fibre insulation will likely be reduced as a higher density is used in the venting configuration, but ventilation airflow should still occur as long as the insulation is considered to be air permeable

Results from the R24 Series indicate that the R24 batts are equivalent to 3 mm clear airspace in terms of venting potential. The drying potential increases when mineral fibre is used in combination with a 3 mm to 6 mm inch clear airspace. Inconsistencies on the inside of masonry wall (roughness) effectively creates an airspace equivalent to 3 mm to 6 mm. Thus, during construction, it may not be required to purposefully create a clear airspace as long as the mineral fibre insulation is not compressed when installed at the interior of the masonry wall.

In the field, the vents will likely not be sharp edged as they will be long holes through the solid masonry. This will likely reduce the flow rate in the field per area of wall as compared to the laboratory experiments. Conversely, the wall will experience a greater pressure differential when wind pressure is added. This can increase or decrease flow depending on the wind's orientation as compared to the orientation of the wall.

The introduction of moisture and convective airflow into the mineral fibre insulation will likely degrade the resistance value of the mineral fibre insulation slightly. This amount of degradation is unknown and needs to be investigated to evaluate whether ventilation and the resulting durability improvements are an acceptable trade-off for reduced thermal efficiency. The designer must be aware of resistance value degradation and increase the amount of thermal resistance during the design phase, to achieve the desired effective thermal resistance.

Overall, this laboratory study has revealed that the drying potential of low density mineral fibre insulation is roughly equivalent to a 3 mm clear airspace. Drying can be achieved when no clear airspace is incorporated into the venting configuration. When an airspace of 3 mm to 6 mm is added to the mineral fibre insulation, the venting configuration is shown to be an effective means of drying solar heated walls.

Chapter 3: Hygrothermal Modeling

This chapter describes hygrothermal model simulations that were created using WUFI Pro 6 modeling software. WUFI 6.0 Pro is a one dimensional hygrothermal analysis program that performs dynamic simulations of coupled heat and moisture transfer across user defined wall assemblies. The simulations are intended to model the long-term performance of the venting configurations tested during the laboratory study. The venting configurations are modeled with typical solid masonry walls found in Toronto, Ontario.

3.1 INTRODUCTION

The laboratory testing presented in Chapter 2 has shown that ventilation drying can be achieved through mineral fibre insulation when moist facades which have been internally insulated are solar heated. The amount of venting that appears to be occurring through the insulation is approximately equivalent to a clear airspace with a thickness of 3 mm. Considering this finding, hygrothermal model simulations were carried out using WUFI Pro 6 modeling software to investigate the potential impact of the ventilation drying on the response of an internally insulated wall system over a five year simulation period.

In total, four venting conditions were simulated. The first case, was an internally insulated wall with no provision for ventilation drying. This case was labelled “No Venting,” and models the case where no provisions have been made for back venting of the façade. The second case was a 3 mm air space which was used to simulate the venting that could occur in mineral fibre insulation with no clear air space. This step was necessary since the modelling program could not simulate flow through the mineral fibre insulation. Thus, a 3 mm air space was modelled in order to evaluate the potential effects of ventilation drying though the mineral fibre insulation with no clear air space. The third and fourth cases were 6 mm and 9 mm air spaces which were used to simulate the venting that could occur in mineral fibre insulation, plus a 3 mm and a 6 mm clear air space respectively.

Venting Configuration	**Modelled Airspace Thickness**	**Applicable Venting Configuration Scenarios**
1 (Base Case)	0 mm	• No flow in mineral fibre insulation
2	3 mm	• 3 mm clear airspace with no venting through mineral fibre • 3 mm clear airspace and venting through mineral fibre
3	6 mm	• 6 mm clear airspace with no venting through mineral fibre • 3 mm clear airspace and venting through mineral fibre
4	9 mm	• 9 mm clear airspace with no venting through mineral fibre • 6 mm clear airspace and venting through mineral fibre

Table 3.1.1: Applicable Venting Configuration Scenarios Given Airspace Thickness in Simulation

3.2 MODEL SET-UP

Table 3.2.1 displays inputs into the model that were common across all simulations. The south orientation was chosen for the simulations to best capture the effect of solar radiation during the winter months. The winter is when the walls are most susceptible to freeze-thaw damage. The east orientation was also simulated because it receives the most driving rain in the Toronto, Ontario climate, possibly making this orientation more susceptible to an overall increase in wall assembly moisture content. Previous research showed that the south wall orientation has a large potential for ventilation during winter months due its greater exposure to solar radiation [22]. Solar radiation at the south face can heat the air within the ventilated airspace resulting air density differences that drive ventilation airflow. A five-year time period was chosen as the runtime in order to capture longer-term hygrothermal data and to determine if the wall assemblies were accumulating moisture over time, or if they were able to dry out. The simulations all ran from January 1, 2017 until December 31, 2021. Interior conditions are based upon operating conditions during testing at Gemini building in Toronto.

Model Parameter	**Input**
Orientation	South or East
Rain Exposure	ASHRAE 160
Initial Material RH	80% (default WUFI value)
Simulation Runtime	5 years
Simulation Time Step	1 hour
Interior Boundary Conditions	23°C (1°C amplitude) 39% RH (15% amplitude)
Exterior Boundary Conditions	Toronto Cold Weather Year

Table 3.2.1: WUFI Common Model Parameters

Figure 1 shows the typical wall assembly for the simulations. Different venting configurations that incorporate airspaces of 0 mm, 3 mm, 6 mm and 9 mm between the solid masonry and the mineral fibre insulation in the wall assembly were simulated.

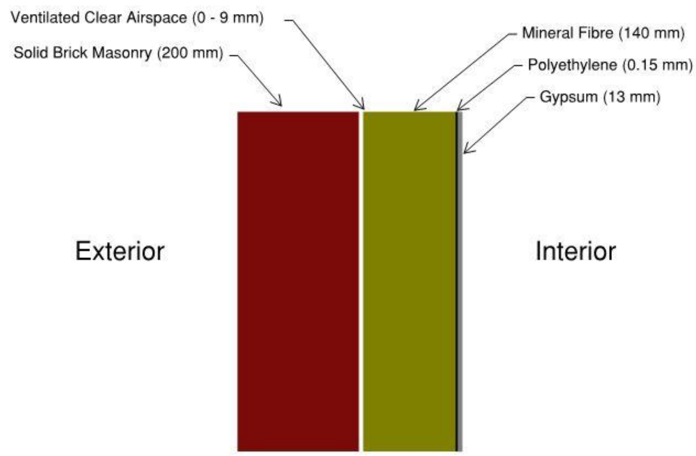

Figure 3.2.1: Wall Assembly for WUFI Simulations

Table 3.2.2 shows the materials that were chosen for the simulations from the databases included in the WUFI Pro 6 software. All material thicknesses were changed within the model to correspond with the wall assemblies and venting configurations as shown in Figures 1.

Material	**WUFI Material**	**Database**
Solid Masonry	Brick (old)	North American
Mineral Wo	Roxul ComfortBatt	ASHRAE 160
Ventilated Airspace	Air Layer 10mm	Generic Materials
Polyethylene	PE-Membrane (Poly;0.07 perm)	Generic Materials
Interior Gypsum	Gypsum Board (USA)	Fraunhofer-IBP

Table 3.2.2: Materials Used in Model

Brick (old) was chosen because it had similar material properties to solid masonry bricks tested in Toronto [22]. Roxul ComfortBatt R-24 was chosen because it was tested in the laboratory study described in Chapter 2. The air layer was chosen with no additional moisture capacity. Earlier versions of WUFI included additional moisture capacity as a material property for air layers to make the numerical calculations more stable for the software. Choosing air layers with no additional moisture capacity better simulates the actual performance of air in ventilated cavities.

The following monitoring positions for temperature and relative humidity were chosen across the wall assemblies as outputs for the simulations.

- Exterior surface of brick masonry
- Interior surface of brick masonry
- Exterior of mineral fibre insulation
- Mineral fibre and polyethylene interface
- Interior face of gypsum interior finish

WUFI Pro 6 adds a feature of adding a ventilation rate to the clear airspace. This feature was not available in previous versions of the programs. Constant ventilation rates were simulated for each of the venting configurations that included a clear airspace. 10 ACH, 50 ACH and 100 ACH were simulated for each thickness of clear airspace (3 mm, 6 mm, 9 mm).

Constant ventilation rates through the clear air space were simulated for each of the venting configurations in which a clear air space was included. 10 ACH, 50 ACH and 100 ACH were simulated. These ventilation rates were chosen because similar rates had been observed behind solid masonry construction and reported for the Barrymore and Gemini field trials in Toronto, Ontario. At Barrymore, the reported averages were 30 ACH at the east face and 50 ACH at the south face [22]. Average ventilation rates recorded at the Gemini House were approximately 100 ACH at both the north and south elevations [22].

3.3 MODEL ANALYSIS

3.3.1 RESULTS AT SOUTH ORIENTATION

The average moisture content in the brick masonry during the five-year simulation period is shown in Figure 3.3.1 for each venting configuration at given ventilation rates at the south orientation. The average moisture content in the brick decreases when ventilated clear airspaces are present. Increasing the thickness of the ventilated clear airspace reduces the average moisture content in the brick at a given ventilation rate (ACH). A larger clear airspace thickness results in a larger volume of air flow through the ventilated airspace. More moisture is able to be removed because more air is available with a given moisture capacity. In addition, the average moisture content of the brick masonry decreases as the ventilation rate increases for a given airspace thickness.

The 3 mm airspace has an average moisture content of 11.8 kg/m^3 when it has a ventilation rate of 10 ACH, which is slightly reduced from the base case with no airspace and no ventilation (12.2 kg/m^3). When the ventilation rate is increased to 100 ACH, the 3mm airspace has an average moisture content of 8.8 kg/m^3. The 3 mm airspace with 100 ACH ventilation rate has a lower average moisture content in the brick masonry than does a 9 mm airspace with 10 ACH (10.6 kg/m^3). When the ventilation rate of the 9 mm ventilation rate is increased to 100 ACH, the average moisture content is reduced to 7.3 kg/m^3. Given the airspace thicknesses and ventilation rates simulated, varying the ventilation rate has a larger impact than does varying the airspace thickness. With a ventilation rate of 100 ACH, a significant amount of drying is achieved in the brick masonry when a 3 mm air space is incorporated into the wall assembly, for walls in the south orientation.

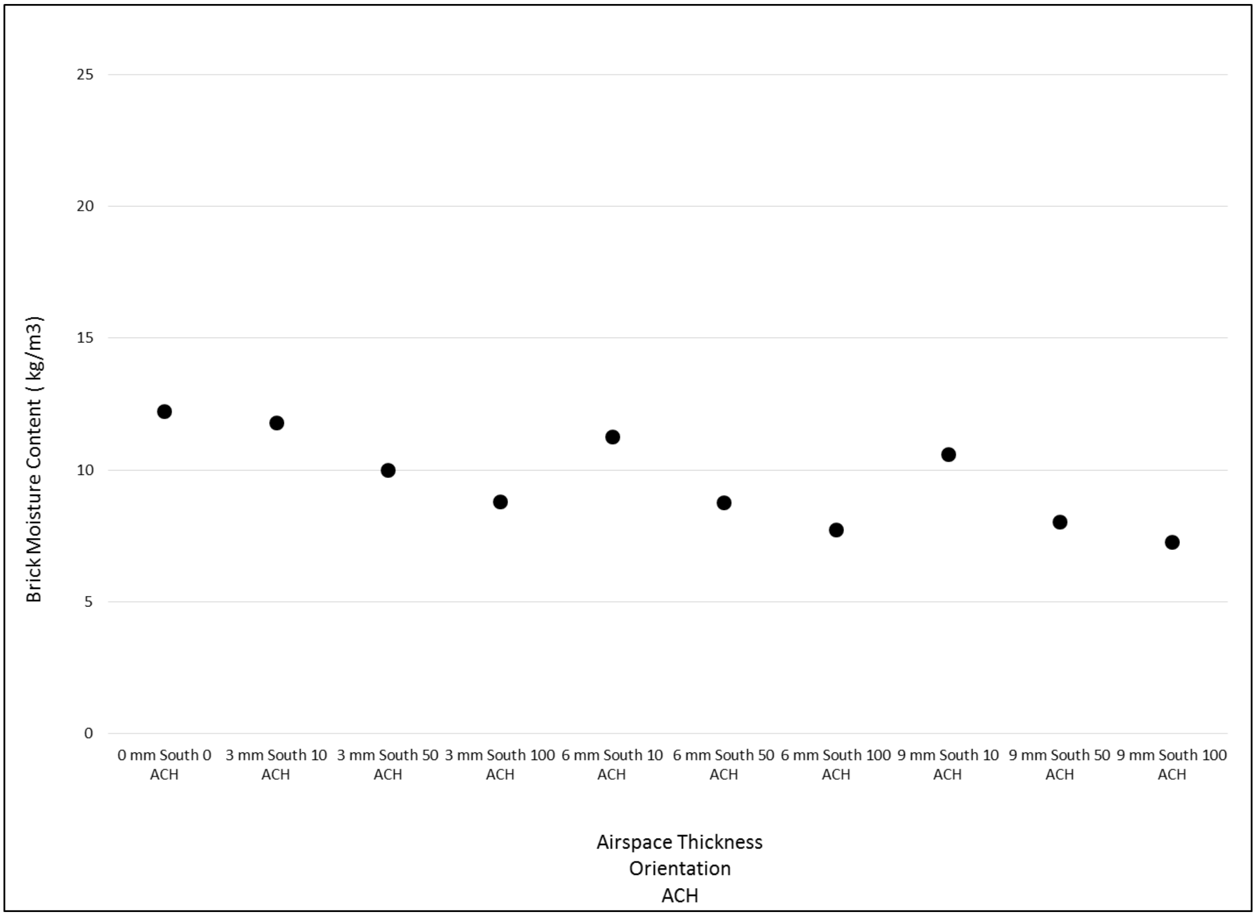

Figure 3.3.1: Average Moisture Content in Brick Masonry during Simulation at South Face for Various Airspace Thicknesses and Air Change Rates

Figure 3.3.2 shows the moisture content of brick masonry for various venting configurations at the ventilation rate of 100 ACH. In general, the moisture content of the brick is lower when ventilation is provided than when it is not. The difference is more pronounced during the winter months. The moisture contents were more similar between venting configurations with 6 mm and 9 mm clear airspaces than they were between the 3 mm and 6 mm clear airspaces. The moisture content in the brick masonry, when no ventilation is provided, grows at a faster rate than it does when a ventilated airspace is provided at the south face.

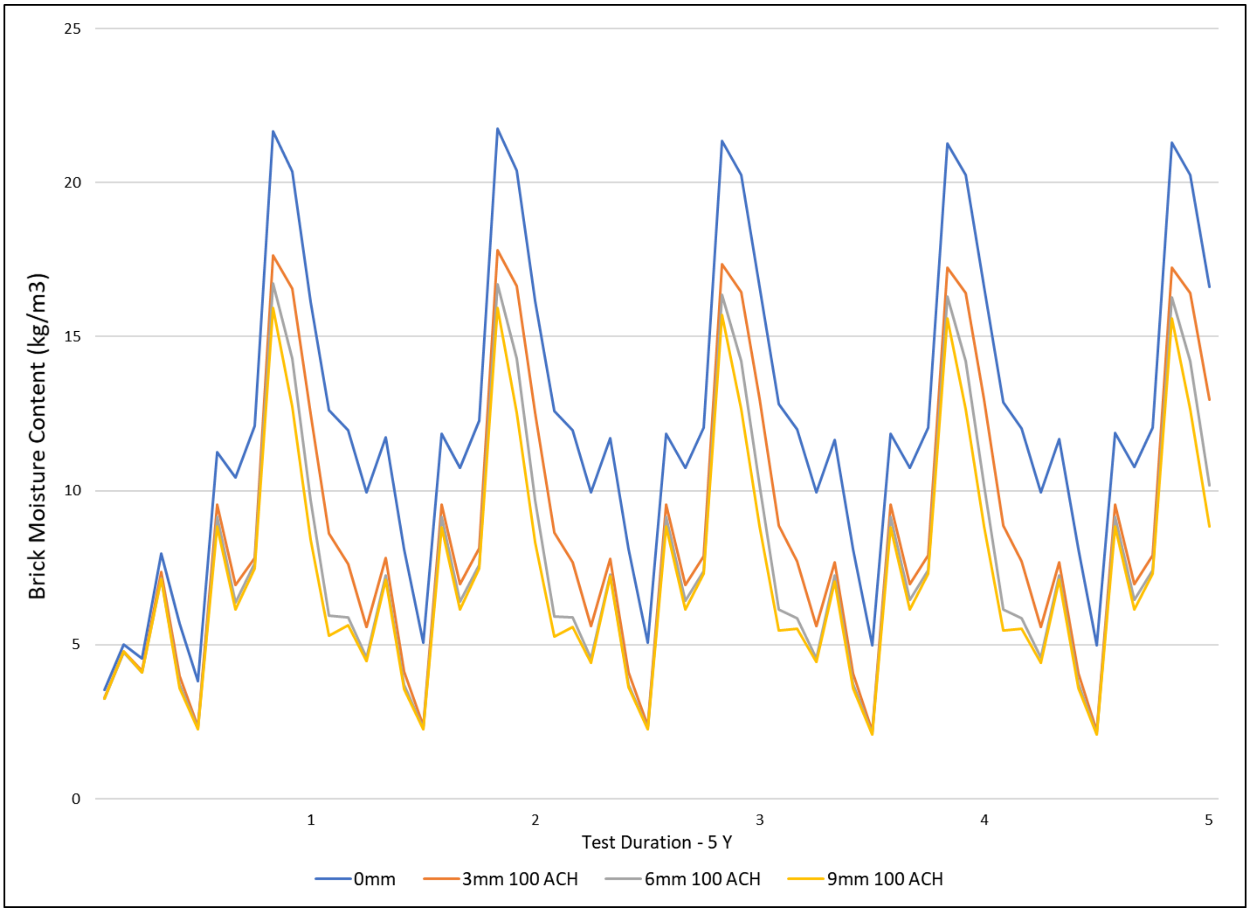

Figure 3.3.2: Monthly Average Moisture Content in Brick during Simulation Duration for Ventilation Rate of 100 ACH at South Face

Figure 3.3.3 shows the average moisture content in the mineral fibre insulation for various venting configurations at the ventilation rate of 100 ACH. Average moisture content values increased during summer months. The effect was most prominent in the non-ventilated configuration. During the summer months, it is likely that moisture was driven into the mineral fibre insulation by vapour diffusion due to solar reversal. Higher surface temperatures due to direct solar radiation at the brick masonry surface would cause a vapour pressure gradient across the wall assembly. Overall, the average moisture content in the mineral fibre insulation is reduced when a ventilated airspace is incorporated into the wall assembly at the south face.

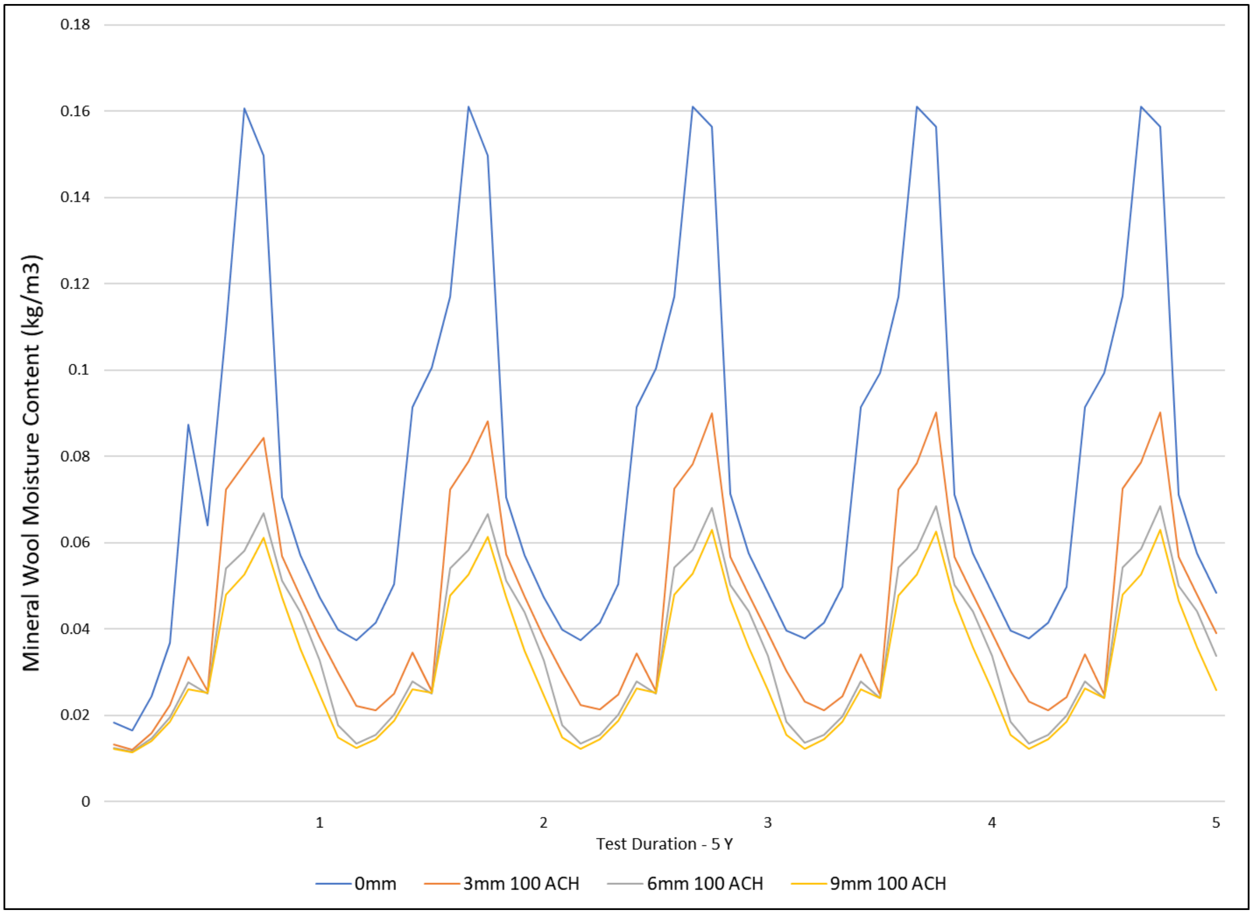

Figure 3.3.3: Monthly Average Moisture Content in Mineral Fibre Insulation during Simulation Period for Ventilation Rate of 100 ACH at South Face

Relative humidity at the exterior face of the mineral fibre insulation for various venting configurations at the ventilation rate of 100 ACH is shown in Figure 3.3.4. This location represents the interface between brick masonry and mineral fibre insulation when no ventilated airspace is incorporated into the wall assembly, and represents the interface between the ventilated clear airspace and the mineral fibre insulation when the clear airspace is present. Relative humidity levels in excess of 90% are experienced at this location in the wall when no ventilated airspace is present for the majority of the simulation. The relative humidity briefly decreases in summers but the relative humidity never drops below 87% at this location in the wall. By contrast, the relative humidity is lower for wall assemblies with a ventilated air space at the exterior portion of the mineral fibre insulation over the simulation period.

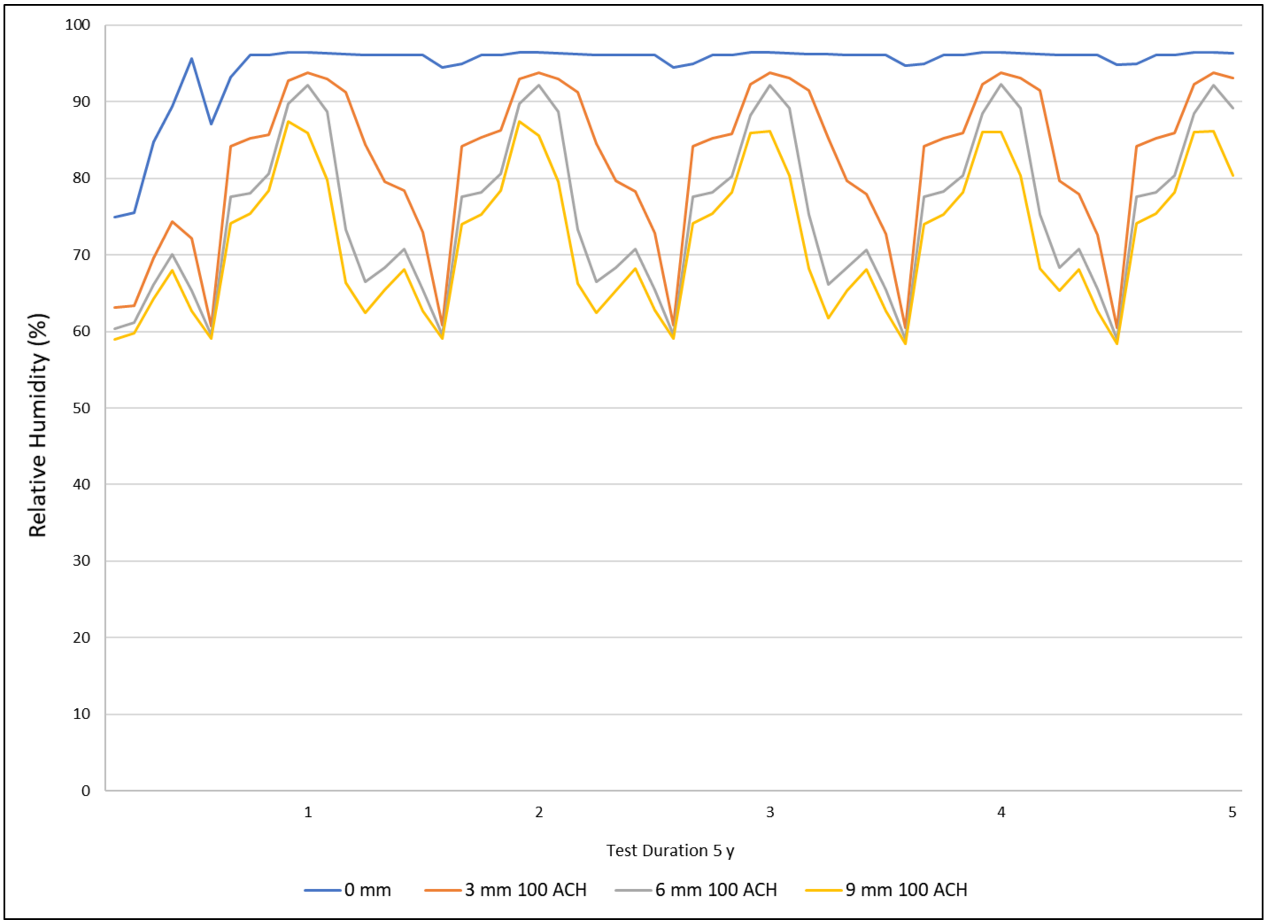

Figure 3.3.4: Monthly Average Relative Humidity at Exterior of Mineral Fibre Insulation for Ventilation Rate of 100 ACH at South Face

3.3.2 RESULTS AT EAST ORIENTATION

The average moisture content in the brick masonry during the five-year simulation period is shown in Figure 3.3.5 for each venting configuration at given ventilation rates at the east orientation. The average moisture content in the brick decreases as ventilated airspaces are introduced to the venting configuration. Larger ventilated airspaces reduce the average moisture content in the brick at the same ventilation rate (ACH). The average moisture content of the brick masonry decreases as the ventilation rate increases for a given airspace thickness.

The 3 mm airspace has an average moisture content of 19.0 kg/m^3 when it has a ventilation rate of 10 ACH, which is slightly reduced from the base case with no airspace and no ventilation (19.6 kg/m^3). The introduction of a 3 mm airspace provides more benefit when the ventilation rate is increased to 100 ACH. The brick masonry in the wall assembly with a 3 mm ventilated airspace has an average moisture content of 16.5 kg/m^3 at this ventilation rate. The brick masonry in the wall assembly with a 3 mm airspace with 100 ACH ventilation rate has a lower average moisture content than it does in a wall with a 9 mm airspace with a ventilation rate of 10 ACH (18.3 kg/m^3). When the 9 mm airspace's ventilation rate is increased to 100 ACH, the average moisture content of the brick masonry is reduced to 13.9 kg/m^3. Given the relative differences of airspace thicknesses and ventilation rates in the simulations, varying the ventilation rate appears to have a larger impact than varying the airspace thickness. With a ventilation rate of 100 ACH, a significant amount of drying is achieved in the brick masonry when a 3 mm air space is incorporated into the wall assembly, for walls in the east orientation.

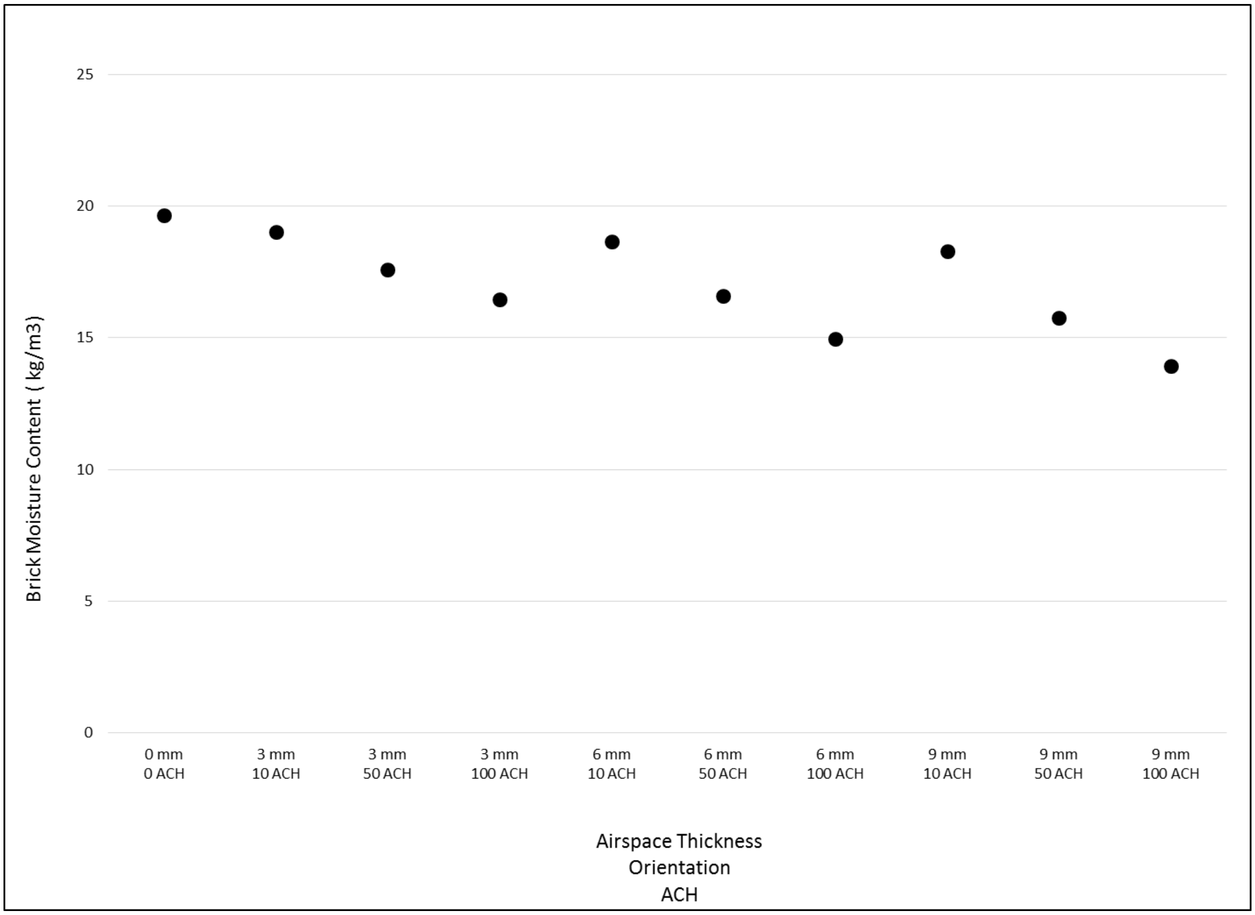

Figure 3.3.5: Average Moisture Content in Brick Masonry during Simulation at East Face for Various Airspace Thicknesses and Air Change Rates

Figure 3.3.6 shows the moisture content of brick masonry for various venting configurations at the ventilation rate of 100 ACH. In general, the moisture content of the brick is lower when ventilation is provided than when it is not. The difference is more pronounced during the winter months.

Figure 3.3.7 shows the average moisture content in the mineral fibre insulation for various venting configurations at the ventilation rate of 100 ACH. Average moisture content values increased during summer months. The effect was most prominent in the non-ventilated configuration. During the summer months, it is likely that moisture was driven into the mineral fibre insulation by vapour diffusion due to solar reversal. Higher surface temperatures due to direct solar radiation at the brick masonry surface would cause a vapour pressure gradient. Overall, the average moisture content in the mineral fibre insulation is reduced when a ventilated airspace is present in the wall assembly at the east face.

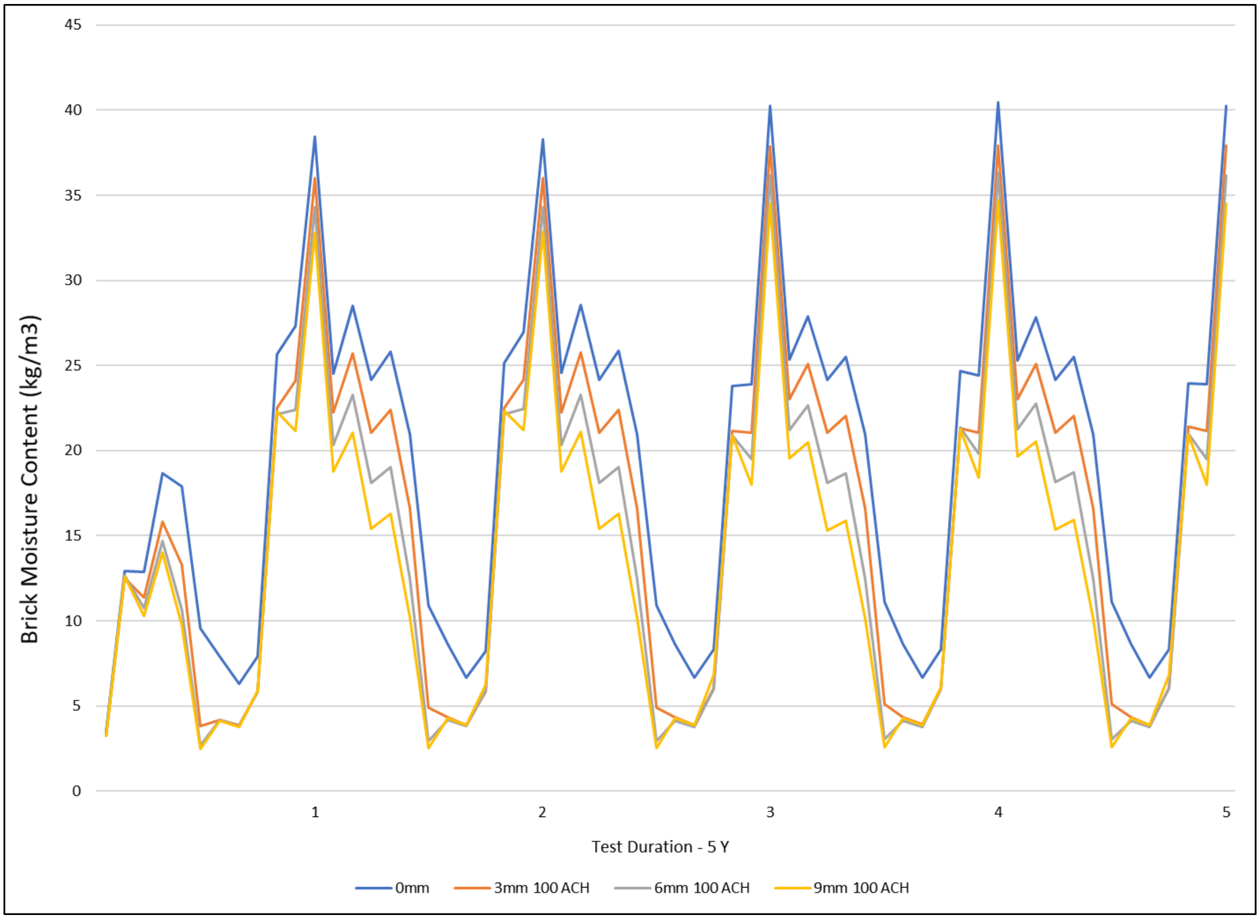

Figure 3.3.6: Moisture Content in Brick during Simulation Duration for Ventilation Rate of 100 ACH at East Face

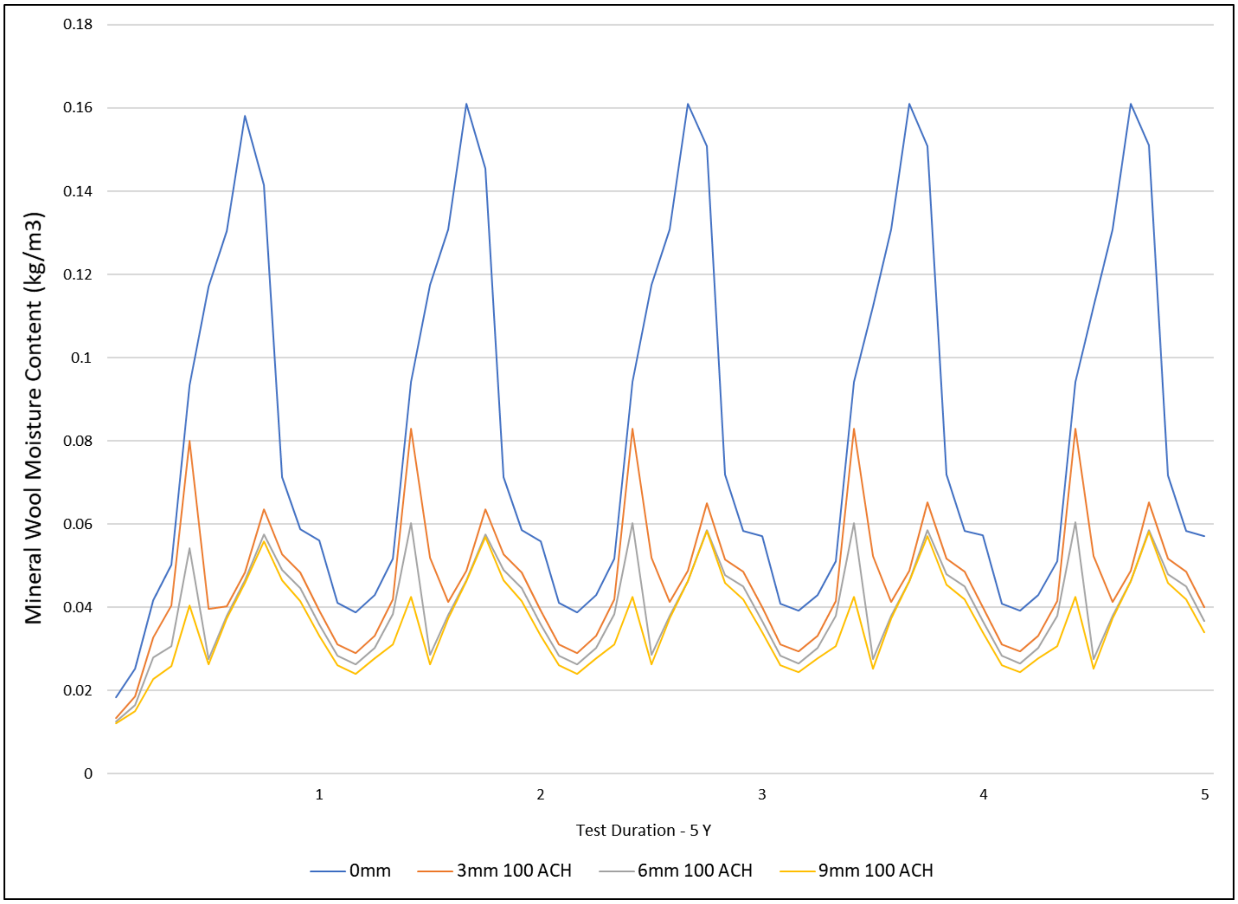

Figure 3.3.7: Moisture Content in Mineral Fibre Insulation during Simulation Period for Ventilation rate of 100 ACH at East Face

Relative humidity at the exterior face of the mineral fibre insulation for various venting configurations at the ventilation rate of 100 ACH is shown in Figure 3.3.8. This location represents the interface between brick masonry and mineral fibre insulation when no ventilated airspace is incorporated into the wall assembly, and represents the interface between the ventilated airspace and the mineral fibre insulation when a ventilated airspace is present. Relative humidity levels in excess of 95% are experienced at this location in the wall when no ventilated airspace is present for the majority of the simulation. By contrast, the relative humidity is lower for wall assemblies with a ventilated air space at the exterior portion of the mineral fibre insulation over the simulation period.

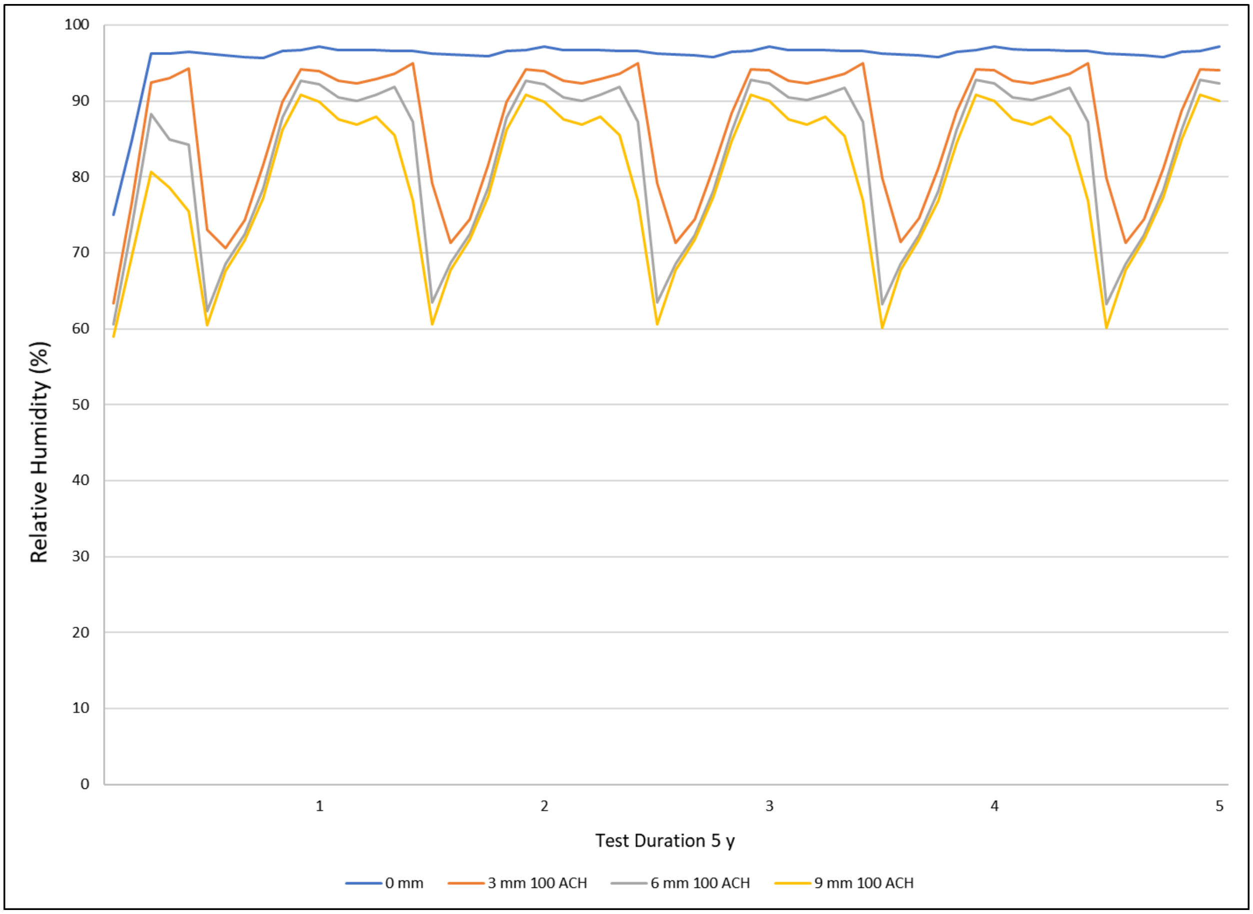

Figure 3.3.8: Monthly Average Relative Humidity at Exterior of Mineral Fibre Insulation for Ventilation Rate of 100 ACH at East Face

3.4 DISCUSSION

Overall, the simulations have demonstrated the potential for incorporating ventilated air spaces behind solid masonry walls in Toronto, Ontario. The simulations have shown that introducing a ventilated air space into the wall assembly reduces the average moisture content of brick masonry and reduces the relative humidity in walls in the south and east orientations. The average moisture content and relative humidity in the wall assembly is lower at the south face than it is at the east face. The east face experiences more driving rain events in the simulated climate and has less solar exposure.

The amount of drying in the wall assemblies increases as the air space thickness increases and as the ventilation rate is increased. The simulations have shown that a vented air space as small as 3 mm can reduce the average moisture content and the relative humidity in the wall assembly. This reduces the potential for freeze-thaw damage and rot and corrosion of embedded structural members.

The 6 mm venting configuration in the model may be most representative of a venting configuration incorporating mineral fibre insulation. If mineral fibre is assumed to be equivalent to a 3 mm airspace as suggested by the laboratory study, then the addition of a 3 mm clear air space to the mineral fibre insulation provides significant venting. If the mineral fibre insulation is not compressed against the inside face of the masonry when it is installed, voids due to the interior roughness of the brick masonry can add additional thickness to the ventilated air space.

The simulations reveal the drying benefits of ventilation. The amount of drying increases significantly as the ventilation rate is increased. There was a relatively small reduction in average moisture content when a ventilation rate of 10 ACH was simulated with the different clear air space thicknesses. The most benefit was shown when 100 ACH was simulated. The average ventilation rate falling in the range 50 to 100 ACH is a reasonable assumption for the south and east faces based upon field data previously obtained in Toronto. Rates may be lower at the north face, due to less exposure to solar radiation that drives some of the ventilation airflow, although wind would still be acting to assist in ventilating a north façade.

There are several limitations to the simulations. The materials used were chosen from generic databases. The properties of materials in existing buildings in Toronto may not be represented.

Properties will vary from building to building, even in the same geographic location. Another significant limitation is choosing a constant rate of ventilation for the simulations. The ventilation rate would change significantly over both the short term and the long term. The ventilation rate is a function of both building characteristics and environmental factors and would not be the same across buildings located in Toronto. A constant ventilation rate gives us an indication, on average, of the moisture that can be removed by ventilation behind solid masonry in a wall assembly.

Chapter 4: Conclusions and Further Research

4.1 CONCLUSIONS

The overall objective of the laboratory testing was to determine how much solar driven moisture can be removed through ventilation using air permeable insulation in various venting configurations. In addition, the work attempted to determine an equivalent airspace thickness of air permeable mineral fibre insulation given its density.

The laboratory tests examined the potential for mineral fibre insulation to act as a venting medium in wall assemblies. The testing incorporated a test apparatus that was loaded with insulation. Absorptive cladding attached to the apparatus acted as a moisture source. A light array increased the pine board temperatures creating a vapour pressure gradient to drive moisture from the pine boards into the test box cavity surface to simulate sun driven moisture from cladding into the wall assembly. The apparatus was sealed during testing to avoid uncontrolled air leakage. By performing a moisture mass balance at the end of each test, the amount of moisture that was ventilated from the system was determined.

The laboratory tests began by examining how much moisture was removed through different venting configurations of the apparatus in the R22 Series. Modifications to the experimental procedure were incorporated into the R24 series. The main difference between the R22 Test Series and the R24 Test Series was the density of mineral fibre insulation used. The density of the R22 mineral fibre insulation was 37 kg/m^3 while the R24 insulation had a density of 55 kg/m^3. The higher density R24 insulation has better properties for testing than does the R22 mineral fibre insulation, including more consistent loft, higher density, and higher rigidity. The combination of these properties allowed confidence in the consistency of the clear airspace in the venting configuration.

The results of the laboratory experiments reveal that ventilation drying can occur through air permeable mineral fibre insulation providing appropriate vents are provided. Moisture was removed by ventilation when no clear airspace is provided in the venting configuration. When combined with a vent area ratio of 1175 mm^2/m^2, RSI 4.2 mineral fibre insulation is roughly equivalent to a 3 mm clear air space. Further, testing showed that a combination of mineral fibre insulation with a clear air space increases the amount of moisture removal than can be removed by ventilation.

The model simulations revealed that in a drying climate like Toronto ON, introducing ventilation into solid masonry wall assemblies reduces the average moisture content and relative humidity of the solid masonry walls. The amount of drying in the wall assemblies increases as the air space thickness increases and as the ventilation rate is increased. The simulations have shown that a vented air space as small as 3 mm can reduce the average moisture content and the relative humidity in the wall assembly.

Improving the drying potential of solid masonry walls that have been internally thermally retrofitted in heating climates means that embedded wood members will be less likely to decay and steel members less likely to corrode. Further, the masonry will less likely to reach its critical saturation point. Thus, using mineral fibre insulation coupled with appropriate vents can improve the durability of internally insulated solid masonry walls.

4.2 AREAS FOR FURTHER RESEARCH

Further laboratory testing should be conducted with different densities of air permeable insulation. Due to the relatively large thickness of the R22 and R24 insulation batts tested, it may be desirable to use a denser and more rigid mineral fibre insulation when internally insulating solid masonry walls. This would reduce infringement on interior space by the insulation. Laboratory testing with more rigid insulation should also investigate the potential for incorporating ventilation through air permeable insulation in low sloped roofs.

Field trials are necessary to assess the long-term performance of internally insulated walls featuring venting configurations with a combination of clear airspace and air permeable insulation. Field trials should attempt to compare the performance of venting configurations using air permeable insulation to the traditional retrofit approach of SPF against the interior face of the masonry, and also to the approach of adding a ventilated airspace between the SPF and the masonry. The field trials would be able to illustrate any negative impacts of introducing moisture into the mineral fibre insulation on the long-term thermal performance of the mineral fibre.

Bibliography

[1] Canada Green Building Council, "About Us - Canada Green Building Council - Greater Toronto Chapter," 2017. [Online]. Available: http://www.cagbctoronto.org/cagbc-toronto/about-us. [Accessed: 11-Jun-2017].

[2] N. R. C. Government of Canada, "Residential Sector Canada Table 2: Secondary Energy Use and GHG Emissions by End-Use." [Online]. Available: http://oee.nrcan.gc.ca/corporate/statistics/neud/dpa/showTable.cfm?type=CP&sector=res&juris=ca&rn=2&page=0. [Accessed: 11-Jun-2017].

[3] J. W. Lstiburek, "Deep-dish retrofits," 2014. Available: https://buildingscience.com/documents/insights/bsi079-deep-dish-retrofits

[4] D. F. Laefer, J. Boggs, and N. Cooper, "Engineering Properties of Historic Brick: Variability Considerations as a Function of Stationary versus Nonstationary Kiln Types," Journal American Institute of Conservation., vol. 43, no. 3, pp. 255–272, Jan. 2004.

[5] J. Der Ananian and S. O'Brian, "Using Measured Data to More Accurately Evaluate Freeze-Thaw Risk When Insulating Solid Masonry Walls." Available: http://www.techstreet.com/standards/using-measured-data-to-more-accurately-evaluate-freeze-thaw-risk-when-insulating-solid-masonry-walls?product_id=1883924

[6] J. Straube, C. Schumacher, and P. Mensinga, "Assessing the Freeze-Thaw Resistance of Clay Brick for Interior Insulation Retrofit Projects," in Proceedings of Buildings XI ASHRAE Conference, 2010.

[7] J. W. Lstiburek, "Thick as a Brick." 2011. Available: https://buildingscience.com/documents/insights/bsi-047-thick-as-brick

[8] B. Straube, John Eric, "Building Science for Building Enclosure Design." Building Science Press, 2005.

[9] M. Guizzardi, J. Carmeliet, and D. Derome, "Risk analysis of biodeterioration of wooden beams embedded in internally insulated masonry walls," Construction Building Materials, vol. 99, pp. 159–168, Nov. 2015.

[10] D. De Rose, N. T. Pearson, P. Mensinga, and J. Straube, "Towards a Limit States Approach to Insulating Solid Masonry Walls in a Cold Climate." Available: http://obec.on.ca/sites/default/uploads/files/members/CCBST-Oct-2014/B6-7-a.pdf

[11] T. P. O'Leary, G. Menzies, and A. Duffy, "The Design of a Modelling, Monitoring and Validation Method for a Solid Wall Structure," Energy Procedia, vol. 78, pp. 243–248, 2015.

[12] J. Little, C. Ferraro, and B. Arregi, "Assessing risks in insulation retrofits using hygrothermal software tools," 2015. Available: https://www.researchgate.net/profile/Joseph_Little4/publication/283710903_Assessing_risks_in_insulation_retrofits_using_hygrothermal_software_tools_-_Heat_and_moisture_transport_in_internally_insulated_stone_walls/links/5643a40908aef646e6c6c367.pdf

[13] J. Straube, R. VanStraaten, E. Burnett, and C. Schumacher, “ASHRAE 1091 - Development of Design Strategies for Rainscreen and Sheathing Membrane Performance in Wood Frame Walls.” Tech. Rep., 2004.

[14] Popp, Meyer, and Keunzel, “Untersuchungen über die not- wendige hinterlüftung an auenwandbekeidung aus grofor- matigen bauteilen,” Fraunhofer Institut fur Bauphysik, Forschungsbericht B Ho, Tech. Rep., 1983.

[15] T. K. Stovall and A. N. Karagiozis, “Airflow in the ventilation space behind a rain screen wall,” in Proceedings of Buildings IX ASHRAE Conference, 2010.

[16] M. Salonvarra, A. N. Karagiozis, M. Pazera, and W. Miller, “Air Cavities Behind Claddings-What Have We Learned?” Tech. Rep., 2007

[17] A. N. Karagiozis and H. M. Kuenzel, “The effect of air cavity convection on the wetting and drying behavior of wood-frame walls using a multi-physics approach,” Journal ASTM International, vol. 6, no. 10, pp. 1–15, 2009.

[18] J. Langmans, T. Z. Desta, L. Alderweireldt, and S. Roels, “Experimental Analysis of Cavity Ventilation Behind Residential Rainscreen Cladding Systems,” *Energy Procedia*, vol. 78, pp. 1750–1755, Nov. 2015.

[19] M. H. Hansen and A. Nicolajsen, “On the influence of cavity ventilation on moisture content in timber frame walls,” in *Proceedings of the 6th Symposium on Building Physics in the Nordic Countries*, 2002.

[20] J. Straube and E. Burnett, “Vents, Ventilation, and Masonry Veneer Wall Systems,” 1998. Available: http://www.civil.uwaterloo.ca/beg/downloads/8th-masonry_ventilated_bv.pdf.

[21] N. T. Pearson, “An Investigation of the Heat and Moisture Performance of a Ventilated Masonry Retrofit for Historic Structures,” MASc. Thesis, Department of Civil Engineering, University of Toronto, 2009.

[22] E. Tzekova, “Improving the Thermal Performance and Durability of Historic Masonry Buildings.” PhD. Thesis, Department of Civil Engineering, University of Toronto, 2015.

[23] SMT, “SMT A2 Datasheet”, 2017. [Online] Available http://smtresearch.ca

[24] Dupont, “SPEC-31 - Physical Properties Data Sheet- DuPont Tyvek HomeWrap.pdf,” 2017. [Online]. Available: http://www.dupont.ca/content/dam/assets/products-and-services/construction-materials/assets/SPEC-31%20-%20Physical%20Properties%20Data%20Sheet-%20DuPont%20Tyvek%20HomeWrap.pdf.

Appendix A: Laboratory Wall Construction – Photos

Photograph 1: View of unloaded test box.

Photograph 2: View of test box loaded with mineral fibre insulation.

Photograph 3: View of partially installed pine siding boards.

Photograph 4: View clear airspace between pine siding boards and mineral fibre insulation.

Photograph 5: View of sealed test box.

Photograph 6: View of test box installed in wall section and light array.

Appendix B: Laboratory Testing – R22 Series

Test	Insulation Type	Clear Airspace	Vent Area Ratio (mm^2 / m^2)	Moisture Lost from Wood Siding (g)	Moisture Found in Wall (g)	Moisture Lost During Assembly / Disassembly (g)
Base	R22	None	None	215.3	95.3 insulation 26.2 cavity/rails 17.0 poly	11.3 assembly 43.9 disassembly
2A	R22 (re-used)	None (6 mm batt compression)	1175	250.4	112.8 insulation 37.9 cavity 9.7 poly	14.1 assembly 41.3 disassembly
2B	R22	None (6 mm batt compression)	1175	222.1	82.0 insulation 49.7 cavity 7.0 poly	14.1 assembly 28.5 disassembly
2C	R22	None (6mm batt compression)	1175	222.0	98.6 insulation 45.4 cavity 7.9 poly	15.6 assembly 20.8 disassembly
2D	R22 (re-used)	None (6 mm batt compression)	1175	238.0	102.5 insulation 45.7 cavity 9.4 poly	14.1 assembly 17.0 disassembly
3A	R22	6mm	1175	221.3	78.2 insulation 31.4 cavity 9.8 poly	17.0 assembly 26.2 disassembly
3B	R22	6mm	1175	274.8	84.3 insulation 34.9 cavity 6.5 poly	12.7 assembly 47.7 disassembly
4A	R22	None	1175	224.6	87.3 insulation 36.7 cavity 16.9 poly	14.1 assembly 33.4 disassembly
4B	R22	None	1175	254.8	119.7 insulation 49.2 cavity 7.3 poly	15.6 assembly 21.7 disassembly
5A	R22 (re-used)	13 mm	1175	272.6	25.1 insulation 21.8 cavity 5.4 poly	14.1 assembly 28.8 disassembly
6A	R22 (re-used)	19 mm	1175	289.5	22.5 insulation 22.8 cavity 7.5 poly	14.1 assembly 25.0 disassembly

Table B.1 – R22 Series Testing Summary Part 1

Test	Guard Room 2 Ambient Temp T_a (°C)	Pine Surface Temp T_s (°C)	Difference T_s - T_a	Inboard Surface Pine Temp (°C)	Insulation / Box Cavity Interface Temp (°C)	Vapour Pressure Difference (Pa)
Base	18.7	48.3	29.6	41.9	24.7	5067
2A	19.1	44.4	25.3	36.1	24.6	2873
2B	18.2	46.6	28.4	35.1	23.7	2734
2C	17.9	44.3	26.4	40.5	23.1	4748
2D	18.3	50.1	31.8	37.2	23.8	3406
3A	18.9	47.6	28.7	35.0	23.3	2767
3B	18.6	48.0	29.4	36.5	23.0	3307
4A	19.1	46.4	27.3	36.0	25.1	2766
4B	18.0	47.1	29.1	34.9	23.4	2798
5A	18.3	44.2	25.9	32.2	21.2	2309
6A	18.6	41.8	23.2	30.2	20.5	1875

Table B.2 – R22 Series Testing Summary Part 2

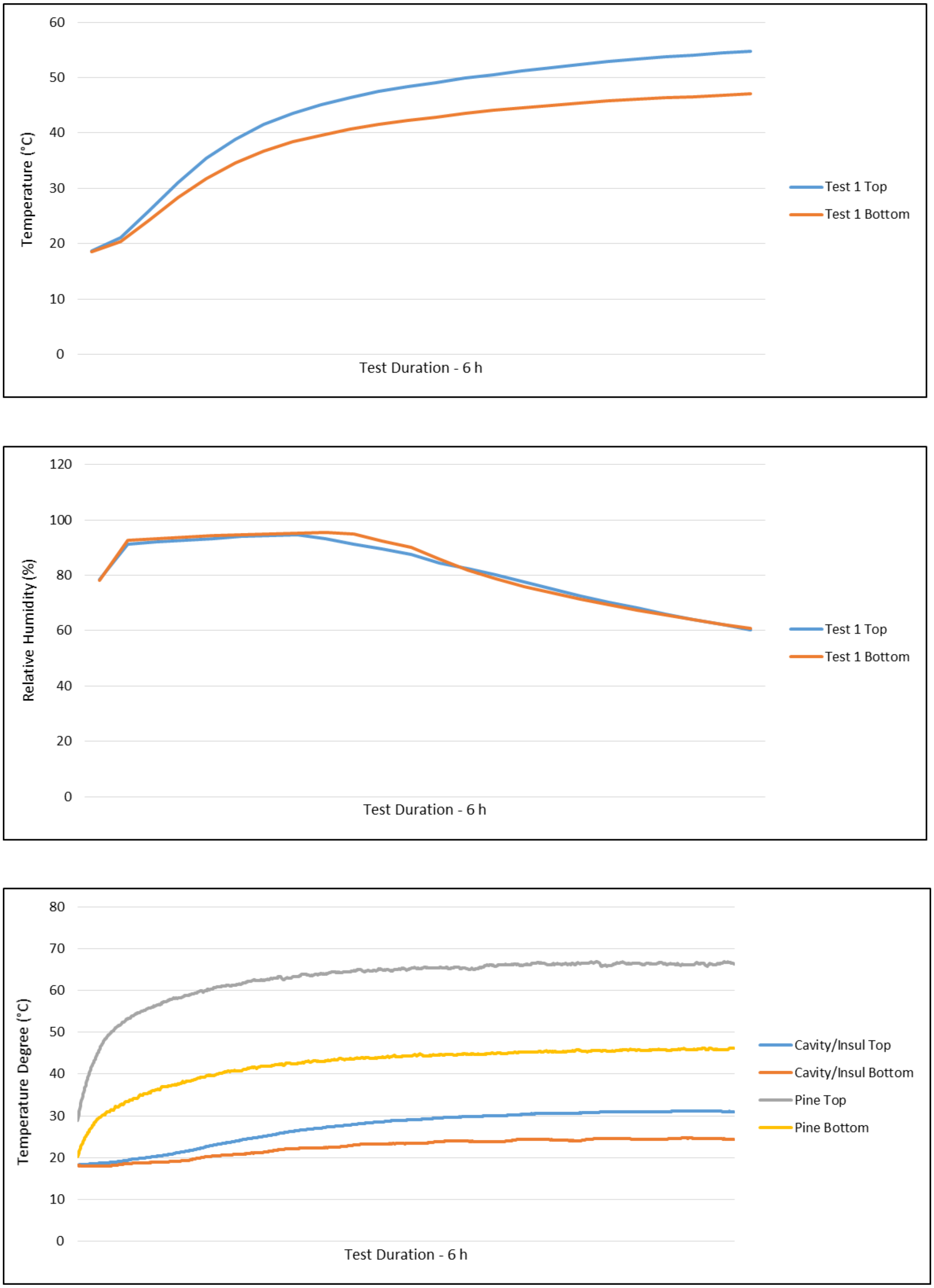

Figure B.1 – Base Test Laboratory Data

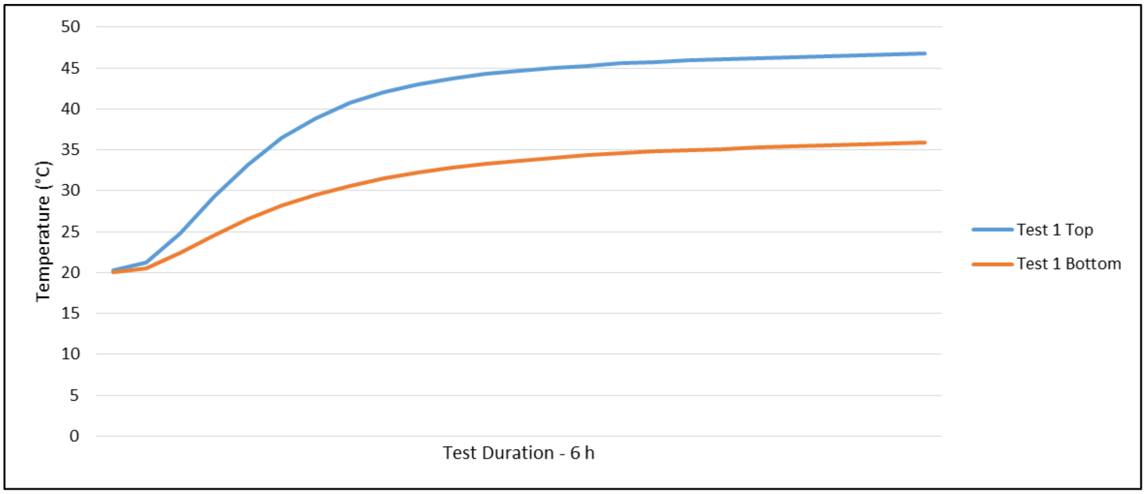

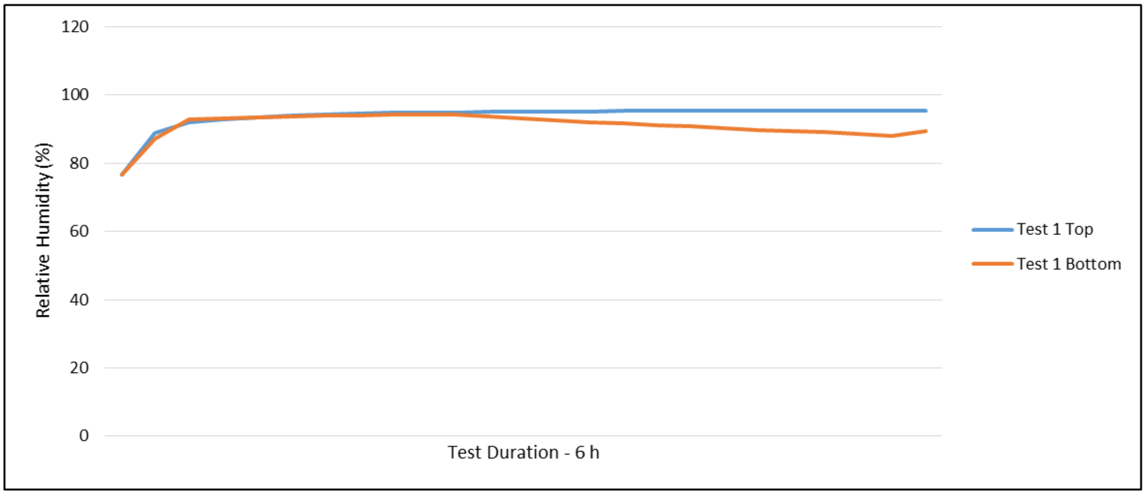

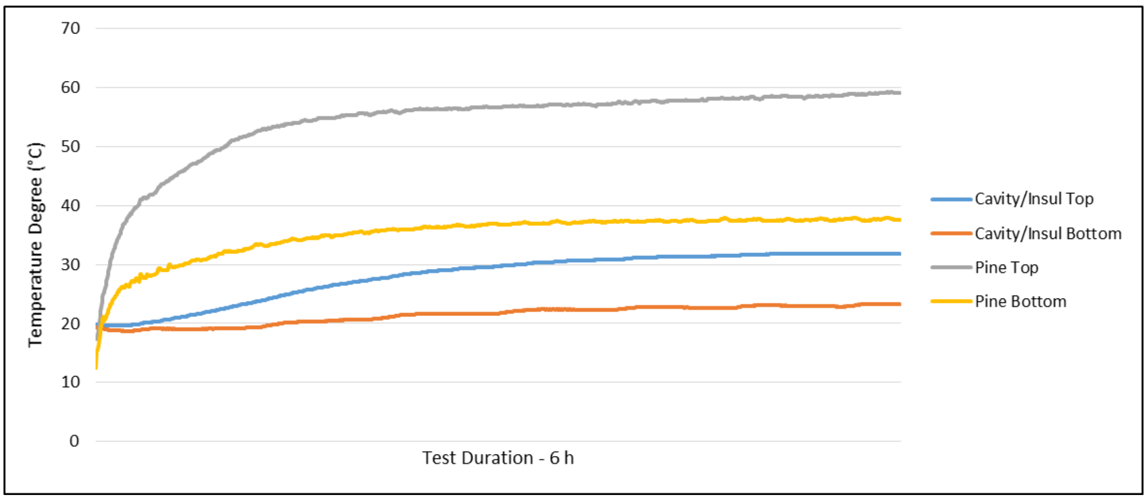

Figure B.2 – Test 2A Laboratory Data

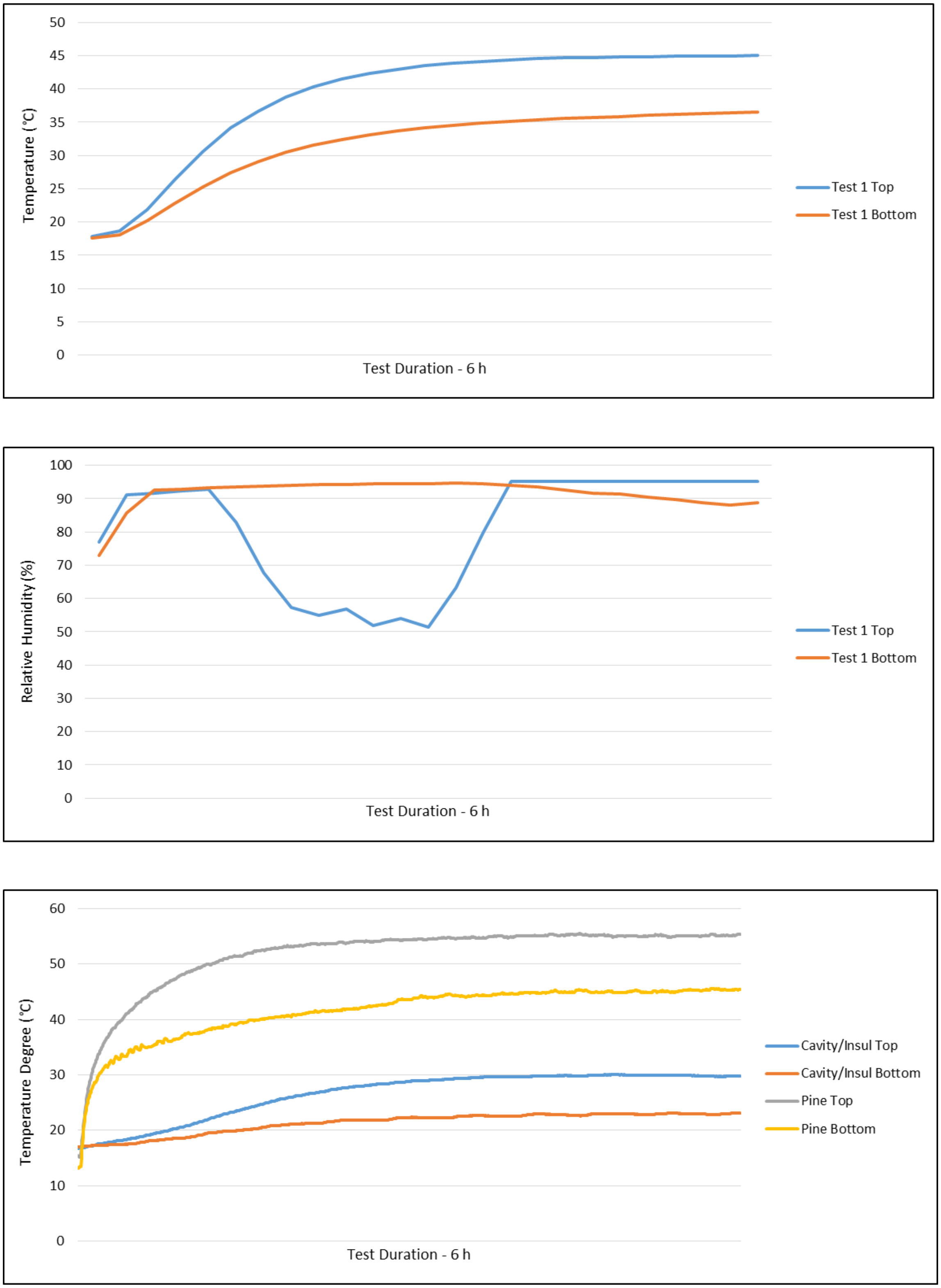

Figure B.3 – Test 2B Laboratory Data

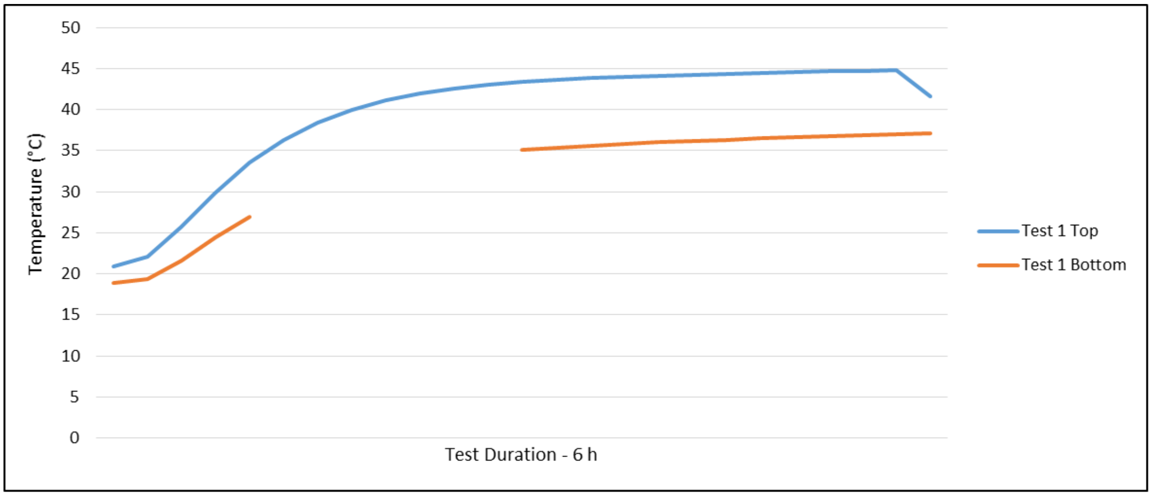

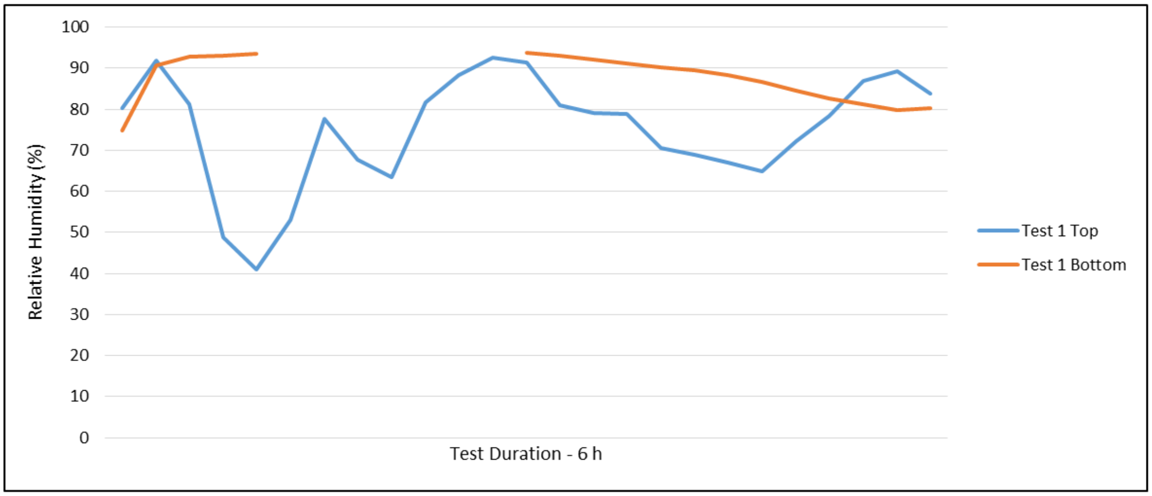

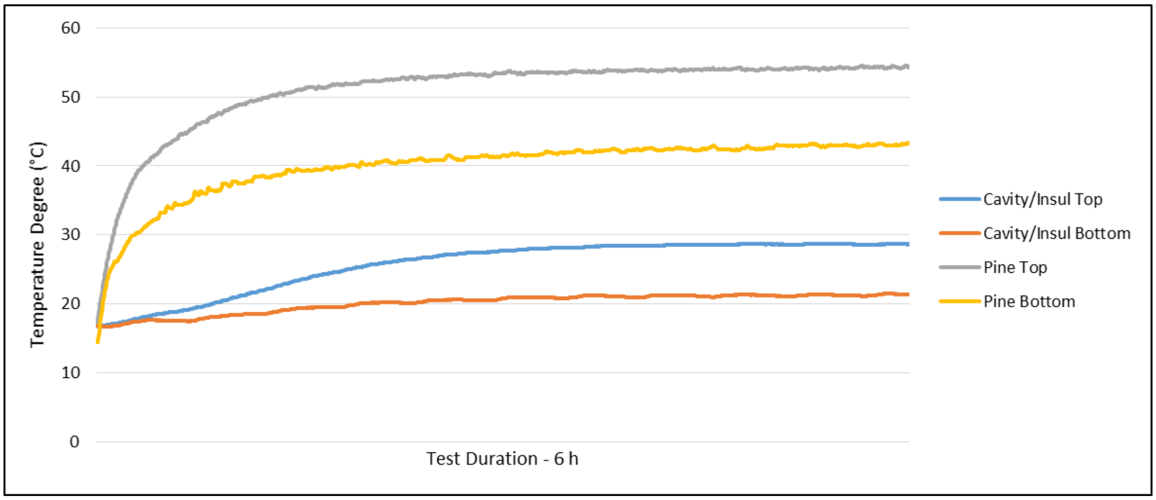

Figure B.4 – Test 2C Laboratory Data

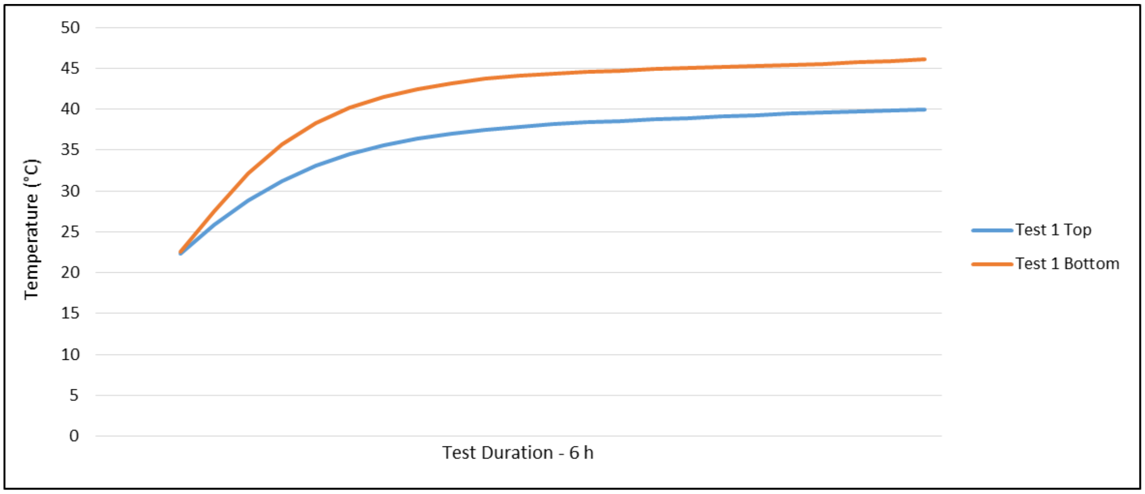

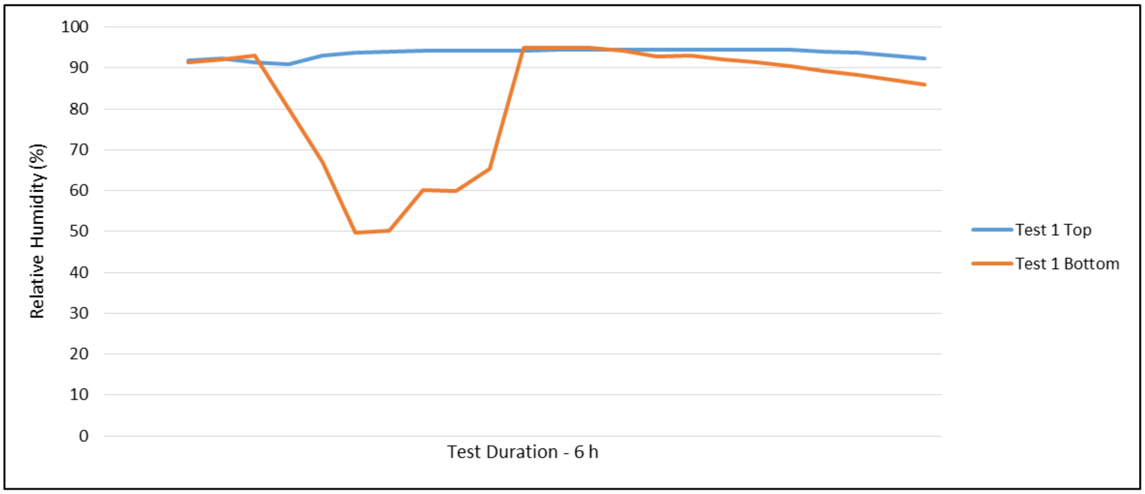

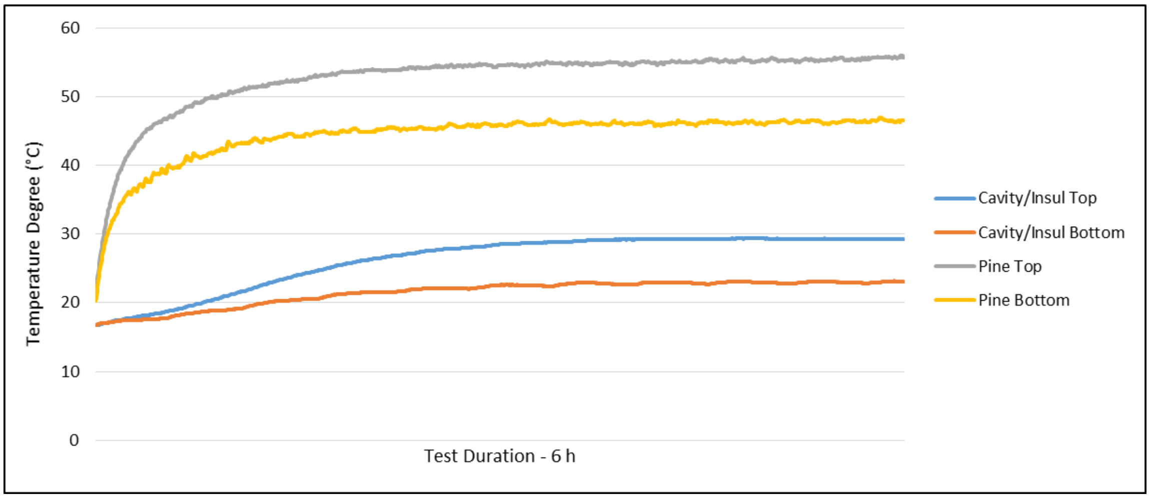

Figure B.5 – Test 2D Laboratory Data

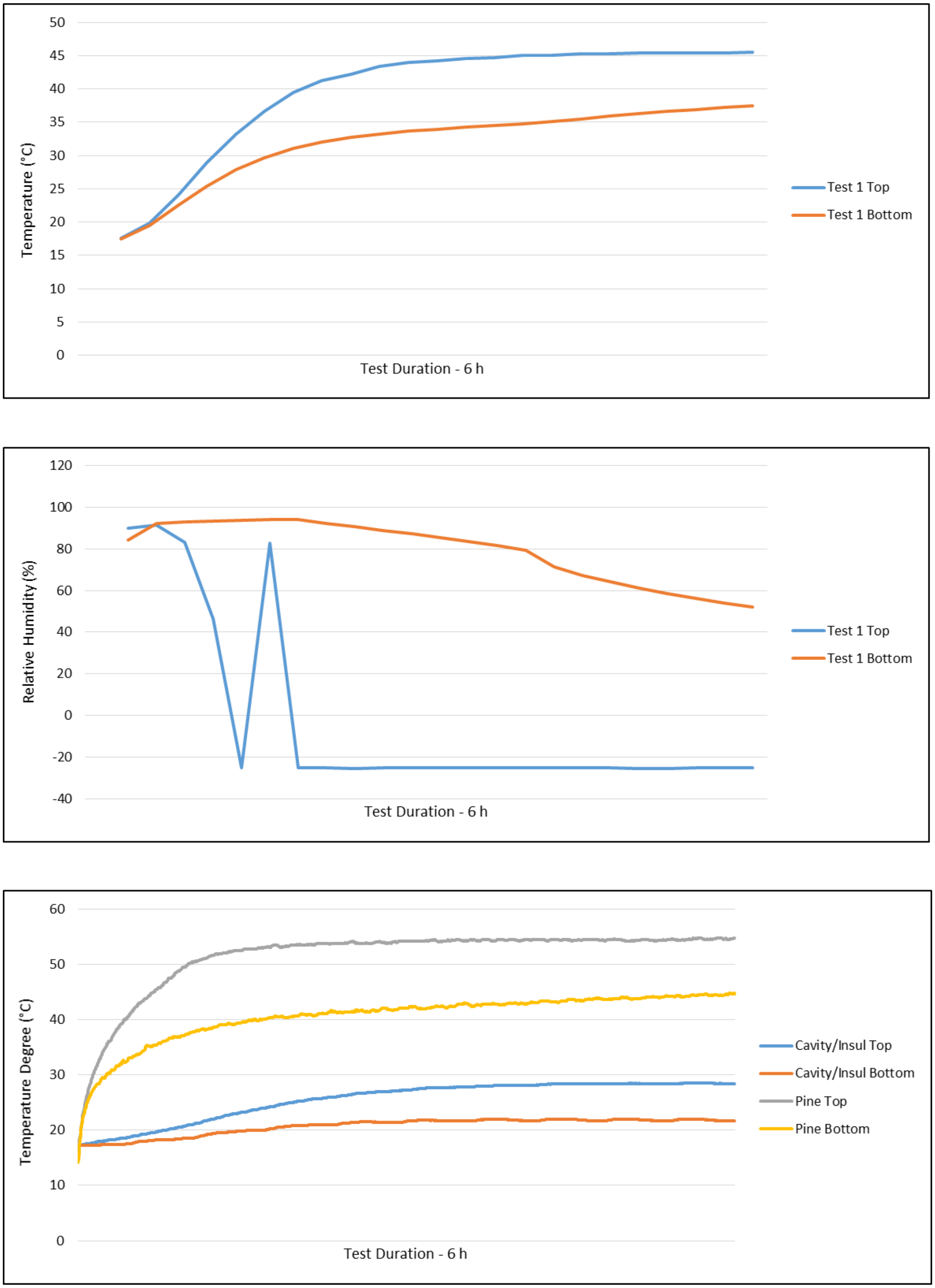

Figure B.6 – Test 3A Laboratory Data

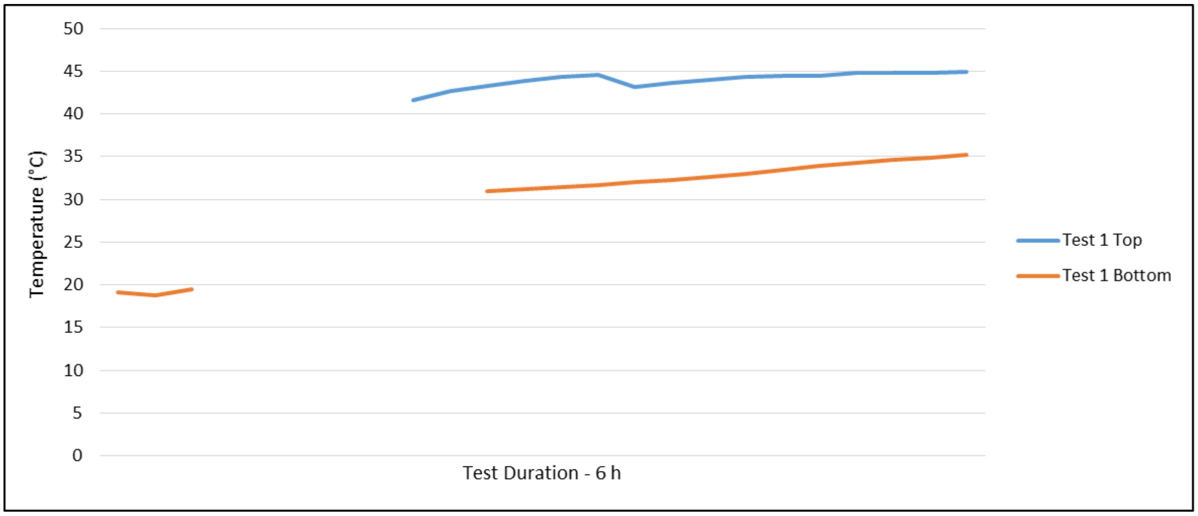

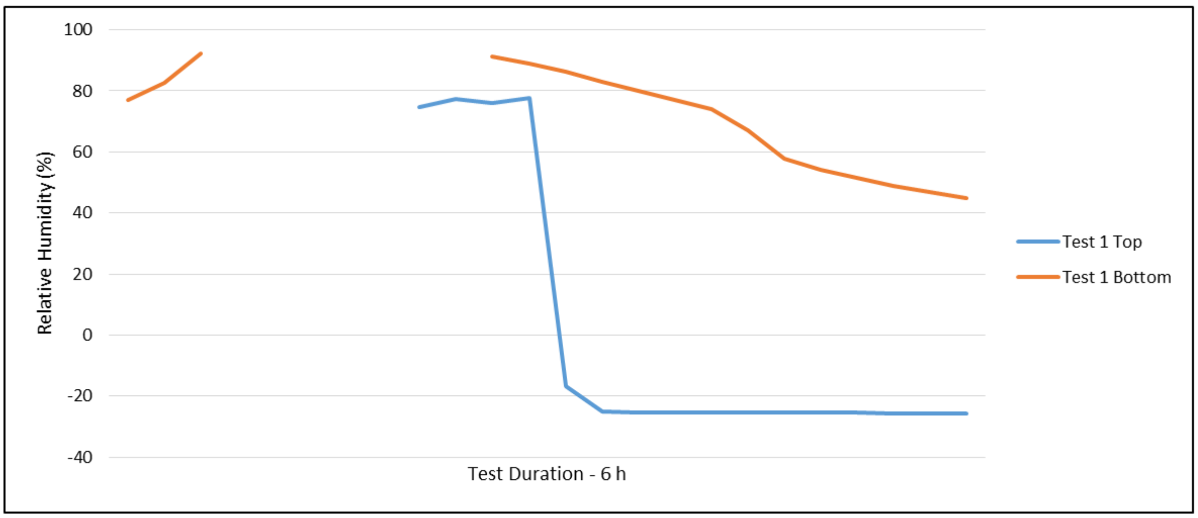

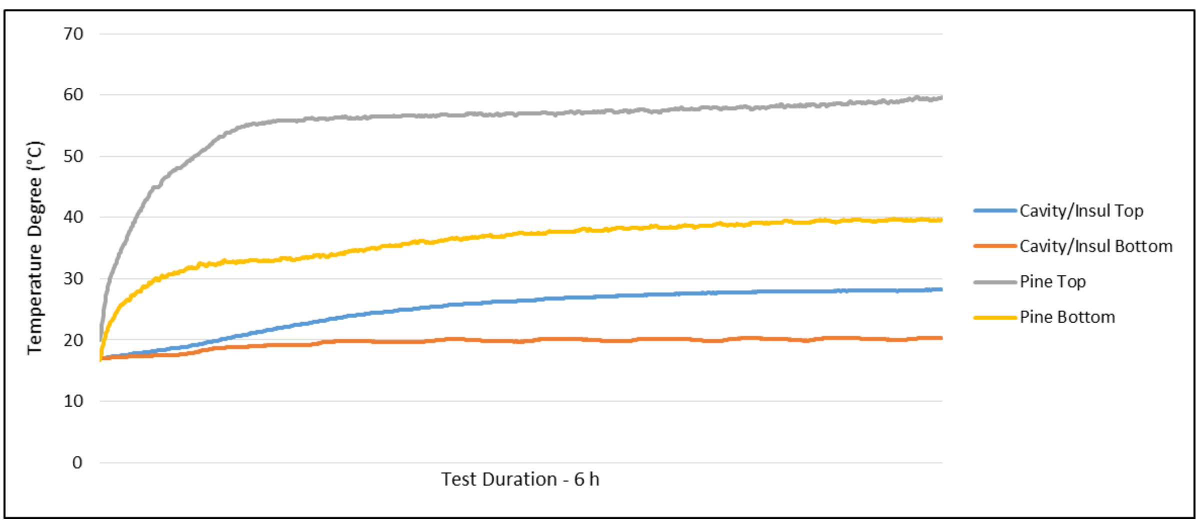

Figure B.7 – Test 3B Laboratory Data

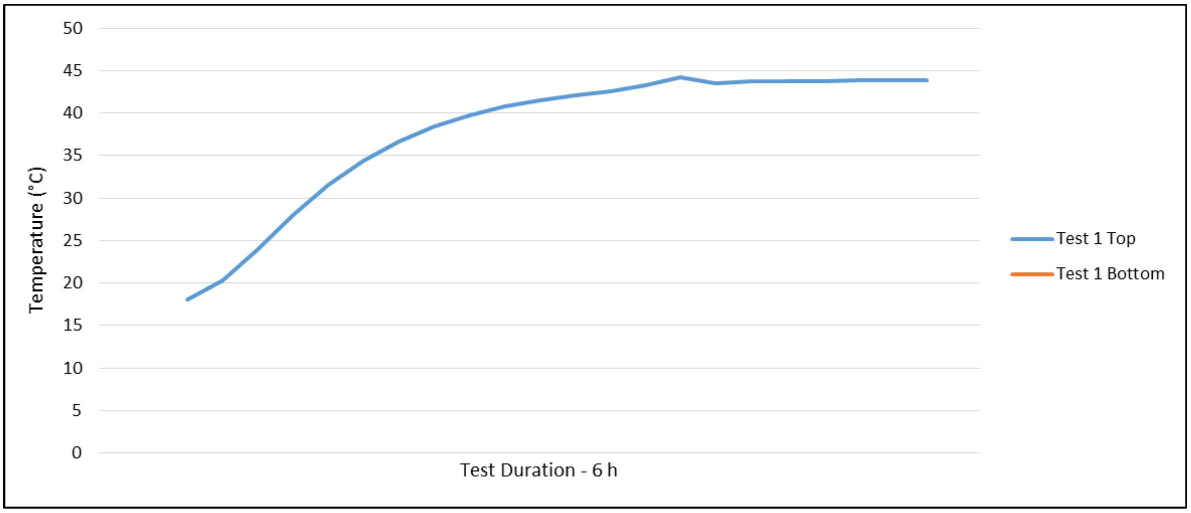

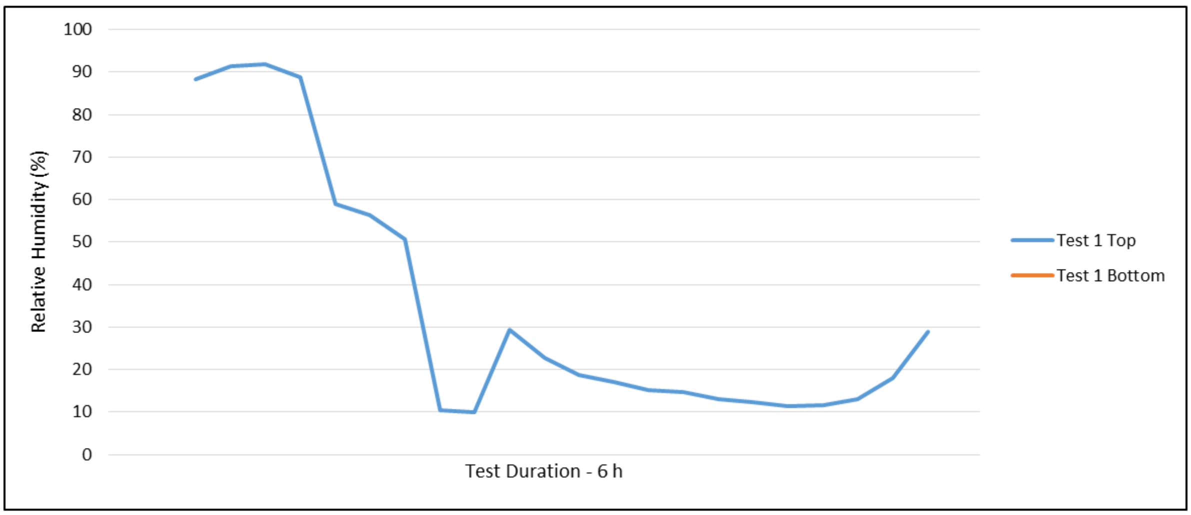

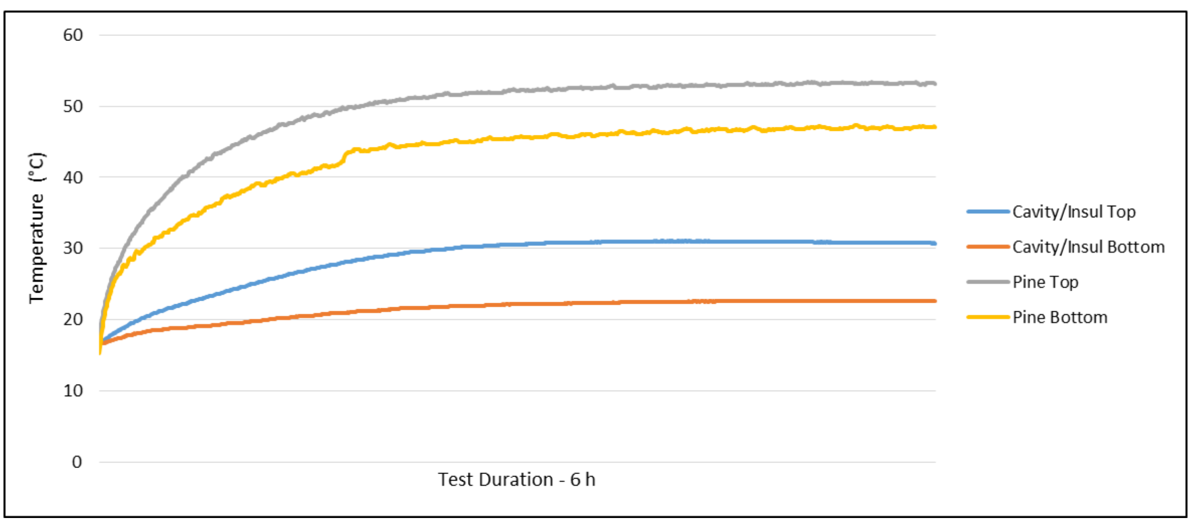

Figure B.8 – Test 4A Laboratory Data

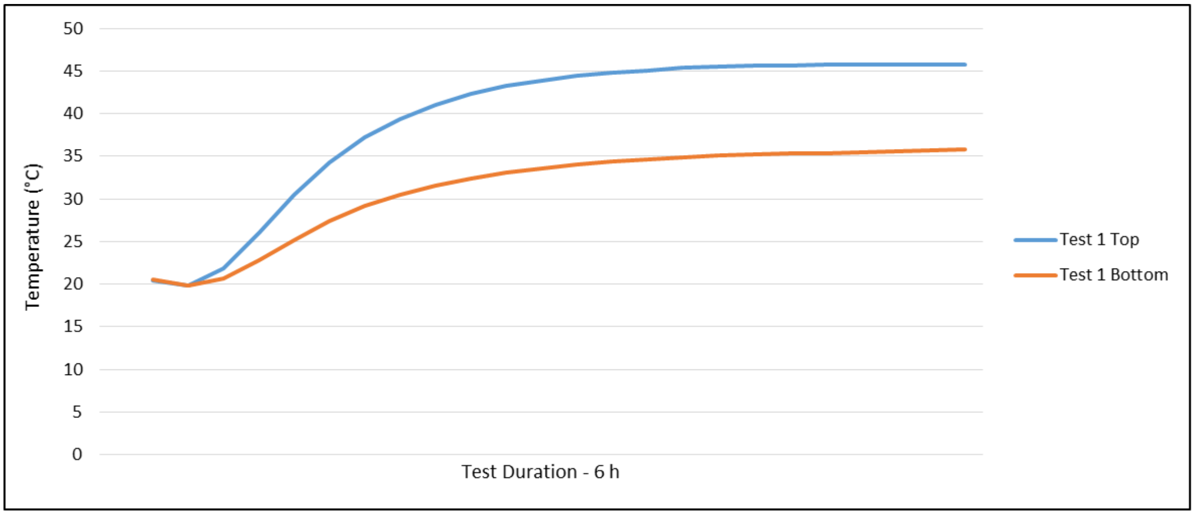

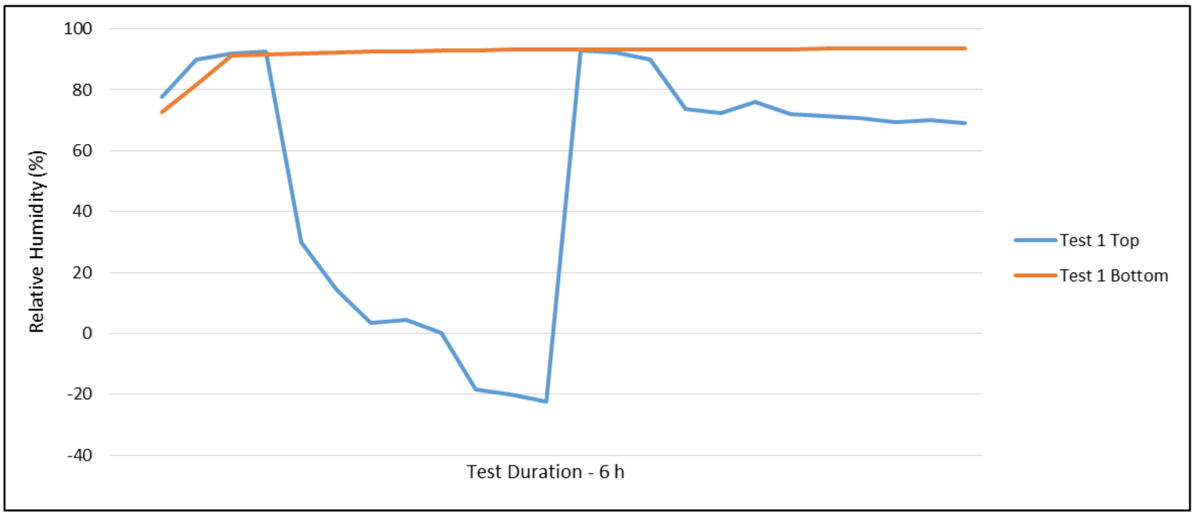

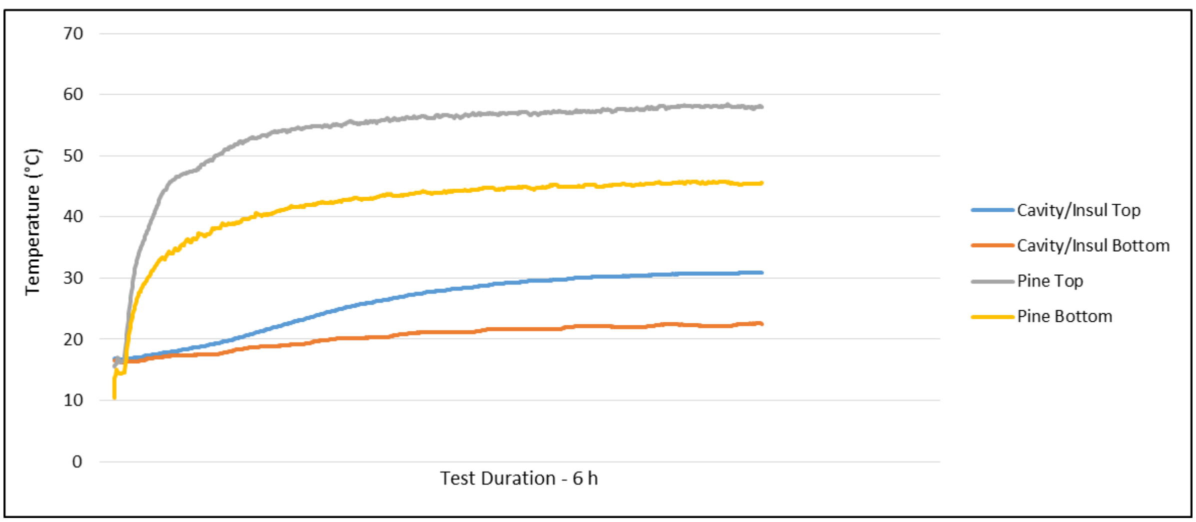

Figure B.9 – Test 4B Laboratory Data

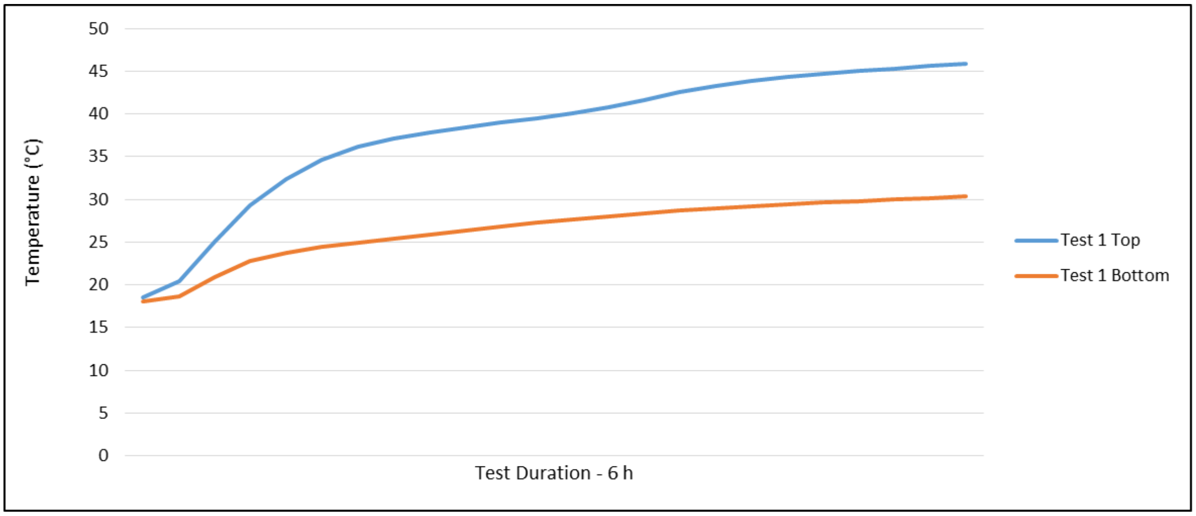

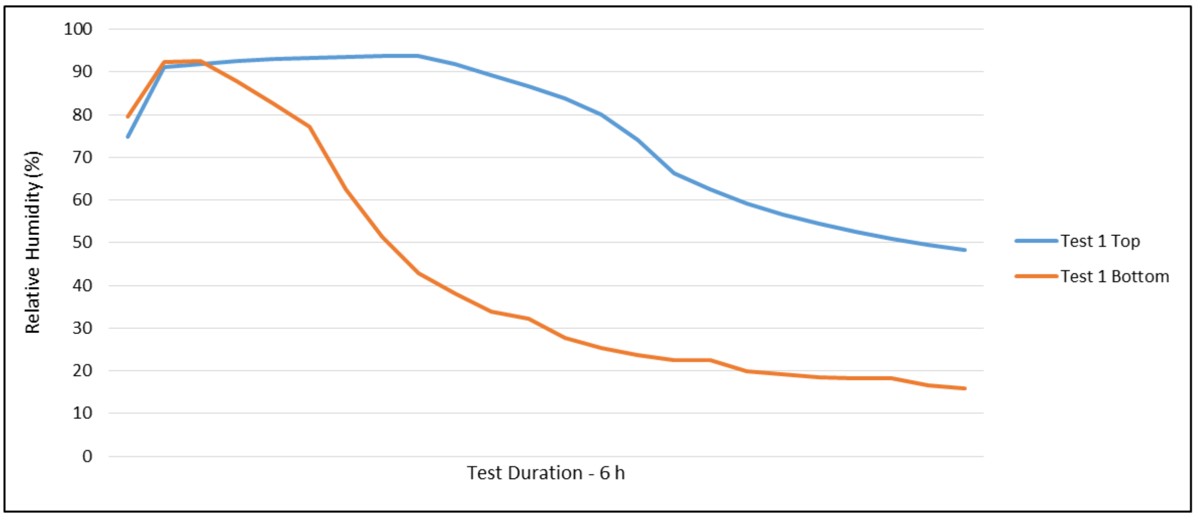

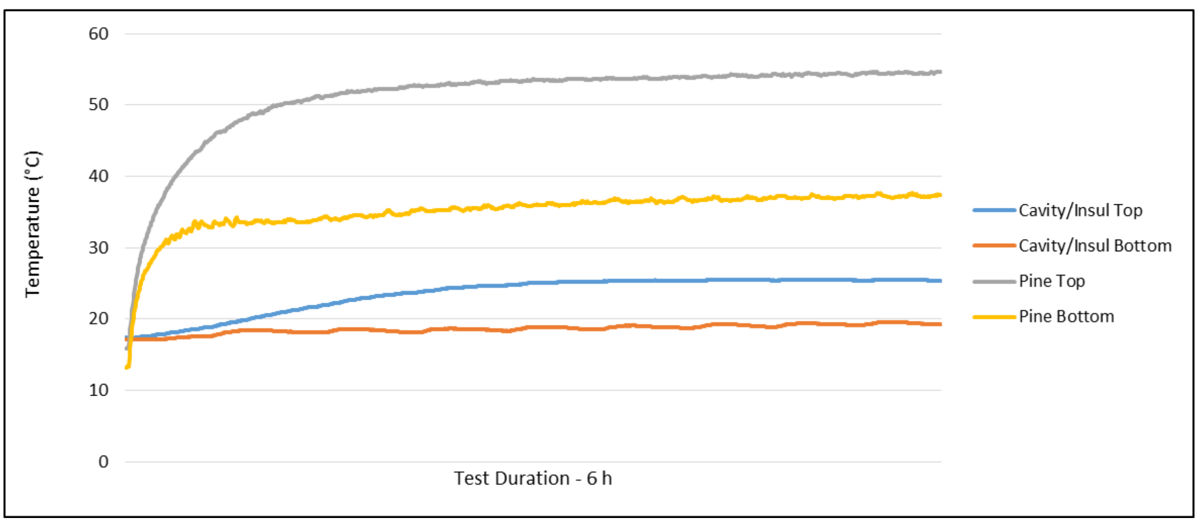

Figure B.10 – Test 5A Laboratory Data

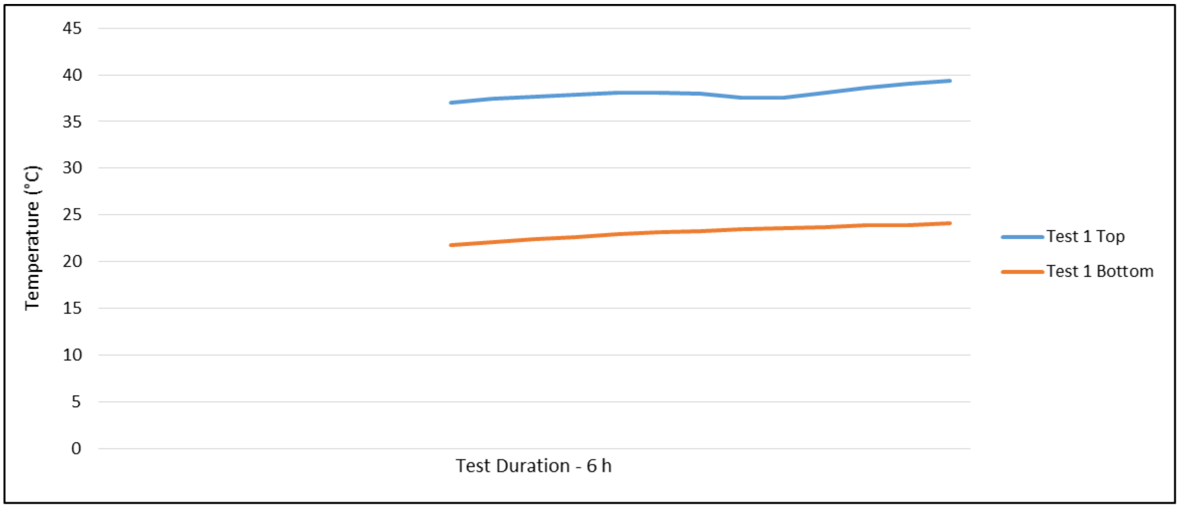

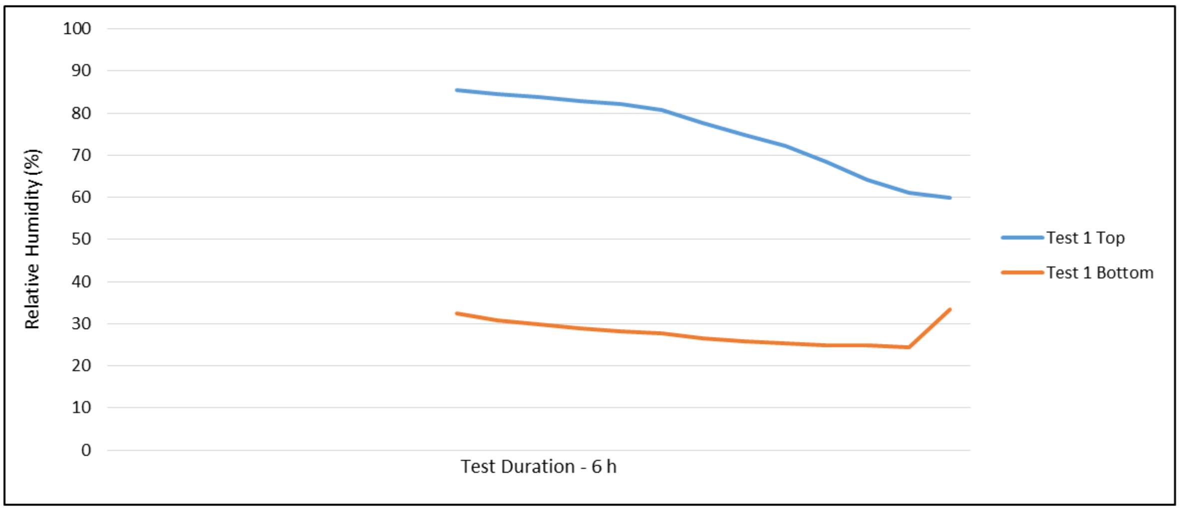

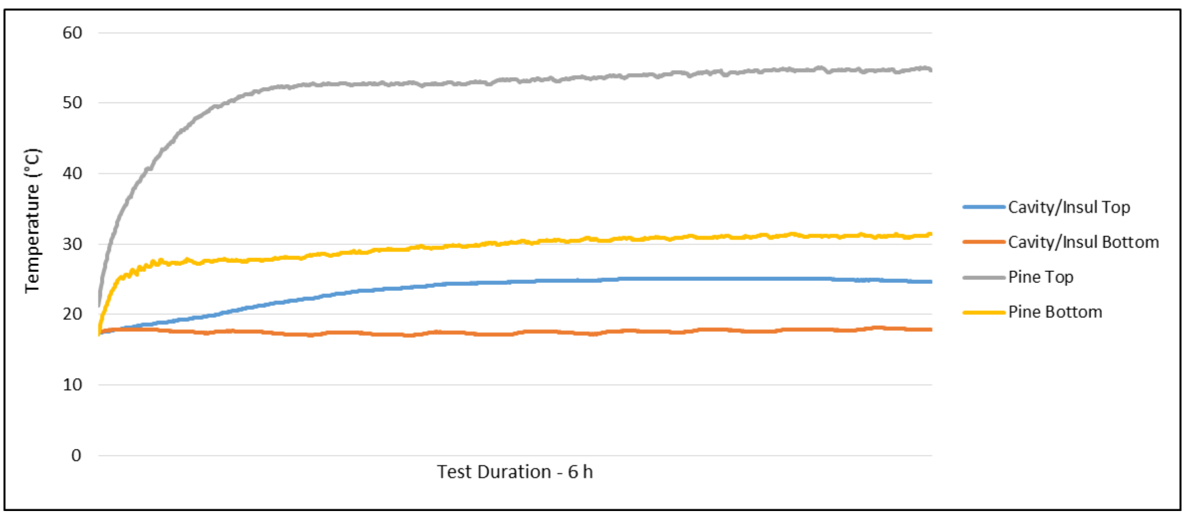

Figure B.11 – Test 6A Laboratory Data

Appendix C: Laboratory Testing – R24 Series

Test	Insulation Type	Clear Airspace Thickness	Vent Area Ratio (mm^2 / m^2)	Moisture Lost from Wood Siding (g)	Moisture Found in Wall (g)	Moisture Lost During Assembly / Disassembly (g)
8A	R-24	6mm	1175	241	22.4 insulation 10.5 cavity/rails 16.9 poly	14.1 assembly 19.7 disassembly
8B	R-24	6mm	1175	282	37.1 insulation 16.9 cavity/rails 6.6 poly	14.1 assembly 17.5 disassembly
8C	R-24	6mm	1175	292	61.8 insulation 36.2 cavity/rails 6.3 poly	12.7 assembly 20.0 disassembly
9A	R-24	None	1175	219	85.1 insulation 32.0 cavity/rails 7.1 poly	12.7 assembly 20.2 disassembly
9B	R-24	None	1175	215	78.4 insulation 31.9 cavity/rails 6.8 poly	11.3 assembly 21.3 disassembly
9C	R-24	None	1175	243	95.6 insulation 37.2 cavity/rails 7.3 poly	11.3 assembly 19.7 disassembly
10A	R-24	10mm SBPO	1175	296	3.5 insulation 8.7 cavity/rails 4.5 Tyvek 7.3.9 poly	11.3 assembly 20.8 disassembly
11A	R-24	0mm (C)	1175	232	91.9 insulation 26.8 cavity/rails 16.4 poly	14.1 assembly 25.1 disassembly
11B	R-24	0mm (C)	1175	252	109.7 insulation 35.6 cavity/rails 4.5 poly	12.7 assembly 27.3 disassembly
11C	R-24	0mm (C)	1175	238	109.1 insulation 22.8 cavity/rails 14.3 poly	12.7 assembly 18.4 disassembly
12A	R-24	6mm SBPO	1175	288	18.0 insulation 27.7 cavity/rails 5.3 Tyvek 7.5 poly	12.7 assembly 19.5 disassembly
13A	R-24	3mm	1175	288	86.4 insulation 22.2 cavity/rails 8.9 poly	12.7 assembly 29.1 disassembly
13B	R-24	3mm	1175	281	49.1 insulation 27.8 cavity/rails 8.8 poly	14.1 assembly 27.1 disassembly
13C	R-24	3mm	1175	261	84.9 insulation 26.2 cavity/rails 11.5.9 poly	12.7 assembly 24.6 disassembly
13D	R-24	3mm	1175	276	65.1 insulation 42.5 cavity/rails 8.6 poly	12.7 assembly 22.0 disassembly

14A	R-24	0mm (C)	2350	237	89.1 insulation 39.7 cavity/rails 12.6 poly	12.7 assembly 26.2 disassembly
15A	R-24	0mm	2350	216	71.5 insulation 38.5 cavity/rails 8.4 poly	12.7 assembly 28.3 disassembly
16A	R-24	3mm	2350	290	78.0 insulation 36.7 cavity/rails 9.1 poly	12.7 assembly 19.3 disassembly
16B	R-24	3mm	2350	262	88.3 insulation 36.4 cavity/rails 16.8 poly	12.7 assembly 25.7 disassembly
17A	R-24	6mm	2350	288	50.3.4 insulation 25.2 cavity/rails 20.8 poly	12.7 assembly 19.7 disassembly

Table C.1 – R24 Series Testing Summary Part 1

Test	Guard Room 2 Ambient Temp T_a (°C)	Pine Surface Temp T_s (°C)	Difference T_s - T_a	Inboard Surface Pine Temp (°C)	Insulation / Box Cavity Interface Temp (°C)	Vapour Pressure Difference (Pa)
8A	18.7	48.3	29.6	29.6	24.7	1037
8B	18.3	45.7	27.3	29.2	21.5	1489
8C	17.9	44.8	26.9	31.1	22.1	1873
9A	18.5	47.5	29.0	36.1	22.9	3180
9B	18.1	49.0	30.9	36.4	23.0	3272
9C	18.5	47.2	28.7	38.7	23.0	4089
10A	18.1	48.5	30.4	29.9	20.7	1756
11A	18.6	47.1	28.5	34.6	23.4	2635
11B	17.8	50.1	32.3	36.9	23.5	3335
11C	17.9	49.6	31.7	36.8	23.6	3299
12A	18.5	47.5	28.9	29.9	20.9	1789
13A	18.8	48.7	29.9	35.2	23.4	2805
13B	18.1	46.8	28.7	31.0	21.4	1941
13C	17.9	45.6	27.6	36.4	22.4	3371
13D	18.0	43.7	25.7	30.9	21.8	1866
14A	17.8	47.2	29.5	38.1	23.4	3777
15A	17.8	46.4	28.6	40.4	21.1	5044
16A	17.9	46.6	28.7	37.0	22.6	3532
16B	18.1	47.4	29.3	36.3	21.2	3536
17A	18.0	47.4	29.4	31.9	22.2	2049

Table C.2 – R24 Series Testing Summary Part 2

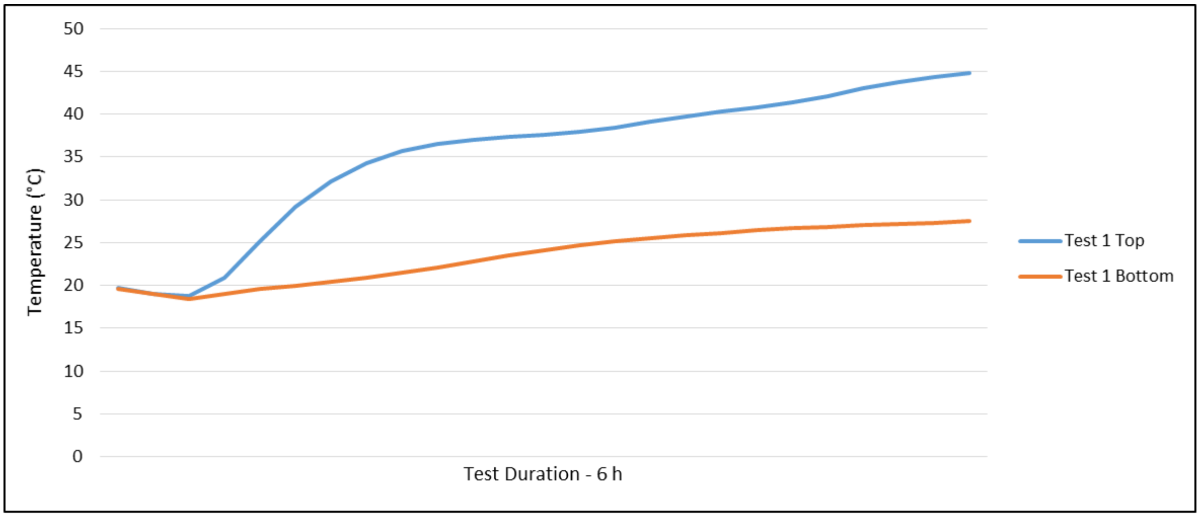

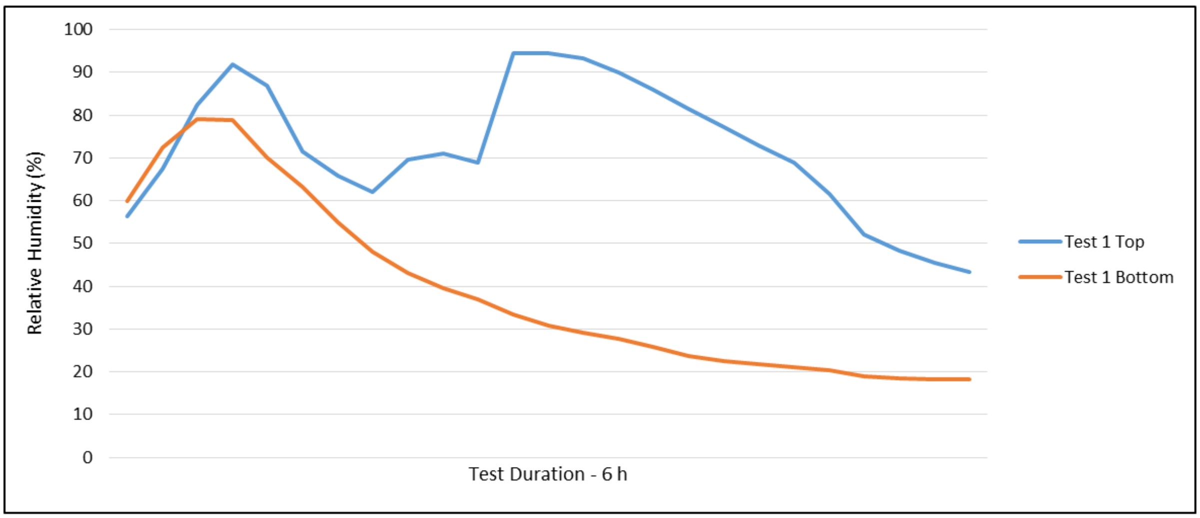

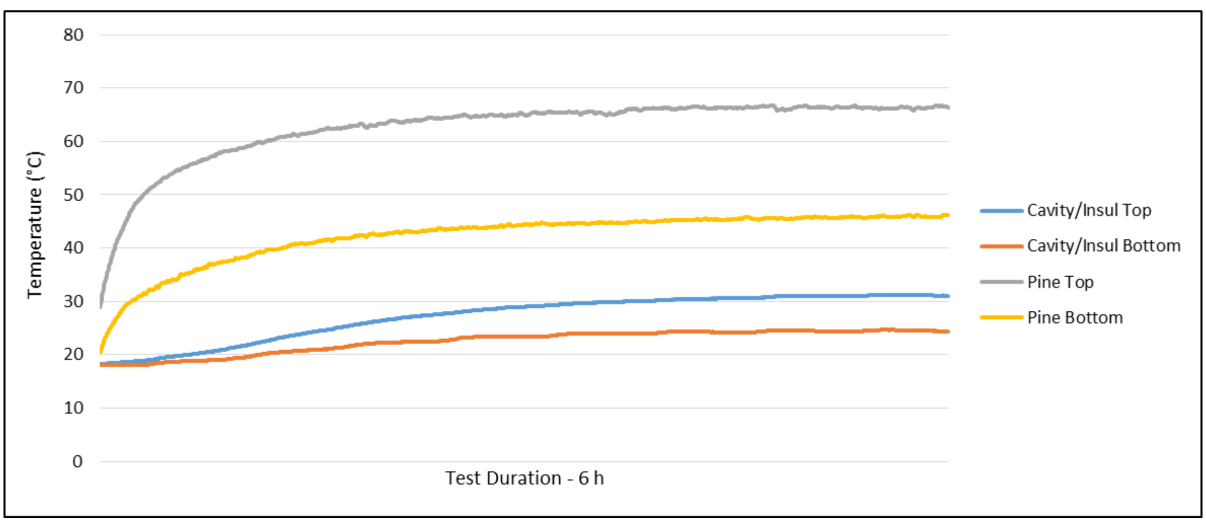

Figure C.1 – Test 8A Laboratory Data

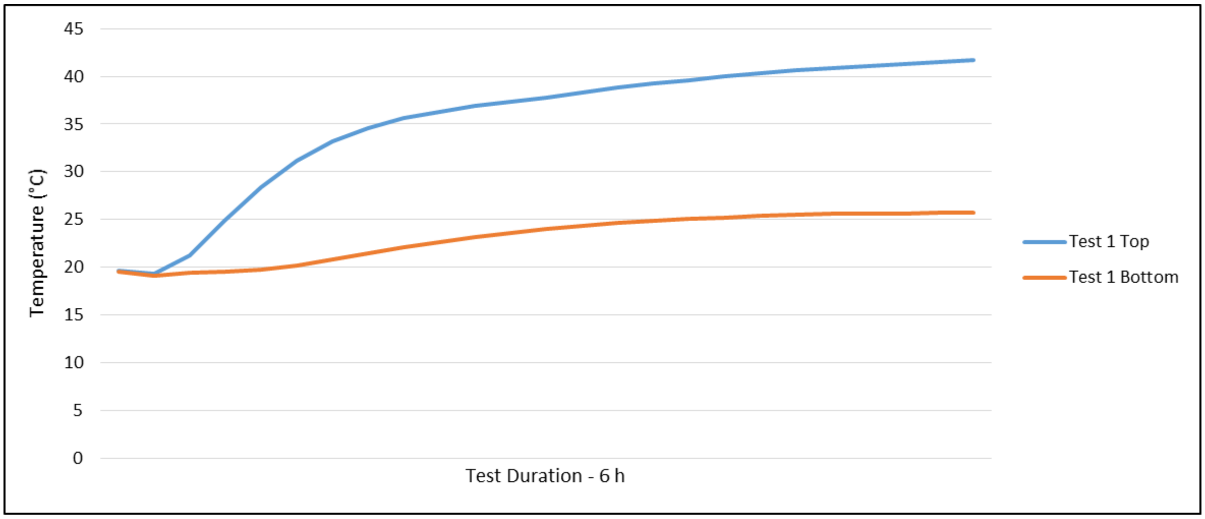

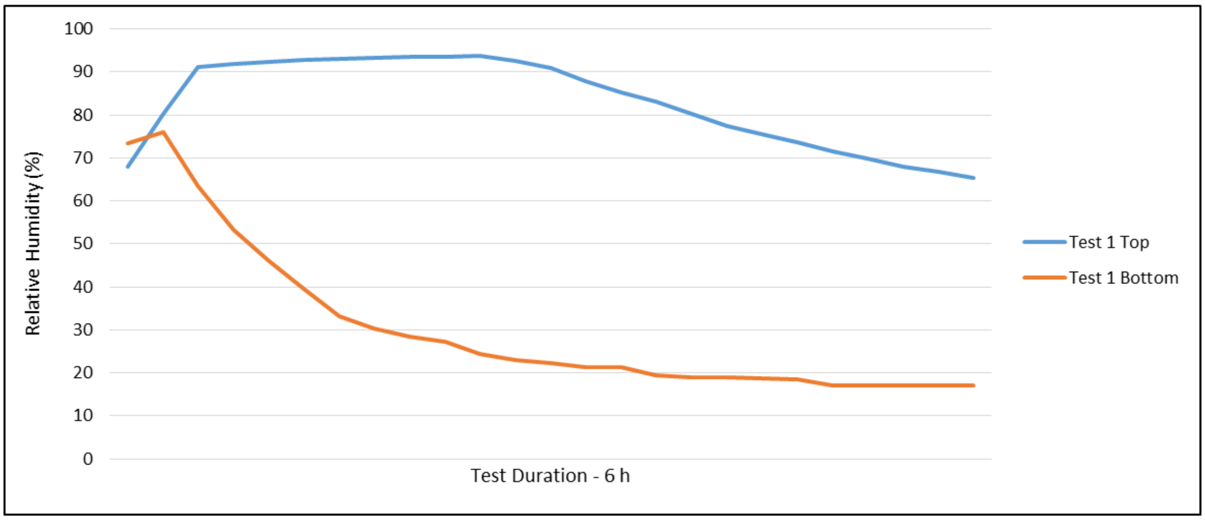

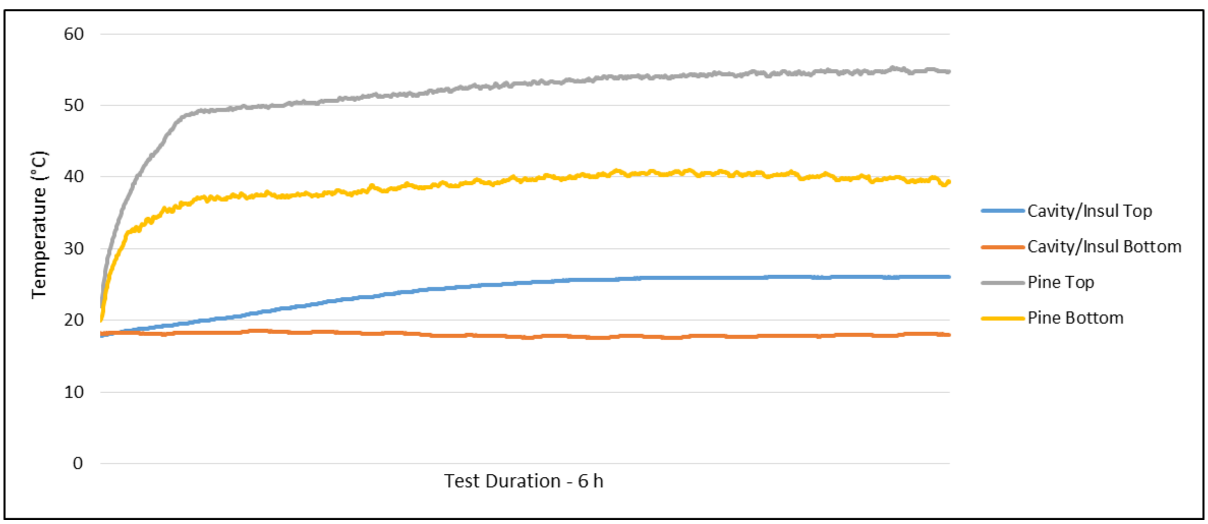

Figure C.2 – Test 8B Laboratory Data

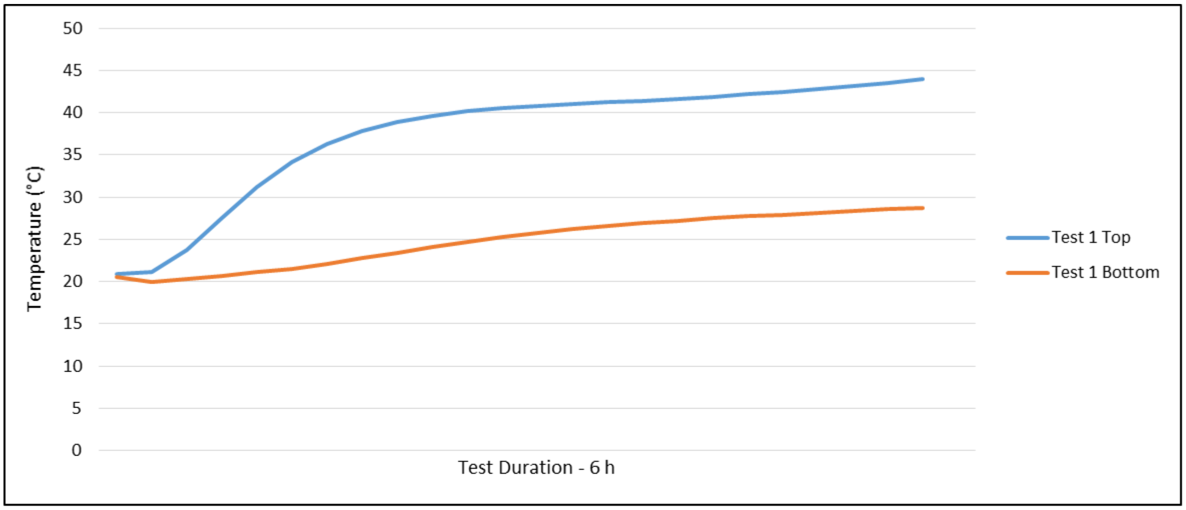

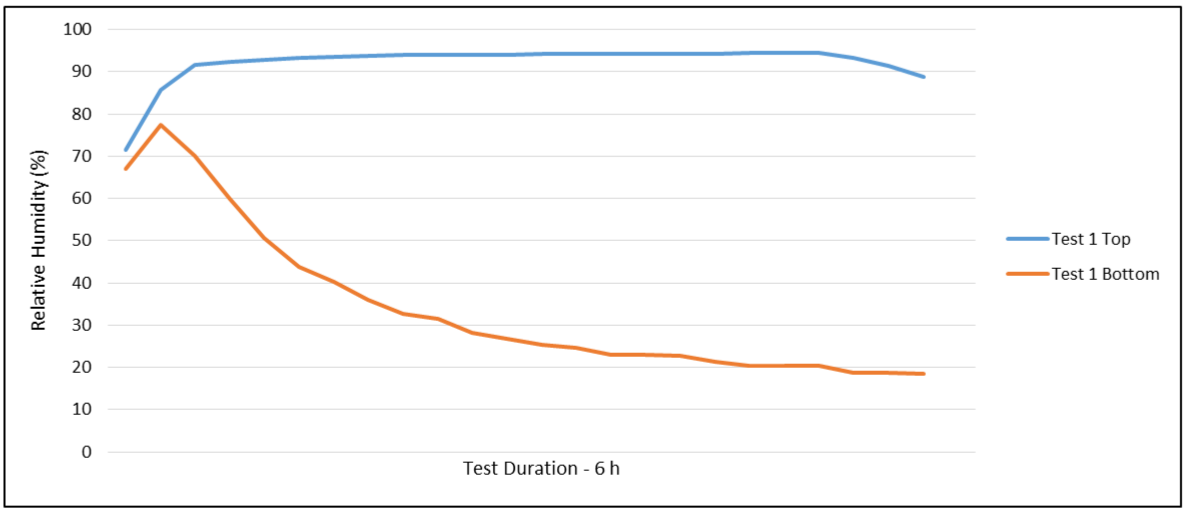

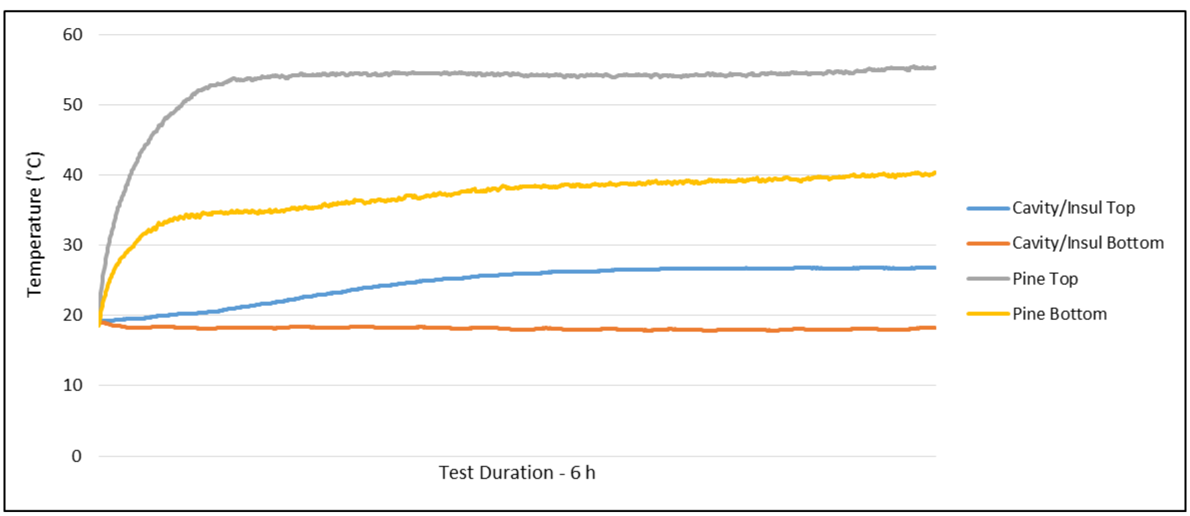

Figure C.3 – Test 8C Laboratory Data

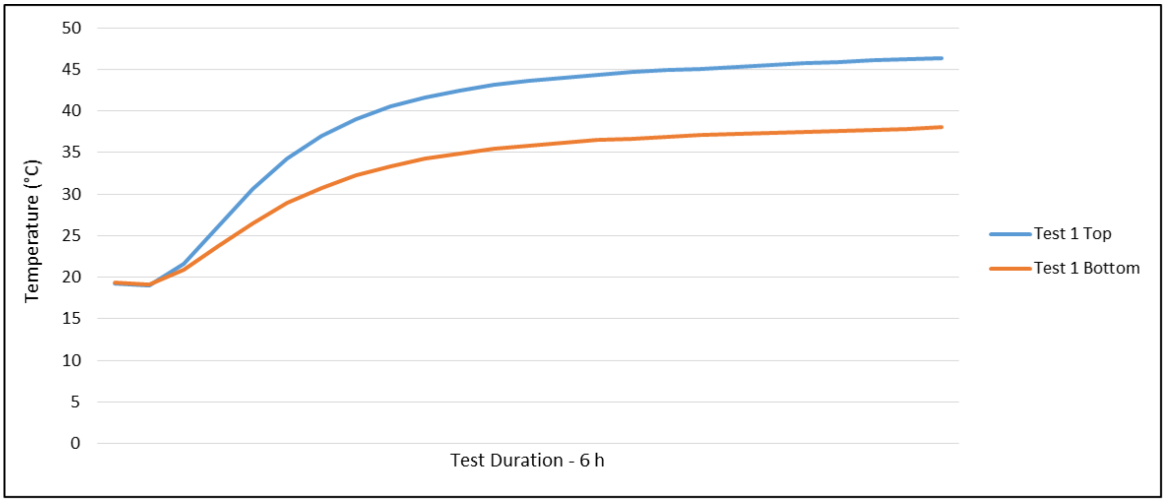

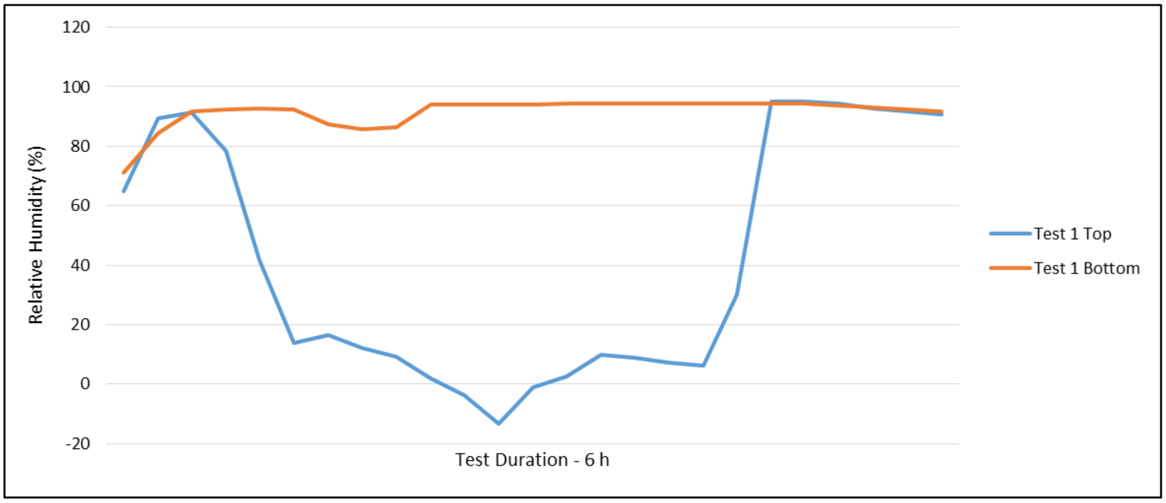

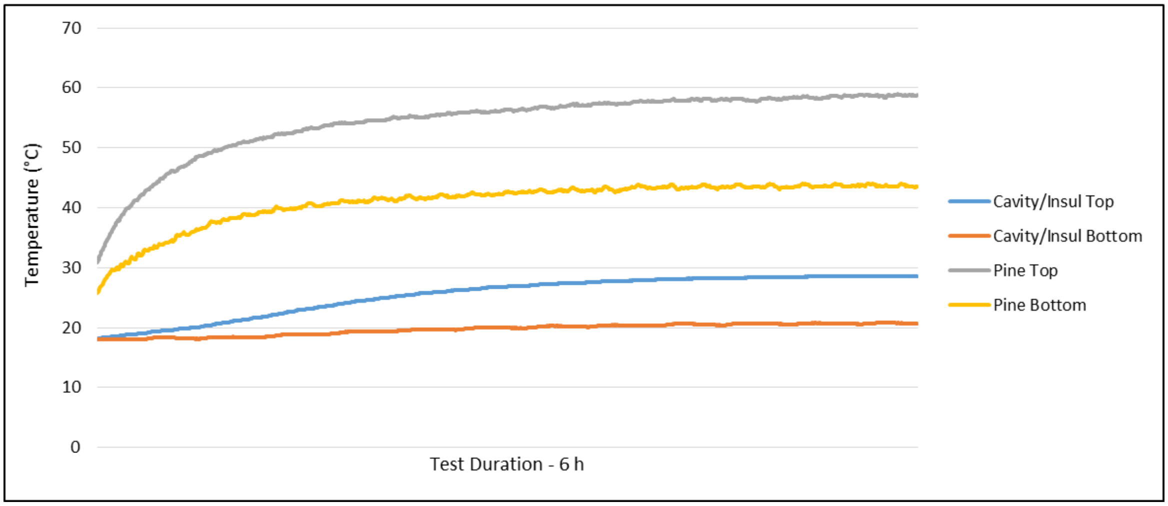

Figure C.4 – Test 9A Laboratory Data

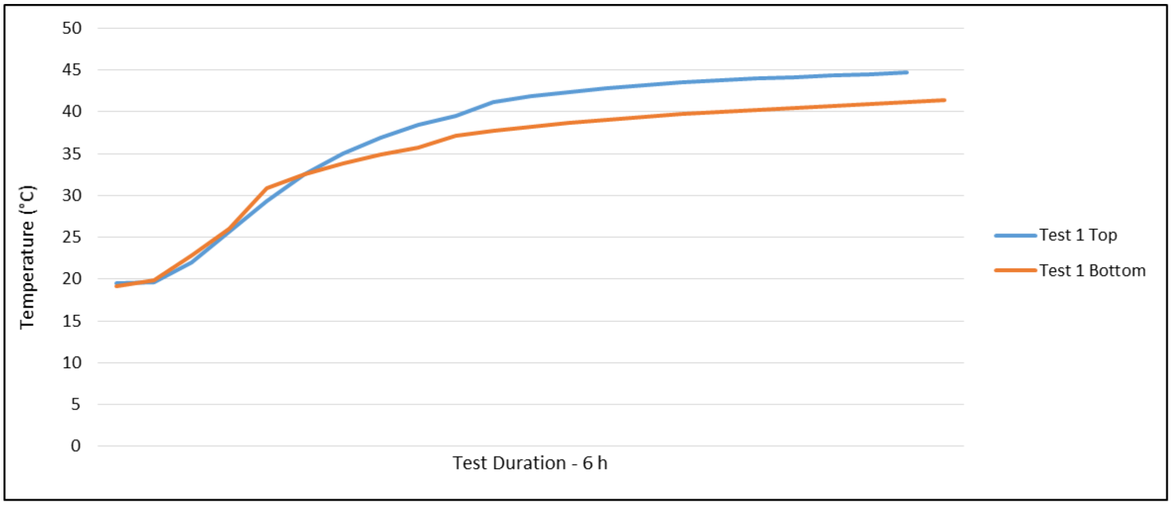

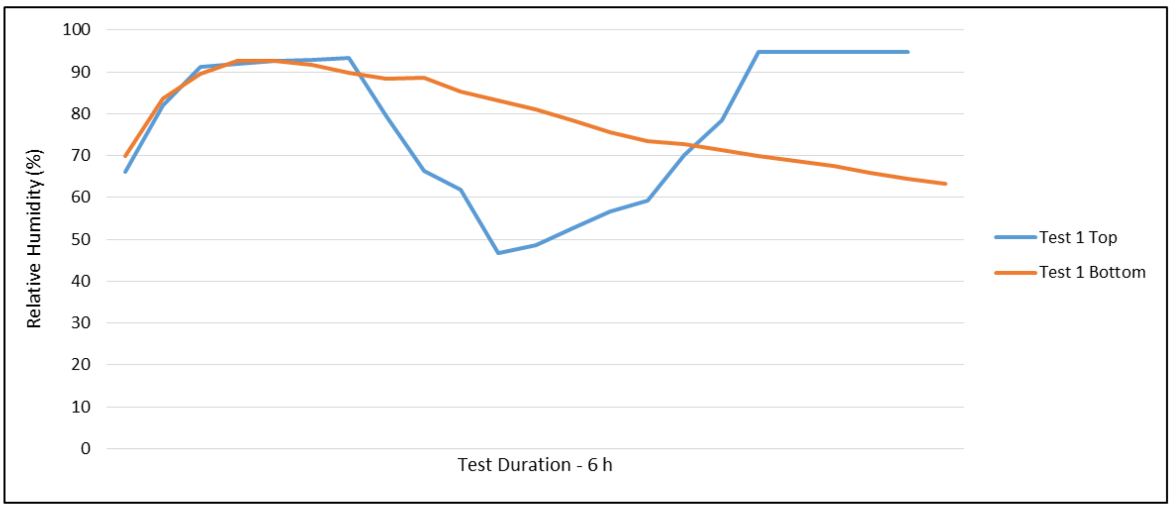

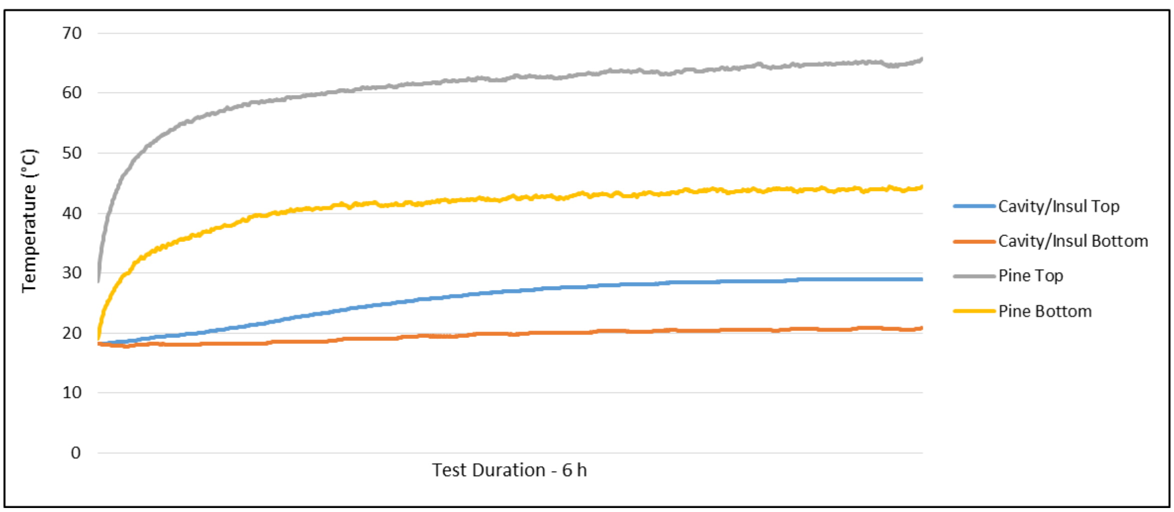

Figure C.5 – Test 9B Laboratory Data

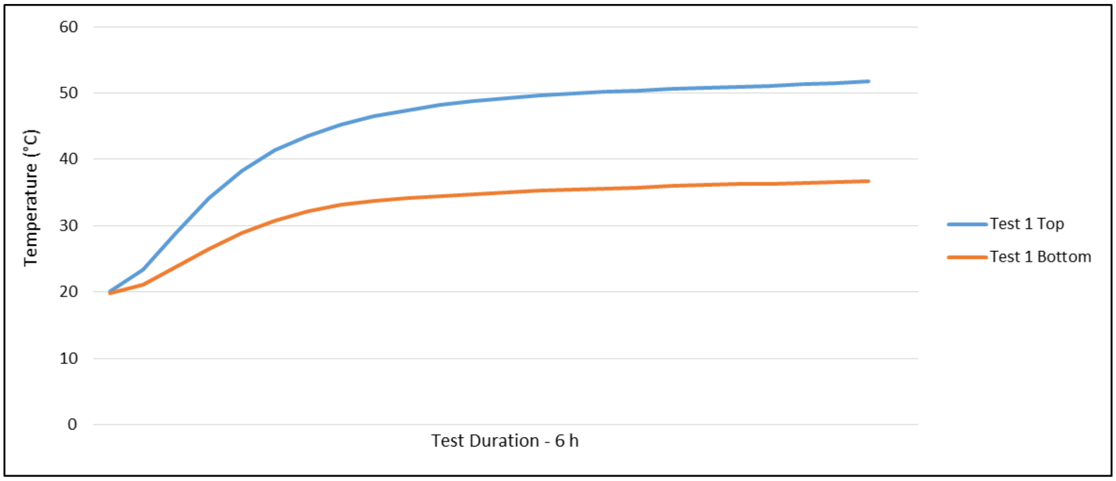

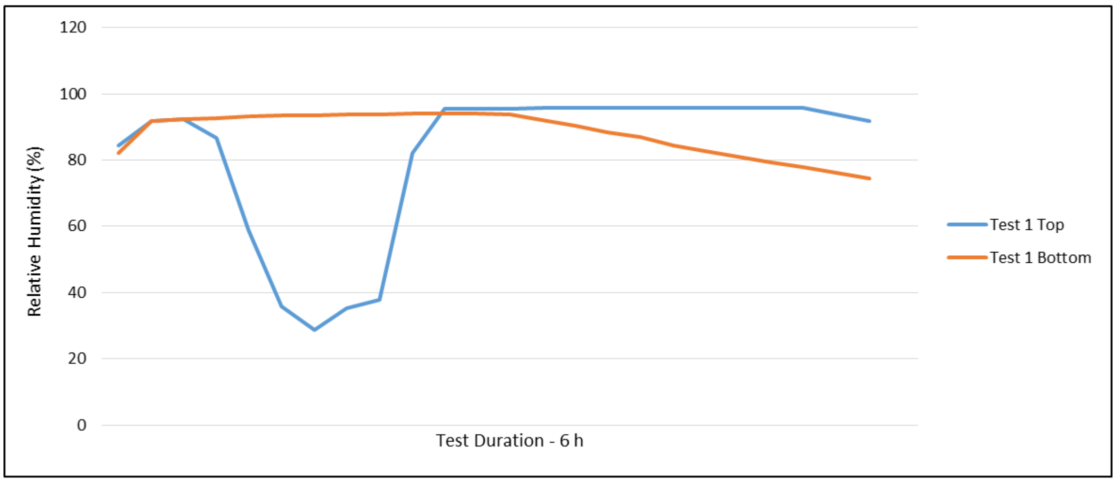

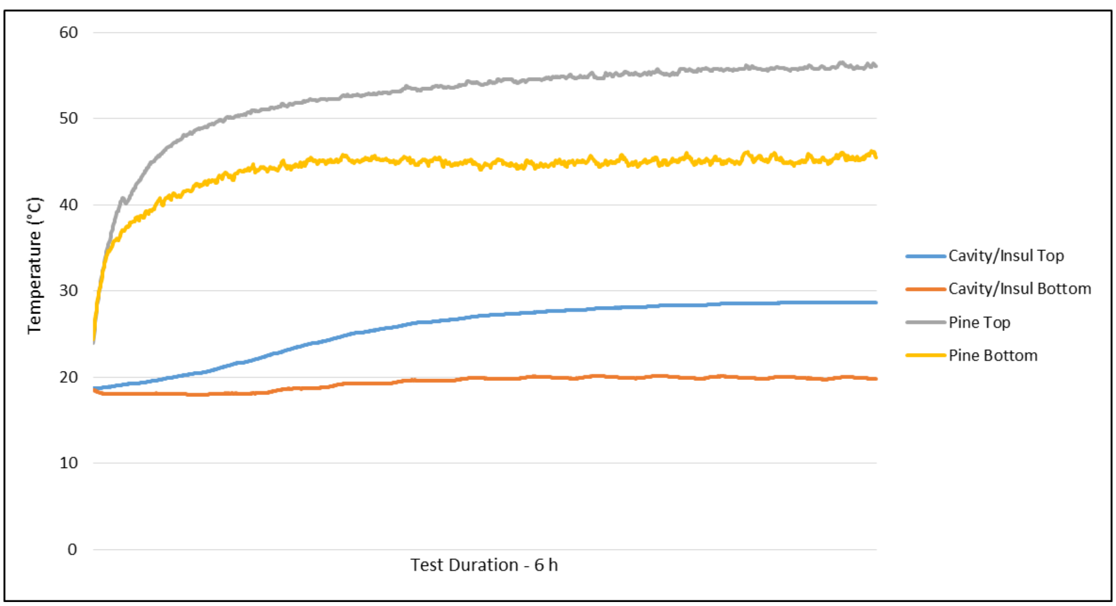

Figure C.6 – Test 9C Laboratory Data

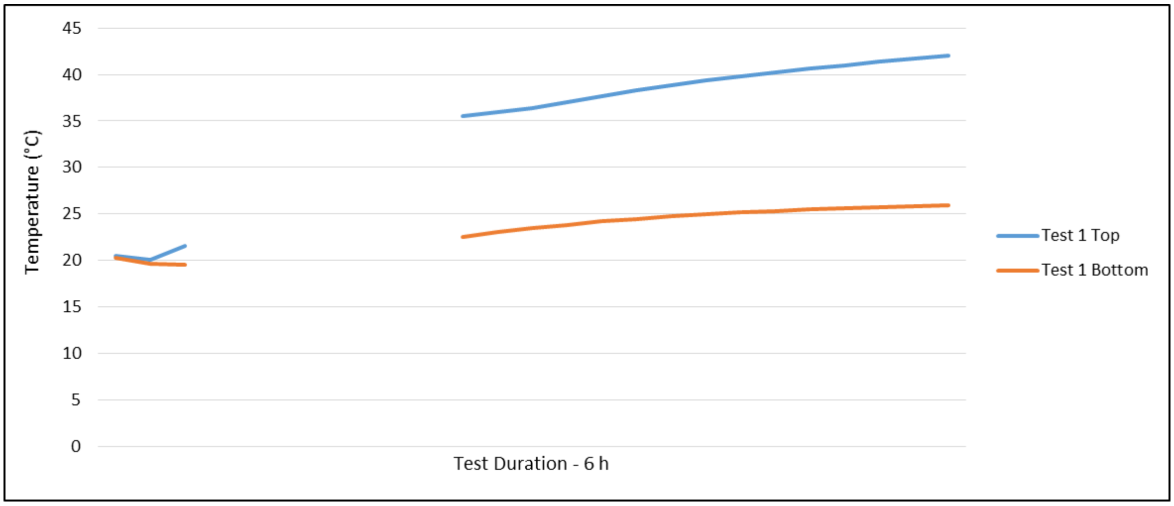

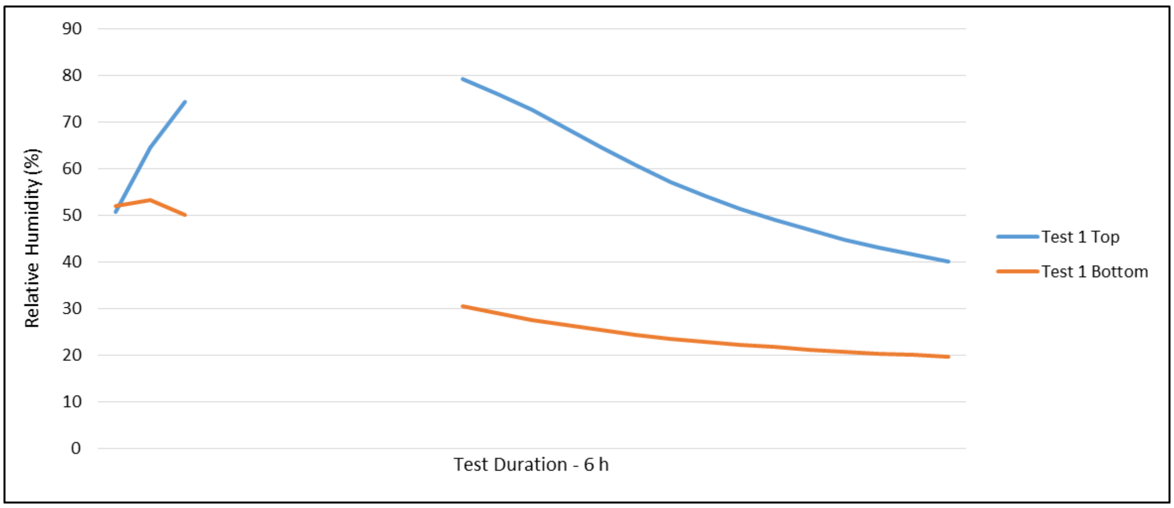

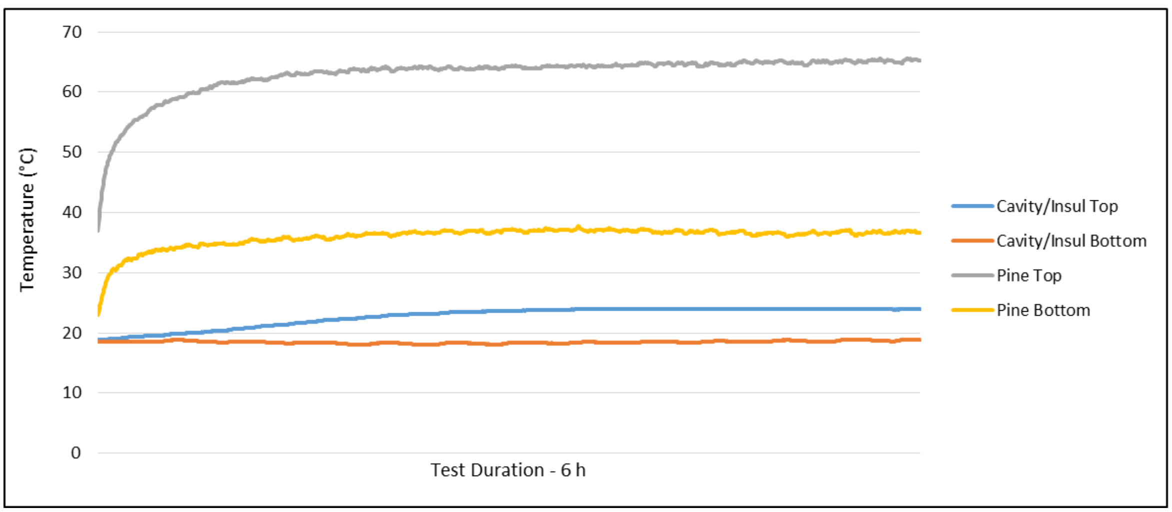

Figure C.7 – Test 10A Laboratory Data

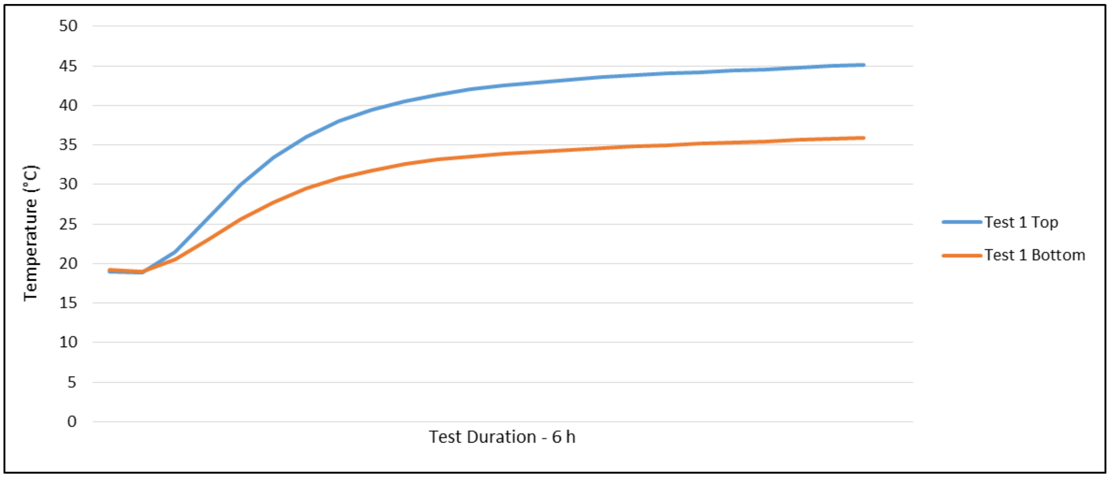

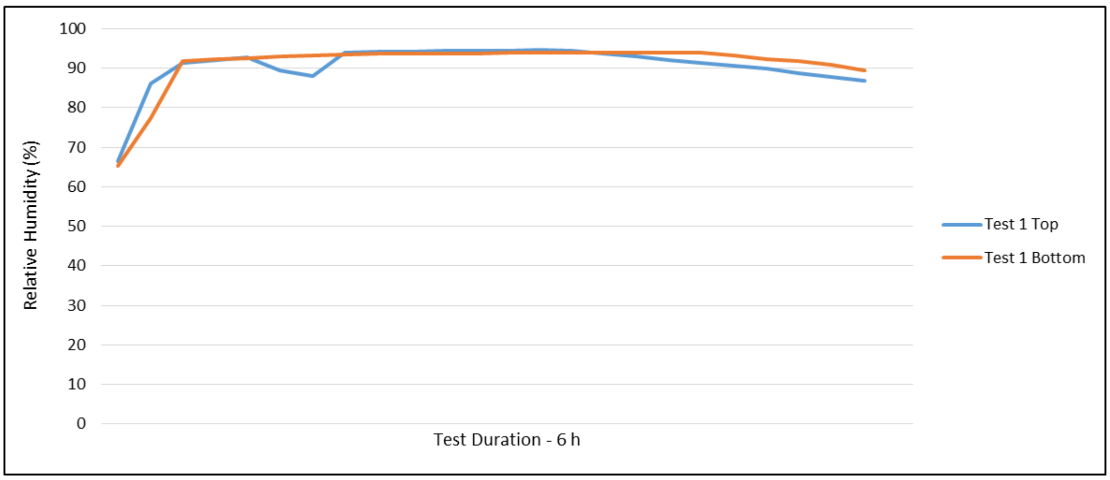

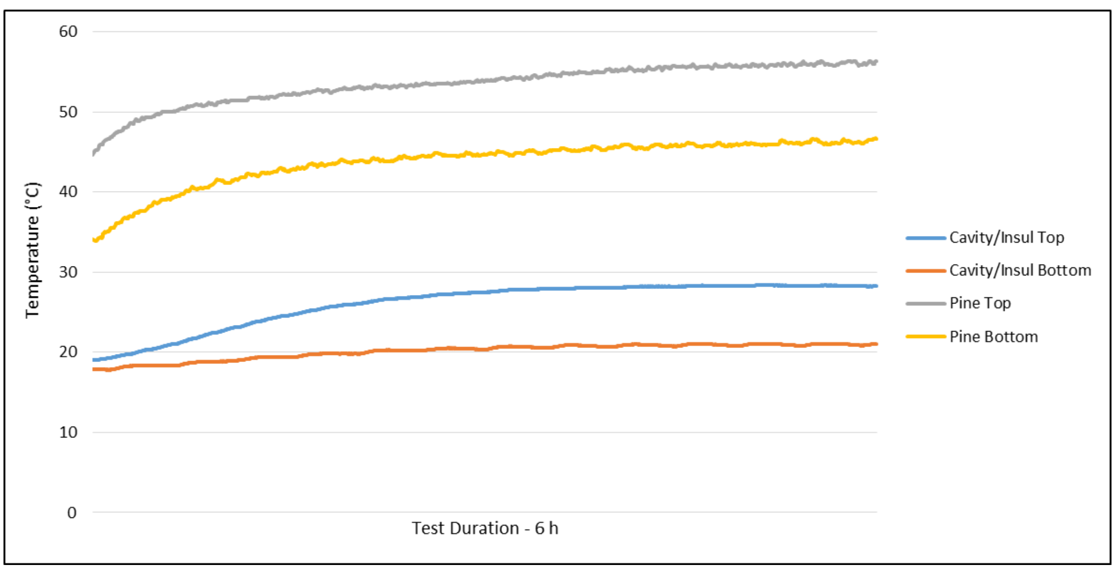

Figure C.8 – Test 11A Laboratory Data

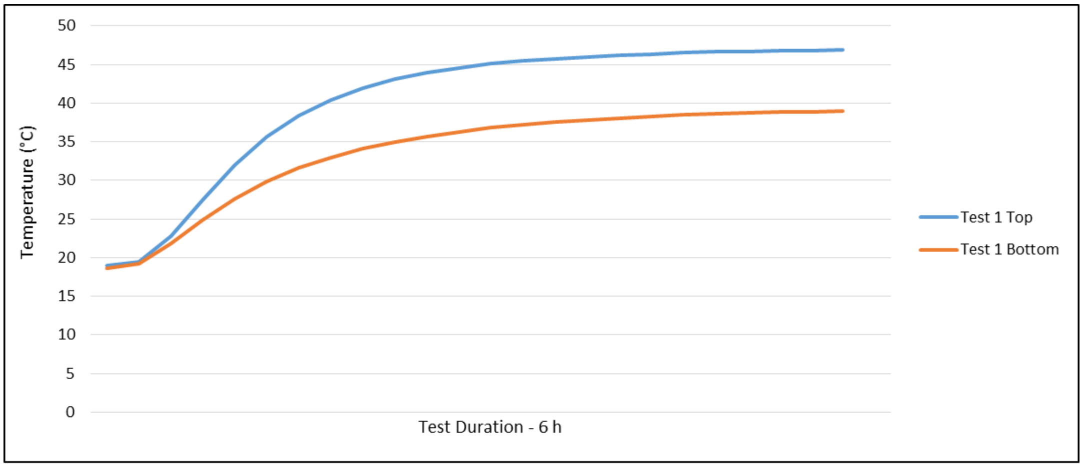

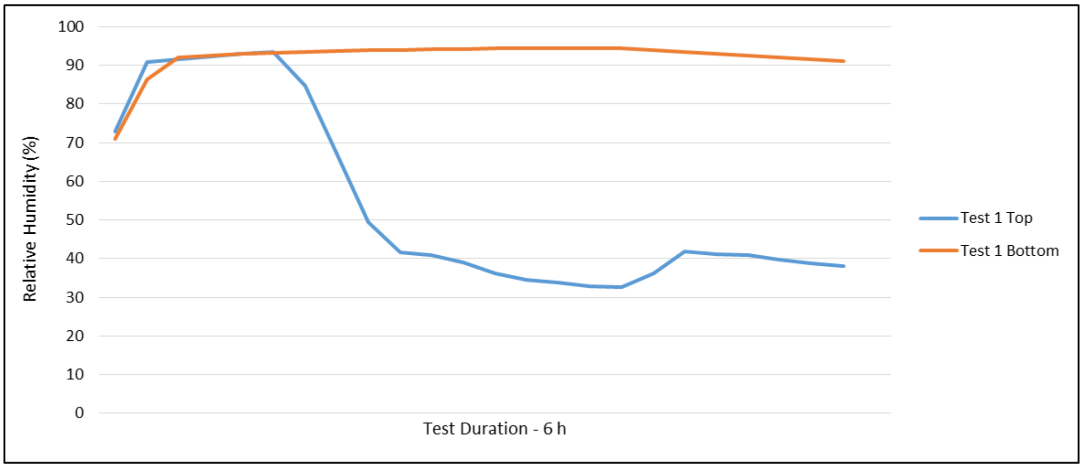

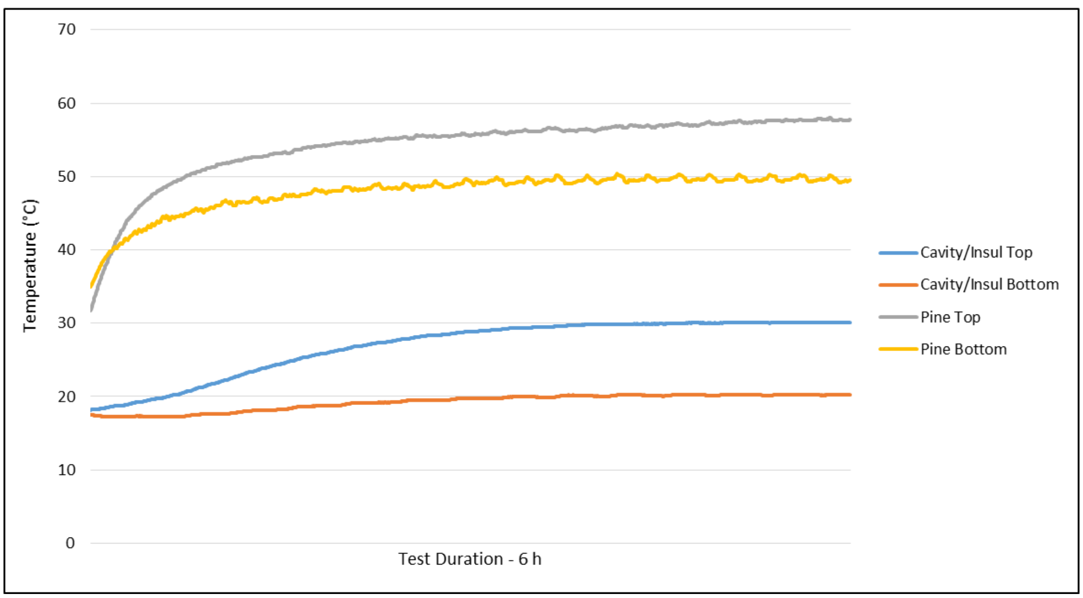

Figure C.9 – Test 11B Laboratory Data

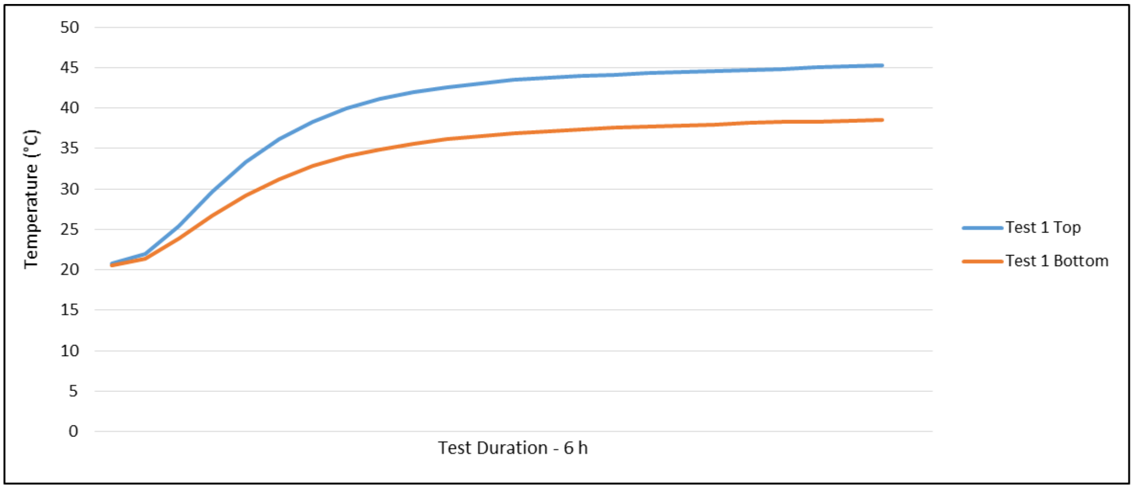

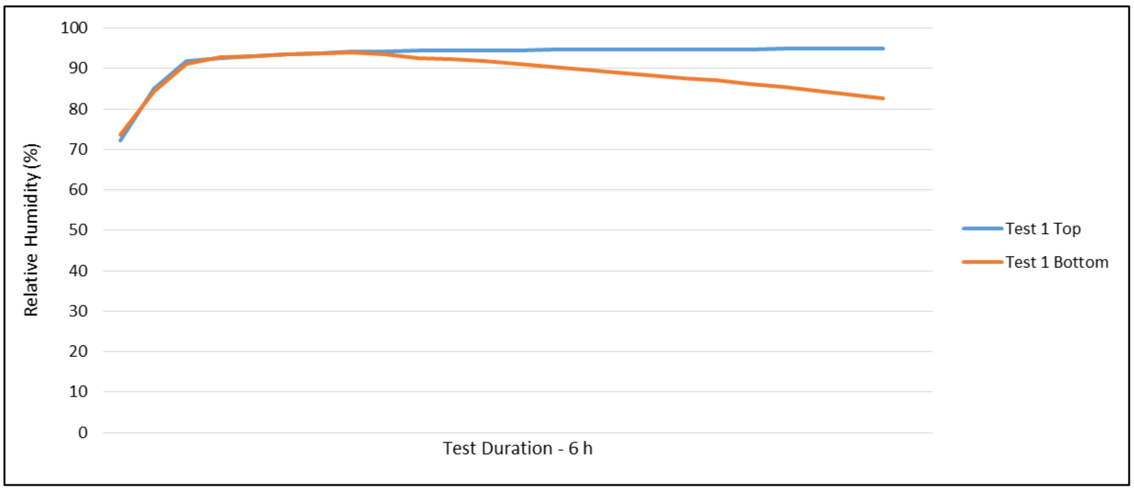

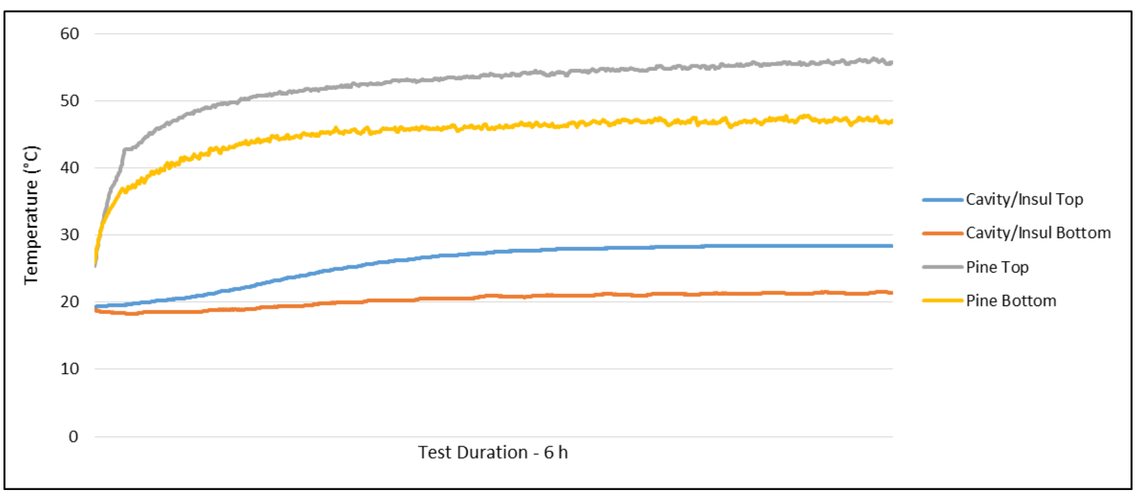

Figure C.10 – Test 11C Laboratory Data

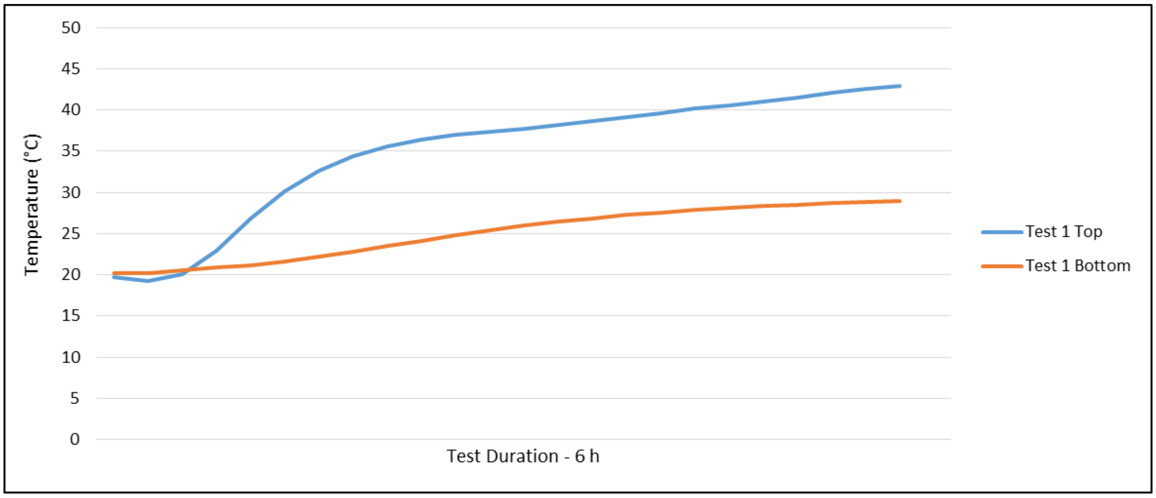

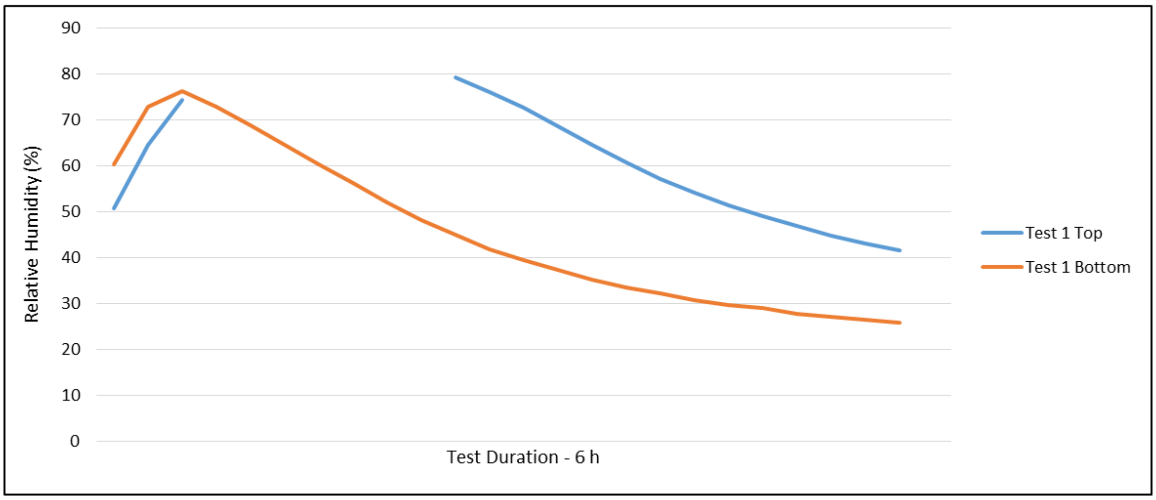

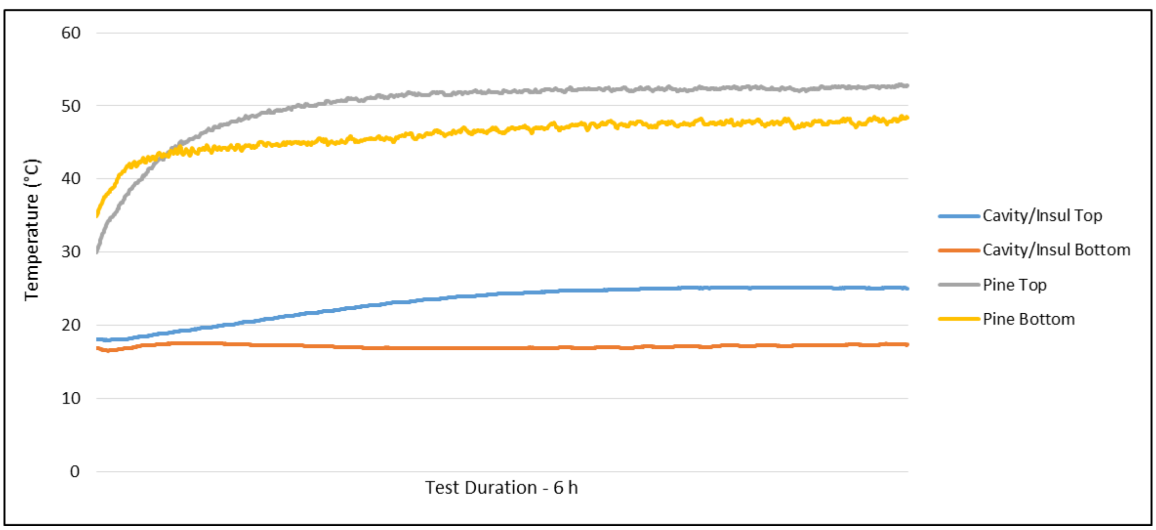

Figure C.11 – Test 12A Laboratory Data

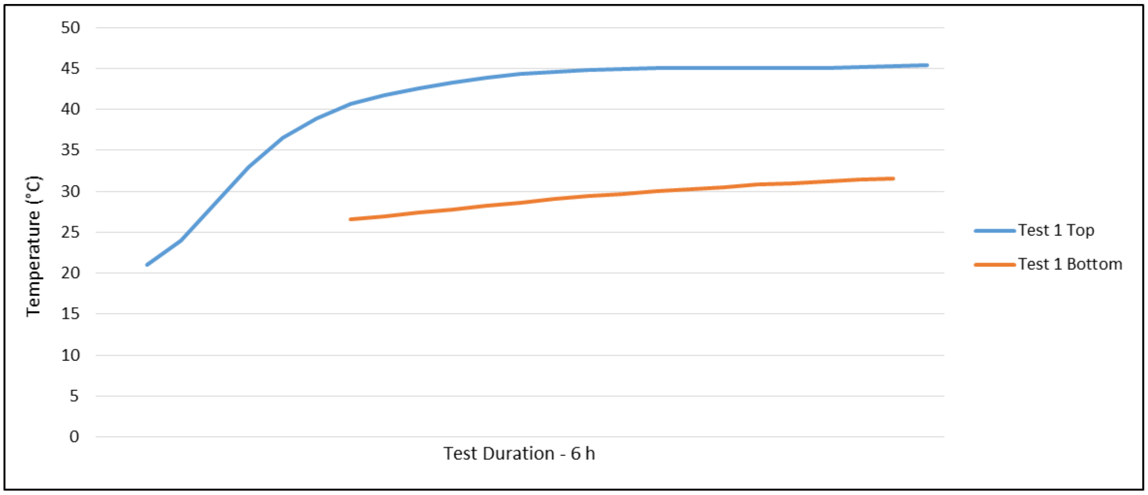

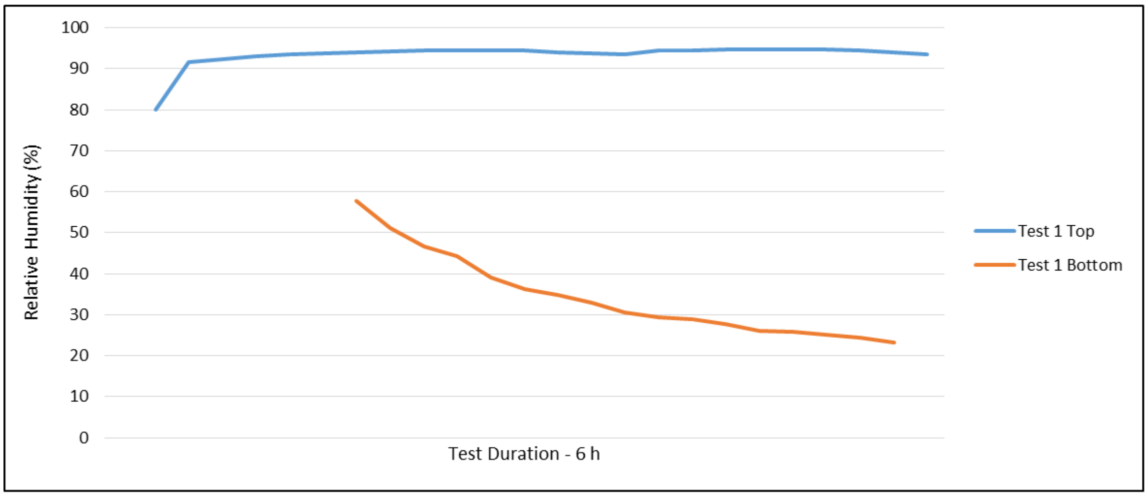

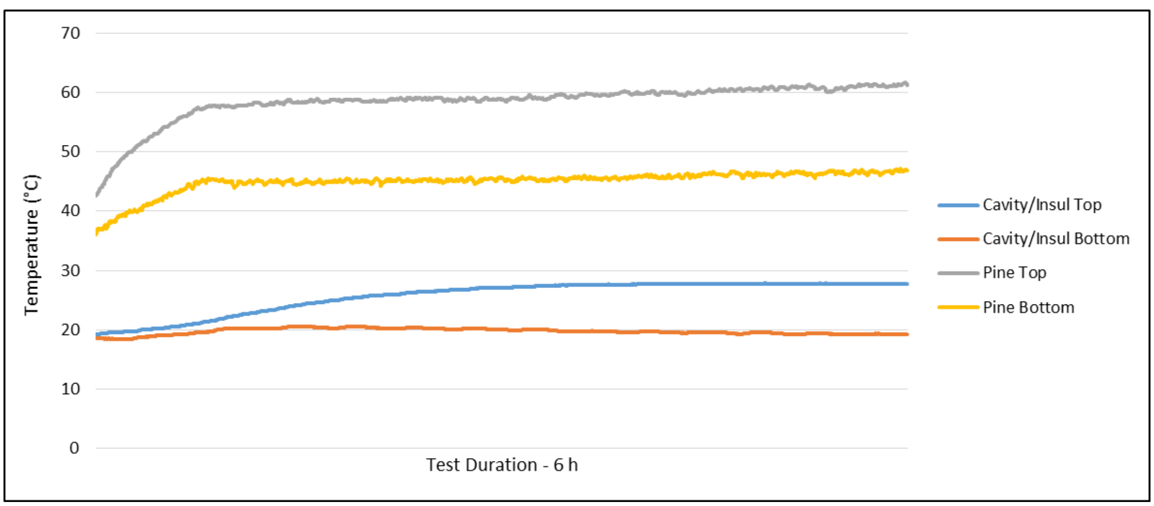

Figure C.12 – Test 13A Laboratory Data

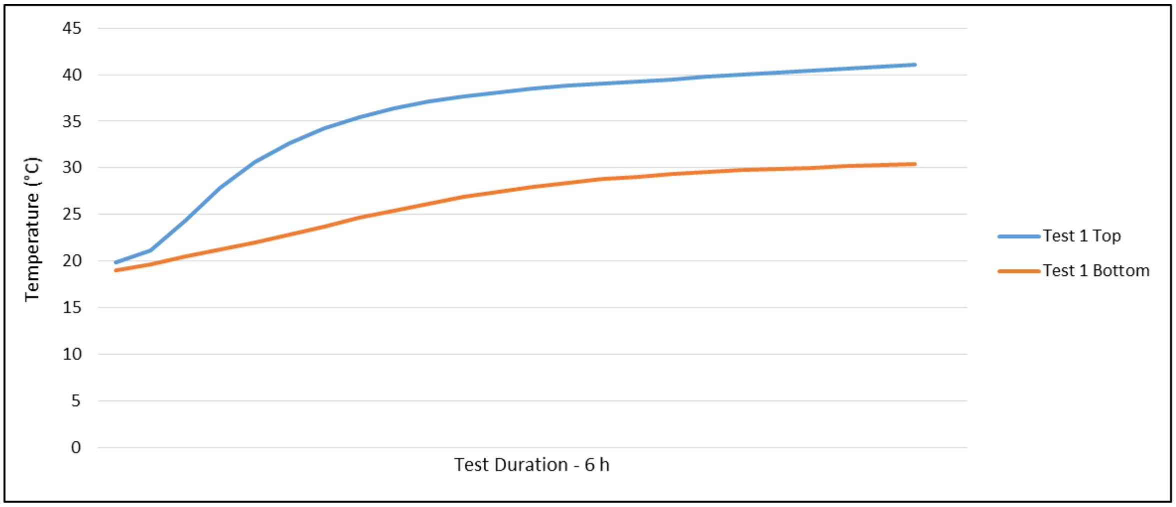

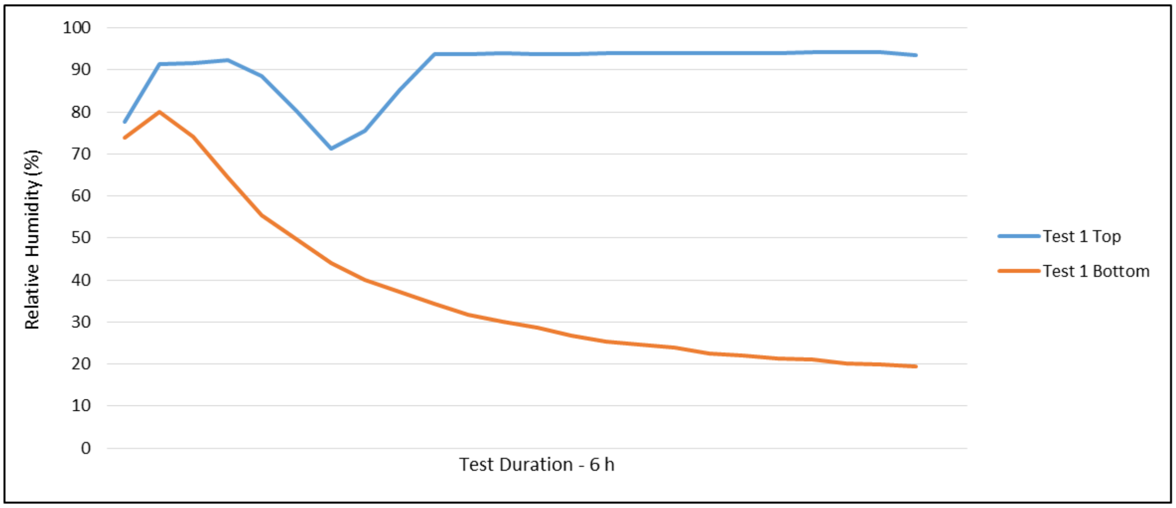

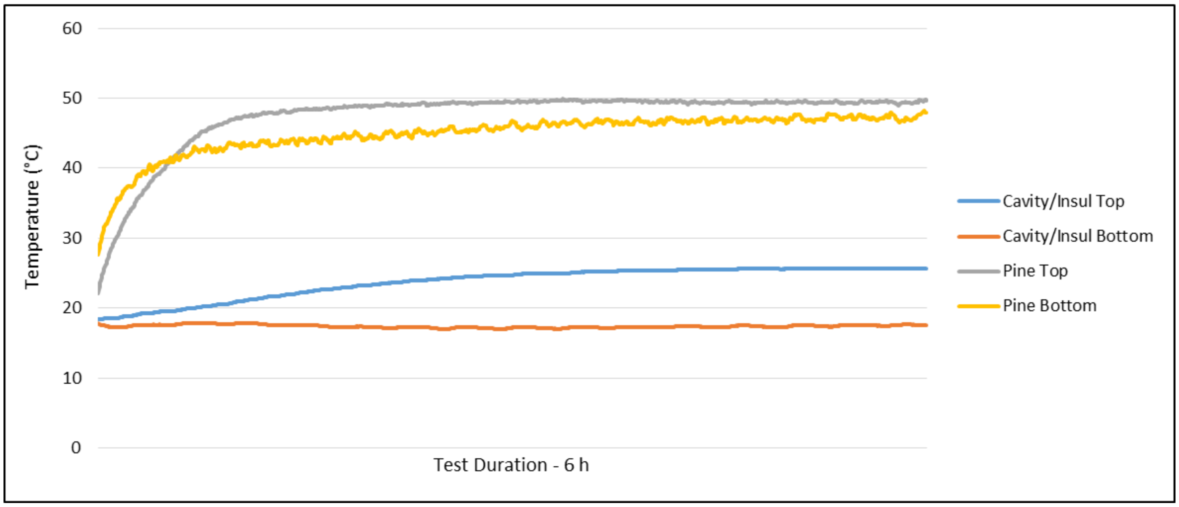

Figure C.13 – Test 13B Laboratory Data

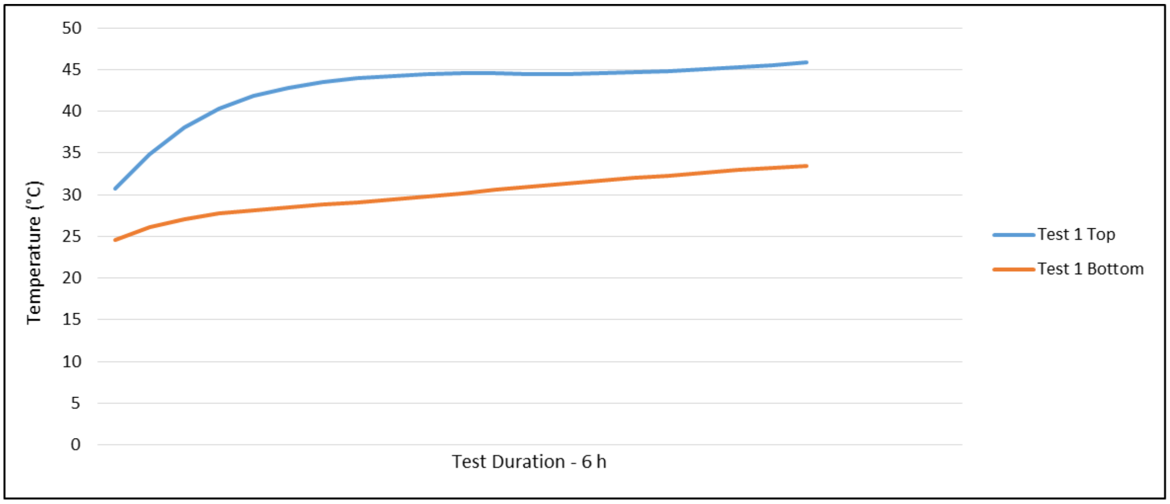

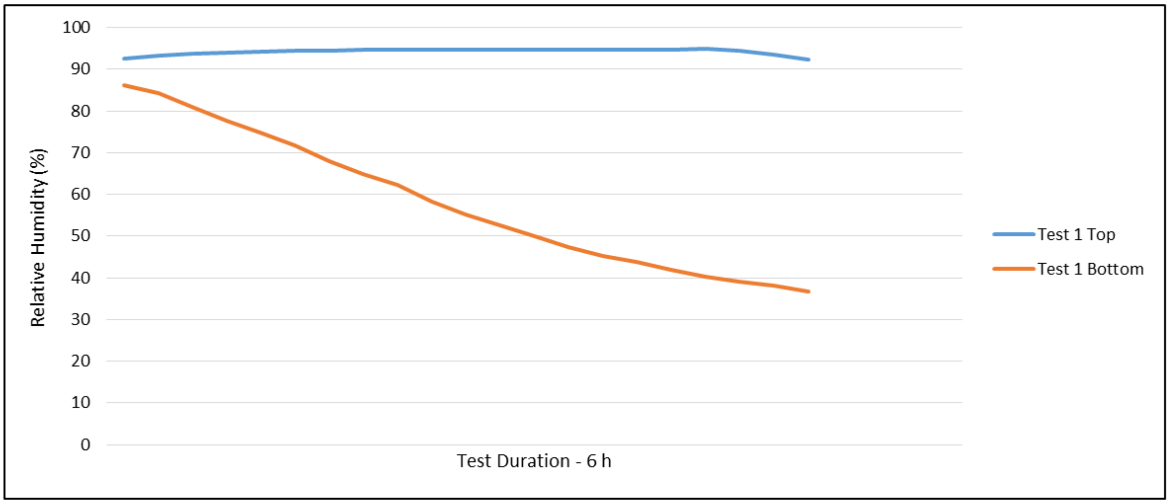

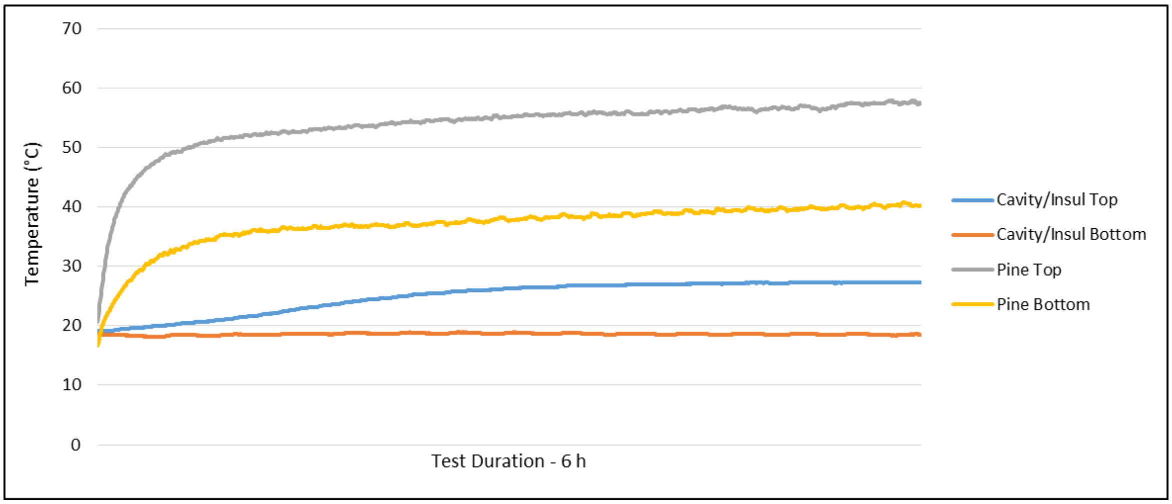

Figure C.14 – Test 13C Laboratory Data

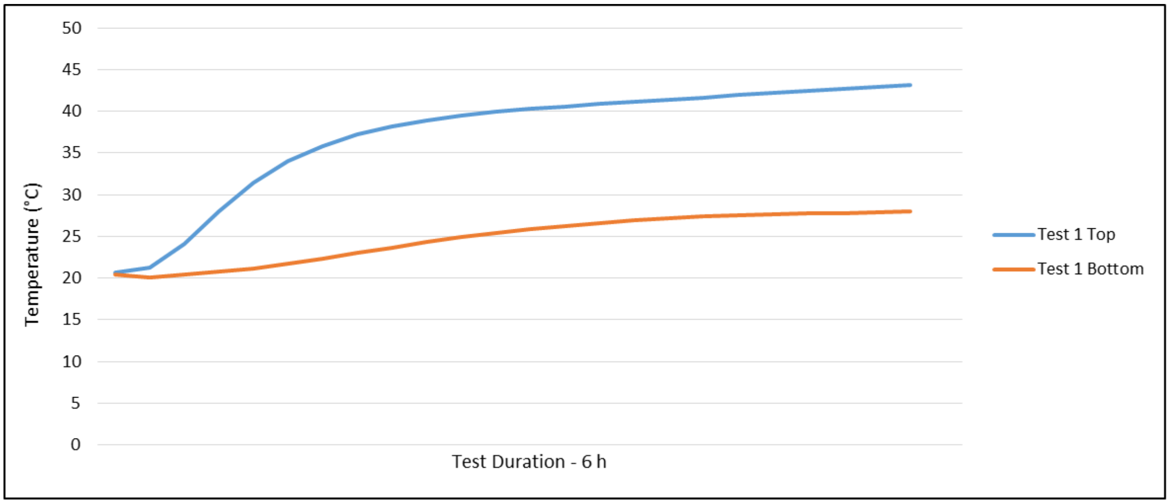

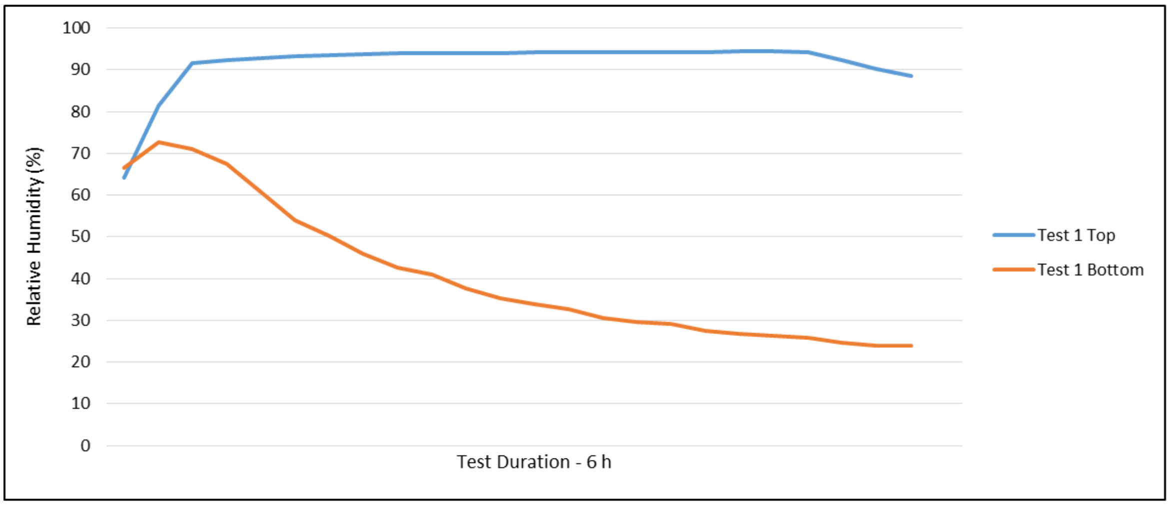

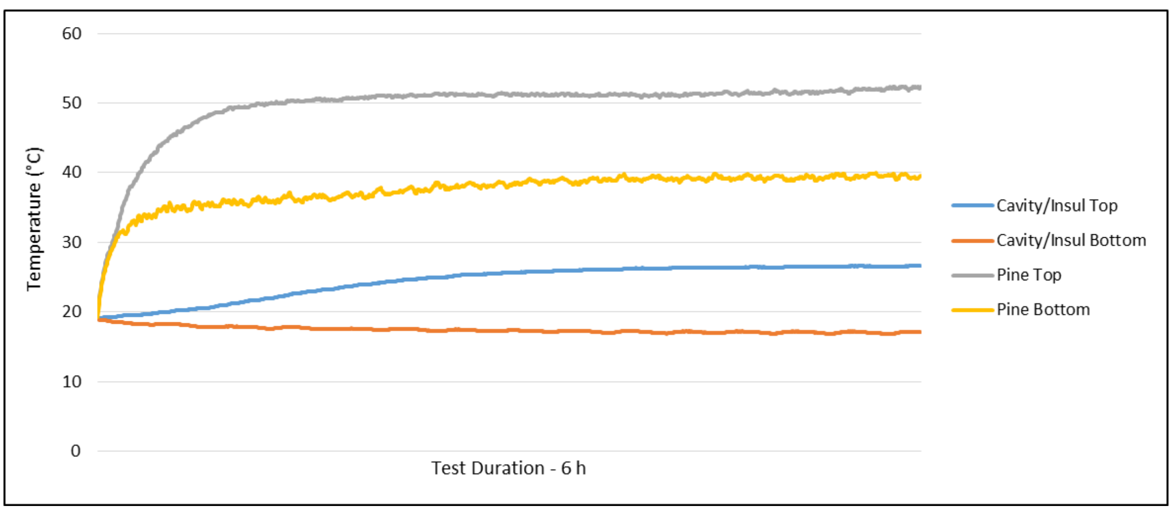

Figure C.15 – Test 13D Laboratory Data

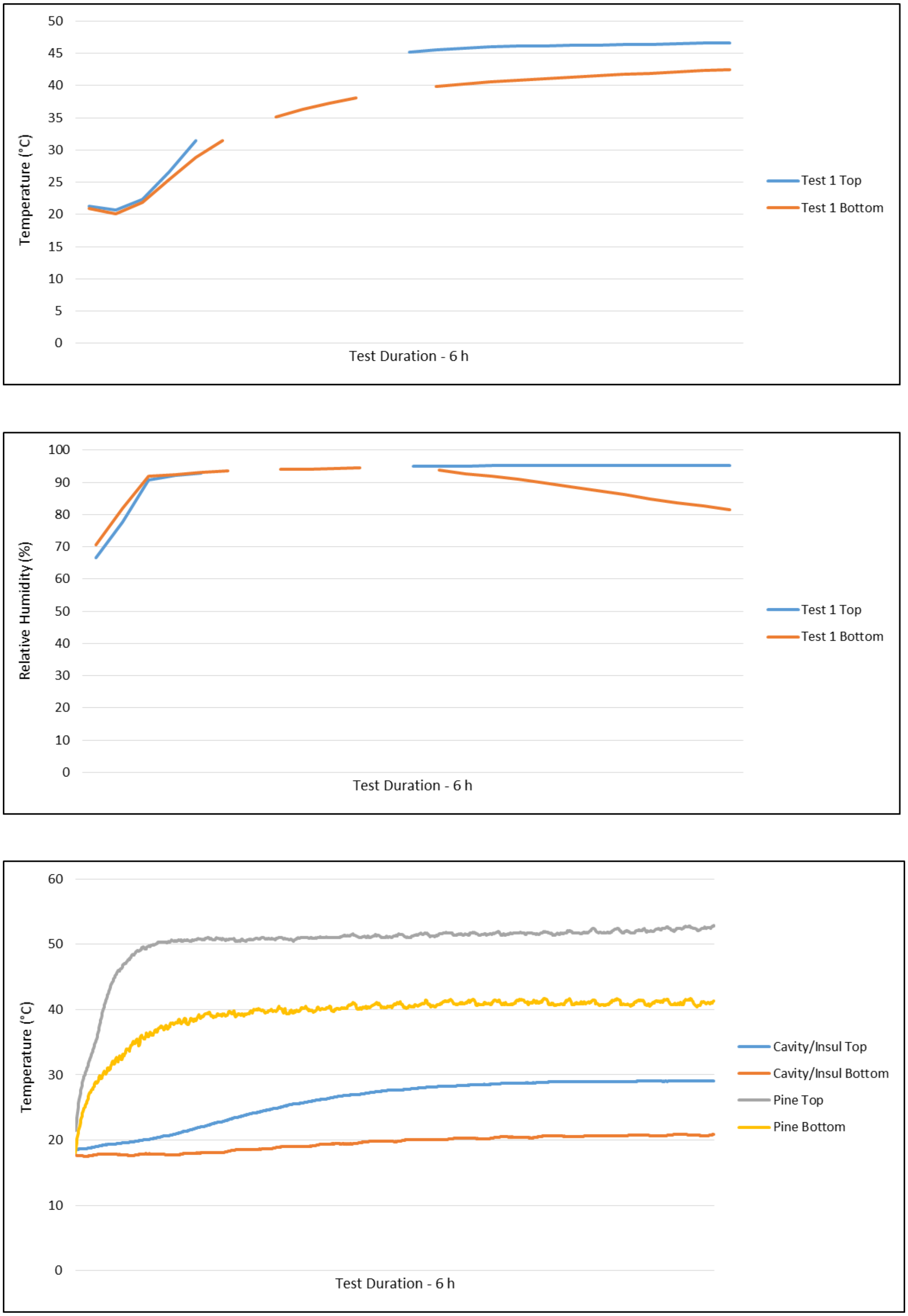

Figure C.16 – Test 14A Laboratory Data

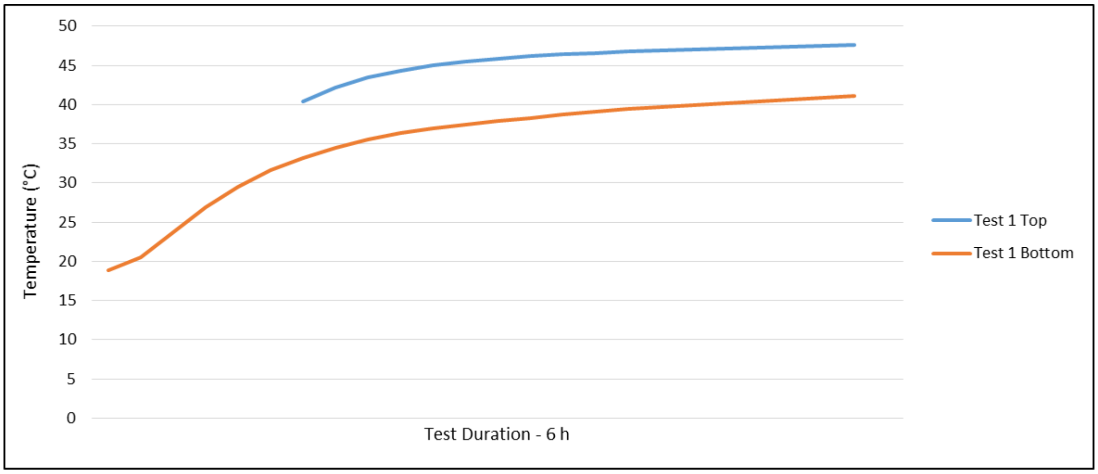

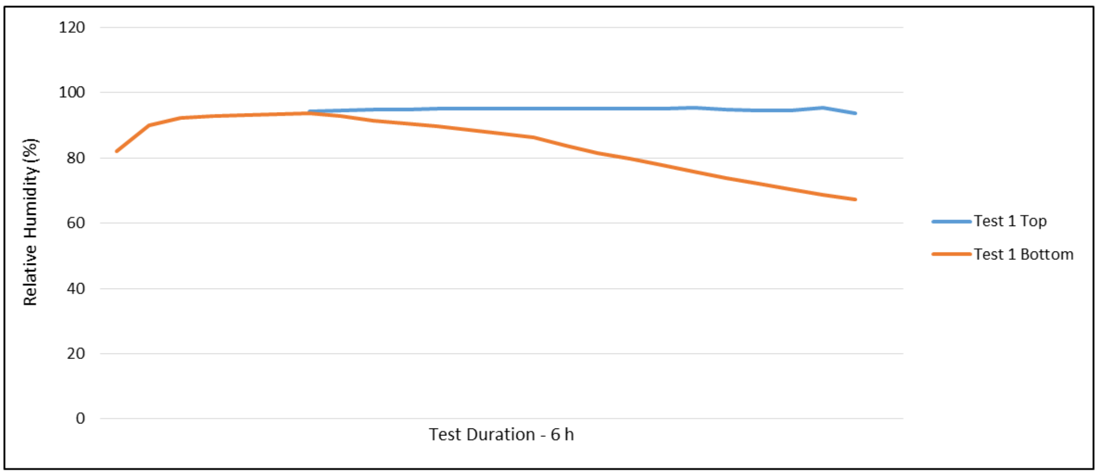

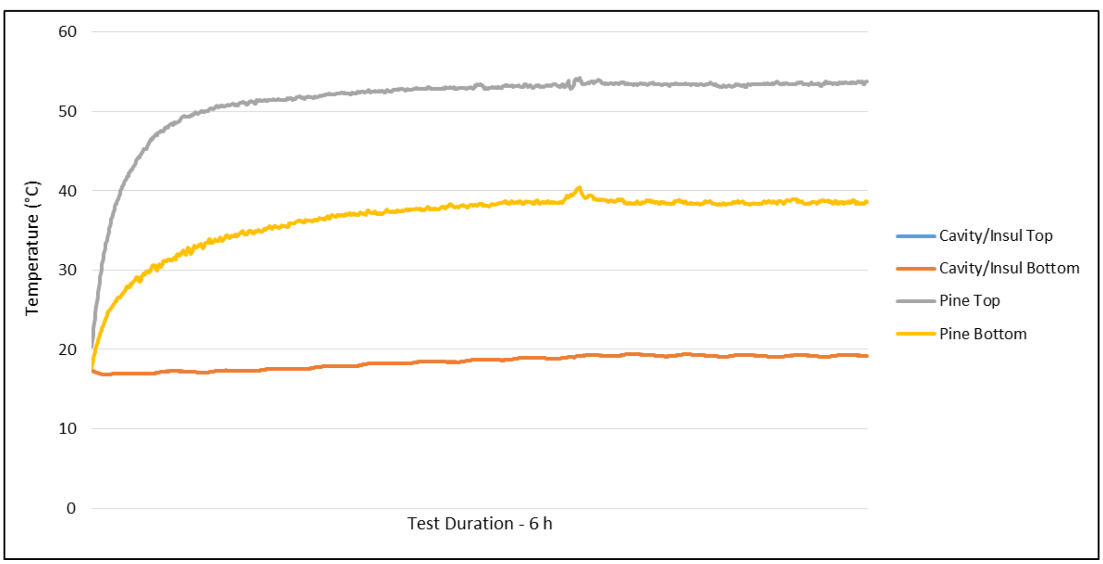

Figure C.17 – Test 15A Laboratory Data

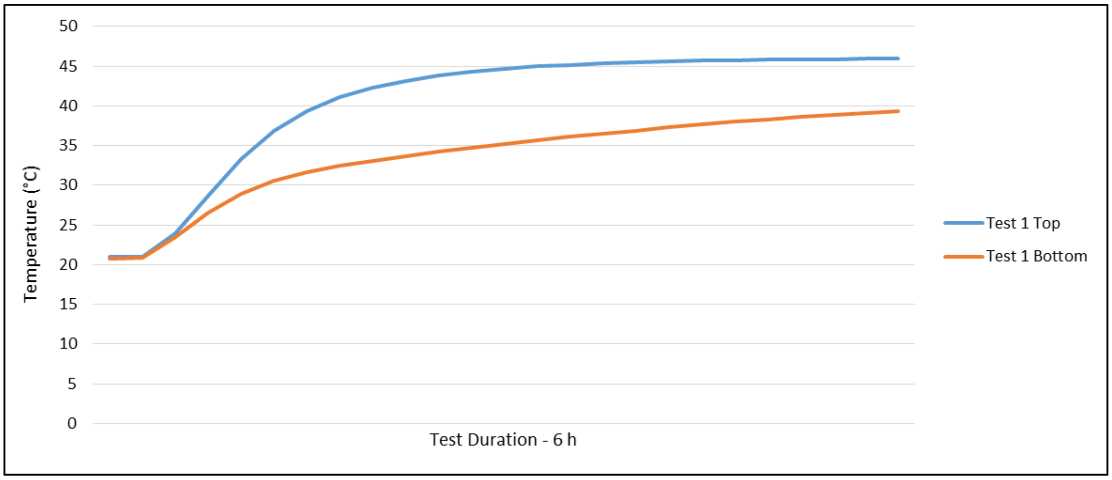

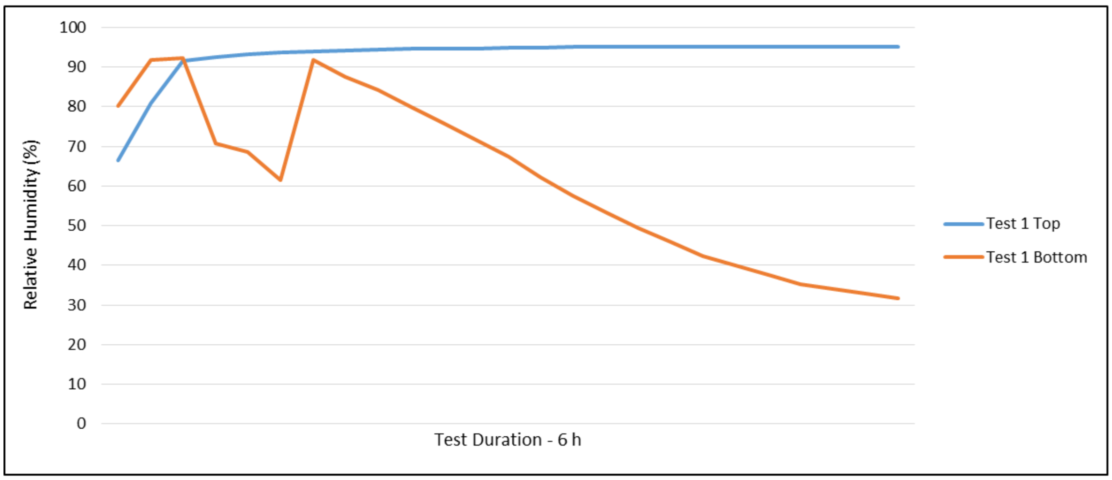

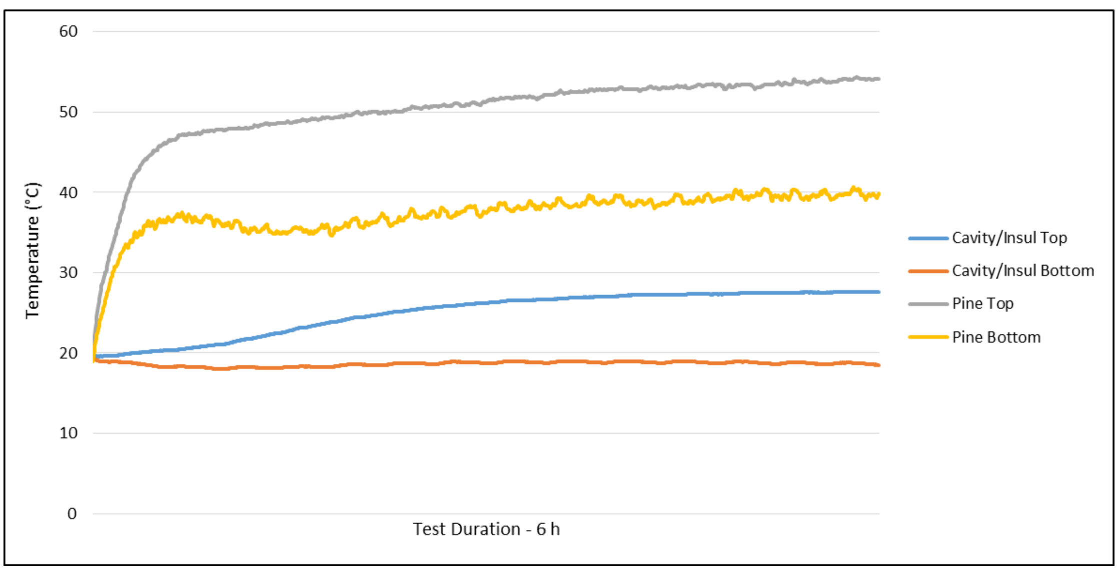

Figure C.18 – Test 16A Laboratory Data

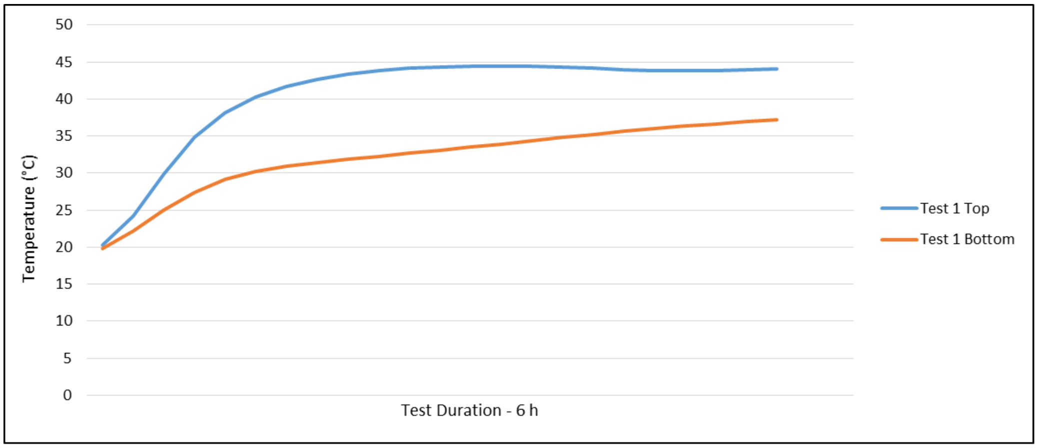

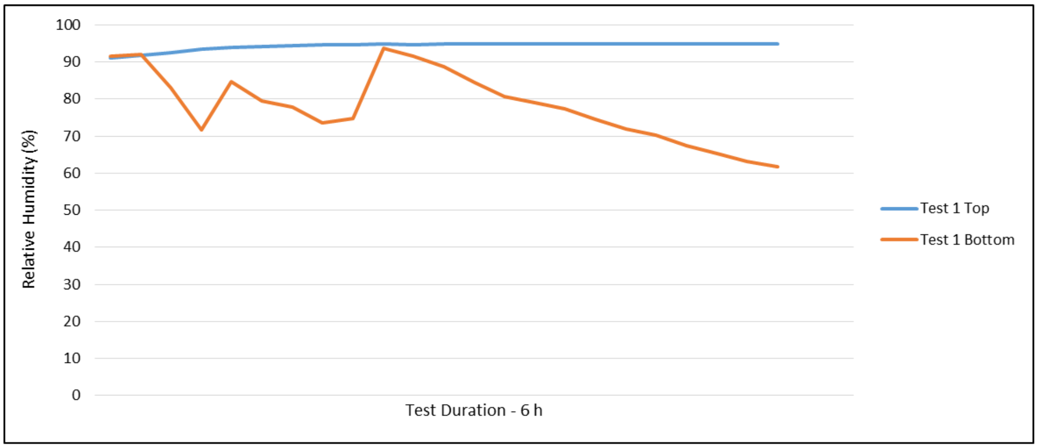

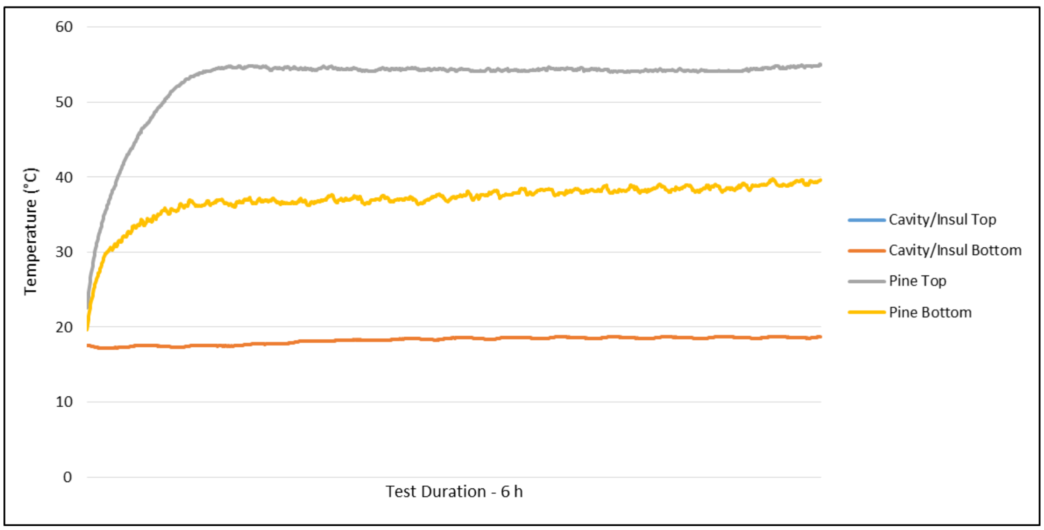

Figure C.19 – Test 16B Laboratory Data

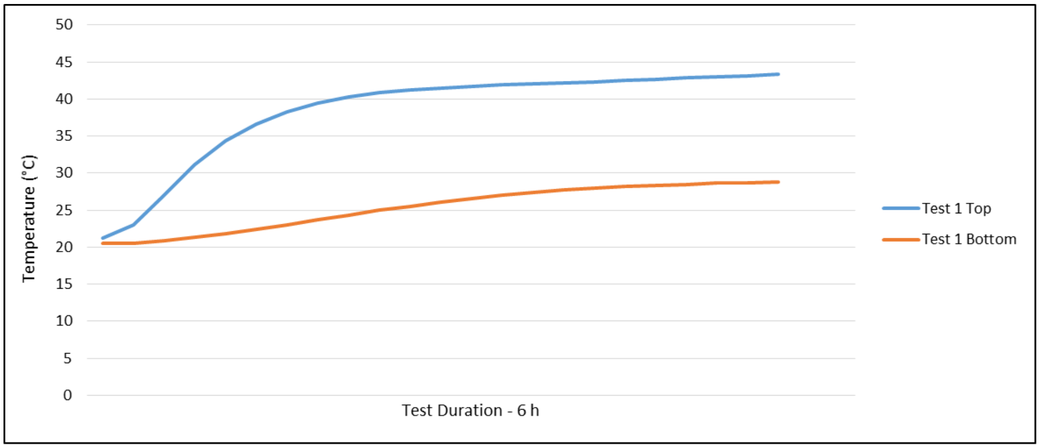

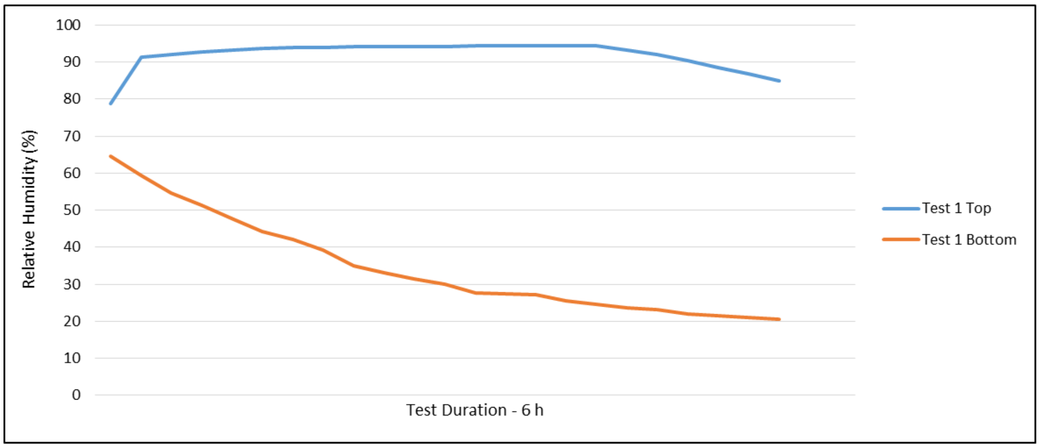

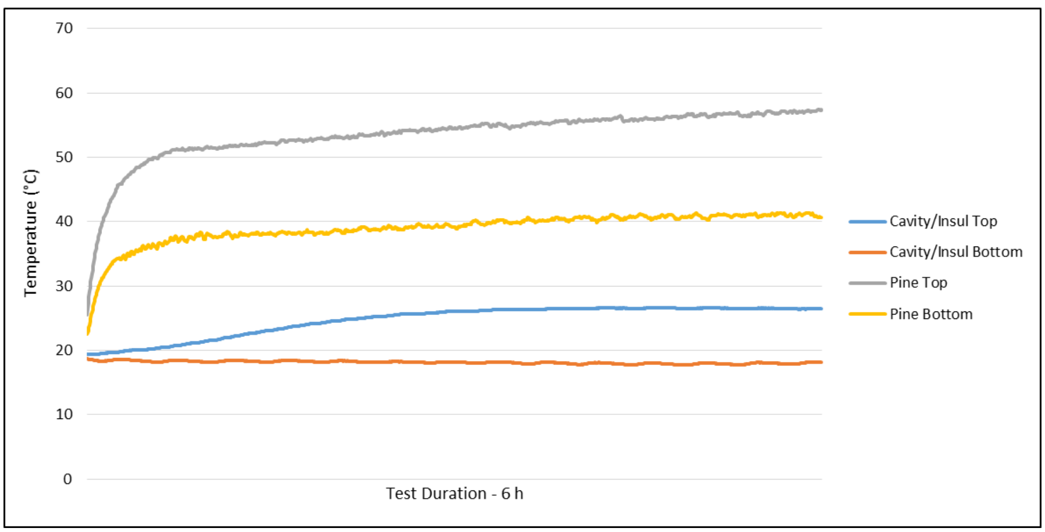

Figure C.20 – Test 17A Laboratory Data